Phase Relationships in the Binary Systems of Nitrides and Carbides of Zirconium, Columbium, Titanium, and Vanadium[1]

POL DUWEZ AND FRANCIS ODELL[2]

Jet Propulsion Laboratory, California Institute of Technology, Pasadena, California

ABSTRACT

Previous investigators have shown that the binary systems involving the monocarbides of zirconium, columbium, tantalum, titanium, and vanadium are of the solid solution type, with the exception of ZrC-VC which are almost completely insoluble in each other. In the present study it is shown that the mononitrides of zirconium, columbium, titanium, and vanadium, which have the same NaCl type crystal structure as the corresponding carbides, are also soluble in each other, with the exception of the pair ZrN-VN. As in the case of the carbides, this exception can be explained on the basis of the atomic size rule governing the formation of solid solution. Furthermore, it is established that most of the binary systems formed by a carbide and a nitride are of the solid solution type, providing the atomic diameters of the metal atoms do not differ by more than about 15 per cent. The systems involving zirconium carbide with the nitrides were not investigated because zirconium carbide decomposed in a nitrogen atmosphere at high temperature.

INTRODUCTION

The present interest in material for use at very high temperature has focused attention on the refractory carbides, nitrides, borides, and silicides of the transition elements. While some of these compounds probably are of interest in the pure state, they might offer greater possibilities when combined in suitable proportions. There is, therefore, a need for studying their alloying properties and for establishing the phase relationships in binary, ternary, and eventually more complicated systems. The first step in this relatively unexplored field is to consider the binary systems between compounds which exhibit a certain degree of similarity. Obviously, the phase relationships will be the simplest in the case of two compounds having the same crystal structure. From this point of view, the carbides and nitrides of zirconium, columbium, titanium, and vanadium constitute a particularly interesting group, since they all have the same cubic NaCl-type crystal structure.

The solubility relationships between monocarbides have been studied by several investigators (1, 2). The most complete and most accurate results were published recently by Norton and Mowry (3) who established that the systems containing any two of the five carbides, ZrC, CbC, TaC, TiC, or VC, are of the solid solution type with the exception of ZrC-VC which are almost completely insoluble in each other. These results are in agreement with the size factor rule, which in the present case is probably the most important one of the three Hume-Rothery rules governing the formation of solid solutions (4). In view of the structural analogy between the mononitrides and the monocarbides, the solubility between the four nitrides, ZrN, CbN, TiN, and VN, also should be complete, with the possible exception of ZrN-VN. The results of the present investigation confirm these predictions.

The considerations of size factor may be extended to the nitride-carbide pairs, in which case the interstitial positions in the lattice are occupied by either a carbon or a nitrogen atom. It was found experimentally that this extension of the size factor rule is justified.

EXPERIMENTAL PROCEDURE

The experiments consisted essentially in heating a mixture of finely divided powder of nitrides or nitride-carbide at sufficiently high temperature to achieve equilibrium. The various powders were sieved through a 325-mesh screen, and the mixtures were pressed at about 10,000 psi (703 kg/cm^2) in a $\frac{1}{2}$ inch (1.27 cm) diameter hard steel die. Acetone or carbon tetrachloride was used in some cases to facilitate compaction. A high frequency furnace and a graphite resistance furnace were used for firing the specimens. In the high frequency furnace a tungsten cylindrical crucible about $\frac{3}{4}$ inch (1.905 cm) inside diameter and 1 inch (2.54 cm) high was placed in the center of the heating coil and a thoria sleeve served as a radiation shield. The whole assembly was maintained in an atmosphere of nitro-

[1] Manuscript received February 6, 1950. This paper prepared for delivery before the Cleveland Meeting, April 19 to 22, 1950.

[2] Present address: Surface Alloys, Inc., Lynwood, California.

gen. The maximum temperature attained in this furnace was about 2350°C.

The graphite resistance furnace was used for higher temperatures up to about 2650°C. The resistance element of this furnace is a tube of graphite 3 inches (7.62 cm) inside diameter and 4 inches (10.16 cm) outside diameter, whose central section is cut in a spiral over a length of about 12 inches (30.48 cm). The heating element is surrounded by a graphite cylinder and powdered magnesia is used as thermal insulator between this cylinder and the outside water cooled jacket. The power requirement to maintain the furnace at 2650°C is approximately 45 kw. As in the high frequency furnace, all firings were made in an atmosphere of nitrogen. The nitrogen was carefully purified and the dew point was lowered by passing the gas through a heat exchanger coil immersed in a bath of liquid nitrogen.

TABLE I. *Source of supply or method of preparation of raw materials*

ZrC.....	A. D. Mackay Company, New York, N. Y.
CbC.....	Fansteel Metallurgical Corporation, North Chicago, Illinois
TiC.....	Titanium Alloy Manufacturing Division, National Lead Company, Niagara Falls, N. Y.
VC.....	A. D. Mackay Company, New York, N. Y.—pure grade.
ZrN.....	Prepared by firing either zirconium hydride (from Metal Hydrides, Inc., Beverly, Mass.) or zirconium metal powder (from Foote Mineral Company, Philadelphia, Pa.) in pure dry nitrogen at 2000°C.
CbN....	Prepared by firing columbium metal powder (from Fansteel Metallurgical Corporation, North Chicago, Ill.) in pure dry nitrogen at 1870°C.
TiN.....	Metal Hydrides, Inc., Beverly, Mass., and also prepared by firing titanium hydride in pure dry nitrogen at 1870°C.
VN.....	Prepared by firing vanadium metal powder (95.5 per cent purity from Vanadium Corporation of America, New York, N. Y.) in pure dry nitrogen at 1650°C.

Precautions were taken to minimize contamination of the specimens during firing. In the tungsten crucible used in the high frequency furnace two or three compacted specimens ½ inch (1.27 cm) in diameter and about ¼ inch (0.635 cm) thick were placed on a thoria support, and the bottom specimen was discarded. In the graphite furnace the bottom specimen in contact with graphite also was discarded. In addition, only the center portion of the other specimens was ground into a powder for lattice parameter measurements.

The raw materials used in this investigation were either obtained commercially or prepared in this laboratory. Table I gives the source of the materials or the method of preparation. No attempt was made to determine the purity of the various raw materials. It may be stated, however, that ZrC and VC were of the same source as those used by Norton and Mowry (3). Vanadium nitride was probably the most impure of all, because the vanadium powder, according to the manufacturer, contained about 95 per cent vanadium, 1 per cent aluminum, 0.27 per cent silicon, 0.35 per cent iron, and 0.4 per cent carbon, the balance being oxygen. No source of purer vanadium could be found, except in too small quantity and at a prohibitive price.

The x-ray diffraction measurements were carried out with a focusing camera covering a Bragg angle range from 17° to 72° and using a copper target with nickel filter. The x-ray $K\alpha$ wavelengths of copper used in calibrating the camera and calculating the lattice parameters were 1.5374 kx for α_1 and 1.5412 kx for α_2. All results are expressed in kx units.

The Lattice Parameter of the Mononitrides and Monocarbides

Several different values for the lattice parameters of nitrides and carbides may be found in the literature (5–14). The main reasons for the lack of consistency of lattice parameter measurements are probably the variation in carbon or nitrogen content and the presence of oxygen. A summary of the work of several investigators is presented in Table II, together with the results obtained in this investigation. It must be pointed out first that the values of Becker and Ebert (5), which are still listed in many tables of physical constants, have been found inexact by most of the subsequent investigators.

As far as the monocarbides are concerned, the recent results of Norton and Mowry (3) are probably the most accurate and are confirmed by the measurements made in the course of the present study (Table II).

Titanium nitride has been studied by several investigators (6, 7, 11, 12). The lattice parameter of the raw material used in this investigation agrees quite well with the value given by Dawihl and Rix (Table II), and is only slightly higher than the values found by Ehrlich, who studied the variation of lattice parameter with nitrogen content (Table II).

For columbium nitride the only parameter found in the literature is that of Becker and Ebert, which is probably not more reliable than the parameters of other nitrides and carbides reported by these investigators. The lattice parameter measured for zirconium nitride differs appreciably from that given by Van Arkel (6). No obvious reason was found for this discrepancy.

In a very complete study of the vanadium-nitrogen system recently published (14) it is shown that

the parameter of VN varies from 4.126 to 4.064 kx with the nitrogen concentration, decreasing from stochiometric down to 0.71 (Table II). The rather low value measured on the material prepared for the present study (4.097 kx) probably can be attributed to a deficiency in nitrogen. The specimens, however, were fired in an atmosphere of purified nitrogen at temperatures as high as 2450°C and no increase in parameter was noticed. Another possible reason for a low parameter is the presence of about 3.5 per cent oxygen in the vanadium powder used for the preparation of the nitride. According to Dawihl and Rix, however, (see Table II) the effect of oxygen on the lattice parameter of VN is not very significant, since there is a difference of only 0.006 kx between specimens containing 3.4 and 10.1 per cent oxygen. Although the main conclusions of the present investigation would not be affected by the presence of oxygen in VN, it should be pointed out that the lattice parameter entered in Table II is that of the particular material used in the experiments and not the true parameter of pure vanadium nitride.

TABLE II. *Lattice parameters of carbides and nitrides (in kx units)*

	Becker, Ebert (5)	Van Arkel (6)	Dawihl, Rix (7)	Scharz, Summa (8)	Kovalskii, Umanskii (1)	Burgers, Basart (9)	Brantley (10)	Norton, Mowry (3)	This investigation
ZrC	4.76	4.73	—	—	4.6734	4.6877	—	4.680	4.685
CbC	4.40	—	—	—	4.4584	—	—	4.461	4.461
TiC	4.60	4.26	4.31 4.316	4.302	4.4442	—	4.320	4.323	4.323
VC	4.30	—	4.159 4.137	—	4.3186	—	—	4.161	4.160
	Becker, Ebert (5)	Van Arkel (6)	Dawihl, Rix (7)	Brager (11)	Ehrlich (12)	Epelbaum, Breger (13)	Hahn (14)		This investigation
ZrN	4.63	4.61	—	—	—	—	—		4.567
CbN	4.41	—	—	—	—	—	—		4.370
TiN	4.40	4.23	4.236	4.235	4.234[c] 4.213[d]	—	—		4.237
VN	4.28	—	4.133[a] 4.129[b]	—	—	4.129	4.126[e] 4.064[f]		4.097[g]

[a] 18.3% N—0.7% C—3.4% O.
[b] 18.4% N—0.1% C—10.1% O.
[c] TiN.
[d] $TiN_{0.42}$.
[e] VN.
[f] $VN_{0.71}$.
[g] Low parameter, probably because of oxygen.

All the pairs of nitrides, with the exception of VN-ZrN, showed a single phase with a variation of lattice parameter approximately following Vegard's law (Fig. 1). The x-ray diffraction patterns of most nitride solid solutions were quite sharp, with well-resolved doublets. Only in the case of CbN-VN were the back reflection lines very weak and not resolved into doublets. Since this condition was probably due to a lack of homogeneity resulting from incomplete diffusion, attempts were made to refire the specimens at higher temperature. The specimens containing more than 50 per cent VN showed evidence of decomposing and melting above 2225°C and the results of x-ray diffraction measurements were inconsistent. Some of the specimens containing 20 to 30 per cent VN were refired at 2400°C, but no improvement was noticed in the sharpness of the powder patterns. It is, therefore, not obvious that the lack of diffusion is the only reason for the broadness of the x-ray diffraction lines in the system VN-CbN, and other factors such as the presence of impurities (mostly oxygen) may have some effect on the observed line broadening.

As stated above, the system VN-ZrN is the only nitride system in which the solubility is not complete. Since no lattice parameter change could be detected with the addition of ZrN to VN, the solubility of the two nitrides is probably smaller than 1 per cent on

Results on Binary Systems

Nitride Pairs

The conditions under which the various binary nitride systems were sintered are summarized in Table III. The results of x-ray diffraction measure-

the VN side. On the ZrN side a small change in lattice parameter was measured and the solubility of VN in ZrN is approximately 5 per cent.

All the results obtained on the binary systems involving the mononitrides are exactly similar to those obtained by Norton and Mowry on the corresponding monocarbides. It is clear that in both cases the size factor controls the relative solubility of the components. The more detailed discussion of this conclusion given in Reference 3 for the carbides may be extended word for word to the nitrides.

TABLE III. *Binary nitride systems*

System	Firing procedure	X-ray pattern
ZrN-CbN	4 hours, 2550°C, graphite furnace 90% CbN melted at 2600°C	doublets resolved
ZrN-TiN	3 hours, 2600°C, graphite furnace	doublets resolved
ZrN-VN	4 hours, 2375°C, graphite furnace 50%—4 hours 2550°C	no reaction
CbN-TiN	4 hours, 2550°C up to 50% CbN 4 hours, 2575°C above 50% CbN graphite furnace	doublets resolved
CbN-VN	2 hours, 2125°C and check runs at 2225°C, high frequency furnace	doublets not resolved
TiN-VN	2 hours, 2425°C 40–70% VN 2 hours, 2125°C other specimens, graphite furnace Reaction incomplete after 2 hours at 2325°C for specimens from 40 to 70% VN	doublets resolved

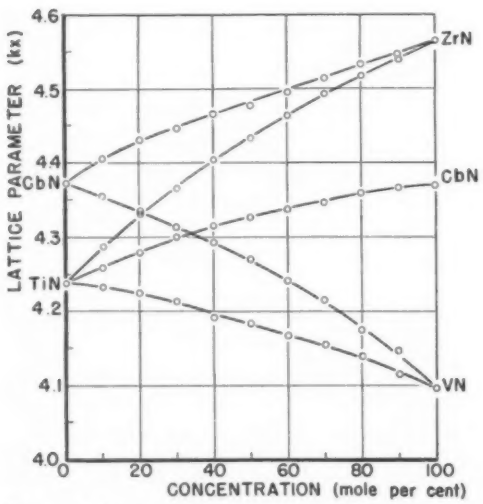

FIG. 1. Lattice parameter vs. composition curves for nitride pairs.

Nitride-Carbide Pairs

The sintering conditions of the systems involving nitride-carbides are summarized in Table IV. Since the firing of the specimens was carried on in nitrogen, it was first necessary to check the stability of the various carbides in such atmosphere at high temperature. The four carbides were heated in nitrogen up to the maximum temperature they would reach when mixed with the nitrides, namely 2650°C for TiC, 2550°C for CbC, 2325°C for VC, and 2400°C for ZrC. After firing the lattice parameters of titanium, columbium, and vanadium carbides were unchanged, and it was concluded that the carbides were stable in a nitrogen atmosphere, at least up to the maximum firing temperature.

TABLE IV. *Binary carbide-nitride systems*

System	Firing procedure	X-ray pattern
TiC-VN	2 hours, 2125°C, high frequency furnace	doublets resolved
TiC-TiN	4 hours, 2425°C, graphite furnace	doublets resolved
TiC-CbN	4 hours, 2550°C, graphite furnace incomplete reaction at 2425°C	doublets resolved
TiC-ZrN	1 hour, 2650°C or 2 hours, 2600°C, graphite furnace incomplete reaction at 2425°C	doublets not resolved
CbC-VN	2 hours, 2375°C, high frequency furnace incomplete reaction at 2250°C	doublets not resolved
CbC-TiN	4 hours, 2550°C, graphite furnace incomplete reaction at 2075°C	doublets resolved
CbC-CbN	2 hours, 2125°C, high frequency furnace	doublets resolved
CbC-ZrN	2 hours, 2450°C, graphite furnace 3 hours, 2550°C, graphite furnace	no reaction
VC-VN	2 hours, 2200°C, high frequency furnace	doublets resolved
VC-TiN	2 hours, 2325°C 70–90% VC 2 hours, 2250°C other specimens high frequency furnace incomplete reaction at 2100C	doublets resolved
VC-CbN	2 hours, 2250°C, high frequency furnace	doublets not resolved
VC-ZrN	3 hours, 2450°C, graphite furnace	no reaction

The x-ray diffraction patterns of ZrC after firing were rather diffuse, but yet sufficiently clear to detect a definite decrease in lattice parameter. This change in lattice parameter, however, was not consistent from test to test. The fact that the lattice parameter of ZrC decreased by firing in nitrogen is enough evidence, however, to assume that nitrogen replaced some of the carbon atoms in the structure, and ZrC may be considered as unstable in the presence of nitrogen at high temperature. In view

of this fact, the study of the binary systems of zirconium carbide with the nitrides was not pursued.

The results of x-ray diffraction measurements of the carbide-nitride systems are shown in Fig. 2, 3, and 4. The systems formed with titanium carbide and the four nitrides are of the complete miscibility type and the variation of lattice parameter with concentration follows approximately Vegard's law

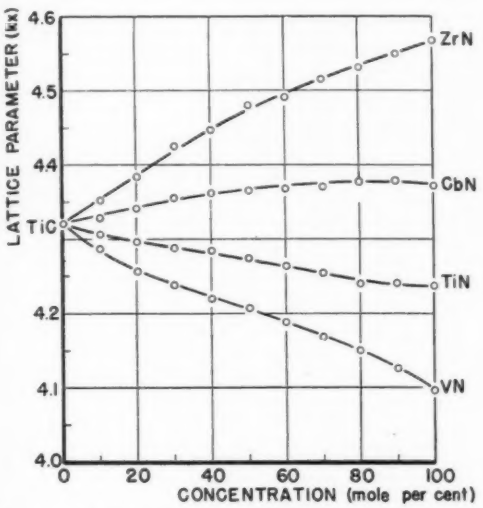

FIG. 2. Lattice parameter vs. composition curves for titanium carbide-nitride systems.

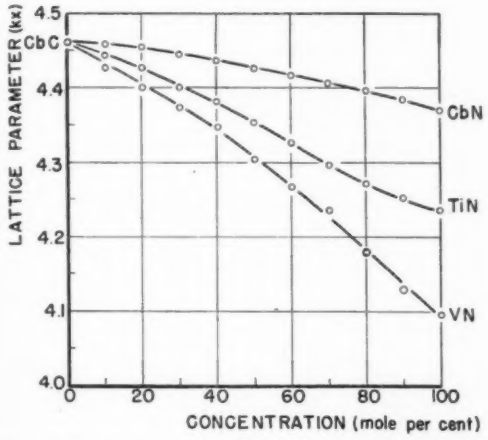

FIG. 3. Lattice parameter vs. composition curves for columbium carbide-nitride systems.

(Fig. 2). The x-ray diffraction patterns of these systems were sharp, except for TiC-ZrN (Table IV) in spite of the fact that these mixtures were fired at very high temperature (2650°C).

The systems involving columbium carbide and three of the nitrides (VN, TiN, and CbN) are also of the solid solution type, with an almost linear variation in lattice parameter (Fig. 3).

The system CbC-ZrN, for which complete miscibility would be predicted by application of the size factor rule, did not seem to have achieved equilibrium even at the highest firing temperature (2550°C). The patterns were very diffuse, but the lines of the two constituents could be identified. Higher firing temperatures were not used because the 50-50 specimens melted around 2600°C. There is no obvious reason for the lack of reactivity in this system at the present time. The size factor cannot be invoked in this case, since it is more favorable than in the CbC-VN system of the same series, for which complete miscibility was observed.

The results obtained with the four systems containing vanadium carbide and the nitrides are in agreement with the size factor rule. With VN, TiN, and CbN, vanadium carbide formed solid solutions (Fig. 4). With ZrN the solubility, if any, is very restricted and this sytem is probably very similar to the systems VC-ZrC (3) and VN-ZrN (see section on nitride pairs above).

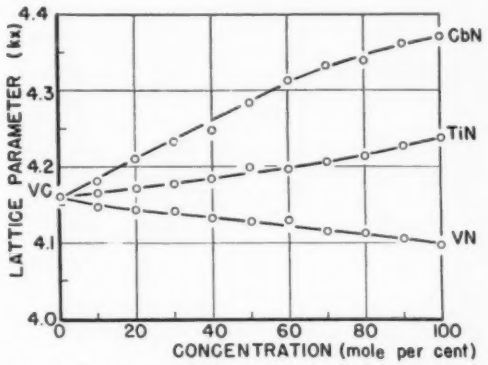

FIG. 4. Lattice parameter vs. composition curves for vanadium carbide-nitride systems.

CONCLUSIONS

1. The binary nitride systems ZrN-CbN, ZrN-TiN, CbN-TiN, CbN-VN, and TiN-VN form continuous series of solid solutions.

2. In the binary nitride system ZrN-VN the solubility of ZrN in VN is less than 1 per cent and the solubility of VN in ZrN is approximately 5 per cent.

3. The following carbide-nitride systems form continuous series of solid solutions: TiC with VN, TiN, CbN, and ZrN; CbC with VN, TiN, and CbN; and VC with VN, TiN, and CbN.

4. The system VC-ZrN shows very limited solubility.

5. In the system CbC-ZrN no reaction took place at a firing temperature of 2450°C.

6. The carbide-nitride binary systems involving ZrC were not investigated because ZrC decomposes when fired in a nitrogen atmosphere at high temperature.

It may be concluded, in general, that the solubility in the nitride and nitride-carbide binary systems is controlled by the atomic size factor rule (No. 1, 2, 3, and 4 above). The only exception to this rule is the system CbC-ZrN for which, in the experiments performed so far, no solubility could be observed.

ACKNOWLEDGMENT

This work was done at the Jet Propulsion Laboratory, California Institute of Technology, under contract number W-04-200-ORD-455 with the Army Ordnance Department, Washington, D. C. The authors wish to thank this agency for the permission to publish the results of this investigation.

Any discussion of this paper will appear in a Discussion Section, to be published in the June 1951 issue of the JOURNAL.

REFERENCES

1. A. E. KOVALSKII AND Y. S. UMANSKII, *J. Phys. Chem., U.S.S.R.*, **20,** 769 (1946).
2. H. NOWOTNY AND R. KIEFFER, *Metallforschung*, **2,** 257 (1947).
3. J. T. NORTON AND A. L. MOWRY, *Trans. Am. Inst. Mining Met. Engrs.*, **185,** 133 (1949).
4. W. HUME-ROTHERY, "The Structure of Metals and Alloys," Institute of Metals Monograph and Report Series No. 1 (1939).
5. K. BECKER AND F. EBERT, *Z. Physik*, **31,** 268 (1925).
6. A. E. VAN ARKEL, *Physica*, **4,** 286 (1924).
7. W. DAWIHL AND W. RIX, *Z. anorg. u. allgem. Chem.*, **244,** 191 (1940).
8. M. VON SCHARZ AND O. SUMMA, *Z. Elektrochem.*, **38,** 743 (1932).
9. W. G. BURGERS AND J. C. M. BASART, *Z. anorg. u. allgem. Chem.*, **216,** 209 (1934).
10. L. R. BRANTLEY, *Z. Krist.*, **77,** 505 (1931).
11. A. BREGER, *Acta Physicochim. U.R.S.S.*, **10,** 593 (1939).
12. P. EHRLICH, *Z. Elektrochem.*, **45,** 362 (1939).
13. V. EPELBAUM AND A. Kh. BREGER, *Acta Physicochim. U.R.S.S.*, **13,** 600 (1940).
14. H. HAHN, *Z. anorg. Chem.*, **258,** 58 (1949).

Improvements in Methods for the Reduction of Zirconium Chloride with Magnesium[1]

W. J. Kroll, W. F. Hergert, and L. A. Yerkes

Northwest Electrodevelopment Laboratory, Bureau of Mines, U. S. Department of the Interior, Albany, Oregon

ABSTRACT

It is shown that gaseous zirconium chloride can be piped to a reactor containing magnesium and that the reaction salts can be repeatedly tapped to make room for more magnesium, in view of continuing the reduction. This permits using the crucible capacity more fully, with consequent reduction of the production cost.

Experiments indicate that part of the magnesium used for the reduction of zirconium chloride can be replaced with sodium. The advantages and disadvantages of this proposition are discussed.

Cast iron is a better crucible material than mild steel when used in contact with hot zirconium. A layer of zirconium carbide is formed by zirconium diffusion, which helps reduce iron contamination.

Introduction

The Bureau of Mines process (1–4) for the reduction of gaseous anhydrous zirconium chloride with magnesium under helium has developed within about 4 years from the test tube to a pilot plant producing regularly 600 pounds of metal a week. The improvements described below concern only the three following phases of this method: refining of the raw chloride, its reduction, and separation of the magnesium chloride from the zirconium sponge. The following subjects and basic principles are discussed before describing the experiments:

1. Purification of, and iron removal from, raw zirconium chloride without the densification operation.
2. Transfer of purified gaseous chloride from a central gas producer, through heated pipes and a valve, to the reactor.
3. Tapping the salts produced in the reduction and refilling the crucible with magnesium under a helium-gas seal.
4. New crucible materials that do not react as readily with zirconium as does iron.
5. Use of a mixture of magnesium and sodium as a reducing agent.

Purification and Transfer of Gaseous Zirconium Chloride, Salt Tapping, and Magnesium Refilling

Items 1 to 3 are discussed as a unit. Purification is accomplished by reducing the trivalent iron contained in the raw chloride with hydrogen, and subliming the zirconium chloride. The salt is densified by condensing it on water-cooled coils which are suspended from a top that floats on a lead-alloy seal to exclude air. The chloride residue contains iron, mainly as the less-volatile dichloride, as well as zirconium oxide and other minor impurities. The vaporization operation is comparatively rapid, requiring less than 24 hours on a pilot-plant scale. Since the reduction lasts about twice as long, it is evident that the purification vessel is used only half the time. For steady plant operation, it would be advantageous to have a large central zirconium chloride gas producer and to pipe the gas to any available reactor. This would eventually also permit purifying the gas more thoroughly—for instance, by filtering it through steel wool for oxide-dust removal.

Simultaneously, the sublimation of zirconium chloride and its condensation on a cool surface could be avoided and the chloride gas could be used directly for the reduction with magnesium. This presumes that iron trichloride can be reduced with hydrogen within the solid raw chloride before sublimation starts.

Elimination of the floating top in the reduction phase, possible with this procedure, has several other advantages. First, the reduction vessel can be shortened considerably because of the absence of a solid block of dense chloride that obstructs the space above the crucible. This gives direct access to the reaction crucible for convenience in rabbling its content and breaking down any crusts formed. Also, refilling with more magnesium, after tapping the salts, is made easy. A small lead-alloy safety valve can be used to relieve any pressure build-up within the reaction vessel. The top itself, provided with a water-cooled rubber gasket, may be bolted to the shell. In this way, the floating top with its large

[1] Manuscript received February 16, 1950. This paper prepared for delivery before the Cleveland Meeting, April 19 to 22, 1950.

lead-alloy seal can be eliminated. The pyrophoric gas-phase reaction product (3) drops back in the bath where it is reduced completely to metal with liberation of magnesium chloride. This may increase the recovery of zirconium by a few per cent.

The possibility of continuing the run, after tapping the salts, offers considerable economic advantages. The volume of the sponge within the crucible does not amount to more than one-eighth of the total, and the crucible, after removal of the salts, appears almost empty. The space available for the sponge in the reduction could be greatly increased by emptying the salts once or even twice and continuing the reduction each time with more magnesium and gaseous chloride. The reduction time would, of course, be extended, but the heating and cooling periods would remain practically the same for a much larger output. The same time saving per pound of sponge produced could be found in the next step, which is the salt separation. The cost for cleaning the inner parts of the retort would be reduced in a similar way.

This proposition necessitated investigation of the following subjects: construction of a new reactor arrangement for tapping the fused magnesium chloride after the reduction, and designing new means for filling in fused magnesium in view of continuing the run.

Crucible Materials

Use of a metal or alloy that could be heated safely beyond the 925°C now possible for zirconium in contact with iron is desirable for shortening the reaction time. Similar advantages would be derived in the vacuum-retort process, where the salt removal could be completed more rapidly or more efficiently at higher temperature, while the sponge would be less pyrophoric because of better sintering. The eutectics of various metals with zirconium were investigated separately, and it was found that silicon and chromium, which form eutectics above 1300°C with zirconium, might be recommendable. However, a 14 per cent silicon-iron alloy proved to be too brittle, and a low-carbon, 65 per cent ferrochrome could not be cast free of pores. Plain cast iron was considered, especially the nodulized graphite type, and it was found to be quite successful because the zirconium does not penetrate beyond the graphite barrier. Other carbon-bearing iron alloys might also work, but the cost would be higher. Carbon lining was not considered because of brittleness, possible gas content, and diffusion into iron above 900°C.

Sodium Addition

Sodium cannot be used readily at atmospheric pressure for the reduction of zirconium or titanium chloride because of its low boiling point of 880°C. Also, an excess of sodium is needed, but this would cause trouble in the removal of the salt from the sponge. The product, sodium chloride, melts at 800°C, leaving only 80°C as a temperature margin within which to operate. This margin can be extended upward by the use of pressure vessels, and the "Hunter" bomb methods were current practice until recently. The limitations of these methods have been stressed before (5). Considerable progress was made in the use of sodium by Freudenberg-Scheideanstalt (6) who tried to extend the temperature margin in titanium reduction at atmospheric pressure by lowering the melting point of the salt with KCl additions. For zirconium, the chloride gas could be bubbled into a KCl bath covered with fused sodium, under inert gas. The lowest melting point in the NaCl/KCl series is 663°C at 50 mole per cent. Such salt composition can, of course, be maintained during the whole reduction run only by addition of KCl. This type of process might yield malleable zirconium or titanium sponge if precautions are taken to obtain an oxide-free KCl bath since oxide would contaminate the sponge produced. Production of an oxide-bearing titanium by this method is shown by the fact that a sample of sponge made in this manner yielded brittle metal when melted in a vacuum arc. When melting KCl in air, oxygen may replace its chlorine to a small extent (7). Moisture trapped in the chloride crystals or present in the air may form potassium oxide and hydrochloric gas. After fusing KCl in air, it gives a slightly alkaline reaction in water, showing the formation of oxide. This is true with many chlorides (8). Despite the fact that it is possible to produce an oxide-free KCl bath—for instance, by fusion of carefully vacuum-dried chloride under helium or by reconditioning an oxide-bearing bath of this salt with CCl_4 or carbon plus chlorine—the use of KCl as a flux to increase the margin of the operation temperature does not seem reasonable, since the flux does not contribute anything to the reduction and subtracts much crucible capacity. It is more logical to produce an oxide-free flux directly from some additional reducing agent, e.g., lithium, potassium, calcium, or sodium. The first two are expensive and calcium produces a low vapor pressure salt that cannot readily be removed by vacuum evaporation at elevated temperature. Sodium and magnesium do not alloy appreciably and sodium may replace part of the magnesium in view of producing a readily fluxing mixture of $NaCl/MgCl_2$. The equilibrium diagram of these series is given by Klemm (9). Calculation shows that a 24 Na-76 Mg mixture reduces the melting point of the salts from 714°C, the melting point of magnesium chloride, to 650°C, the melting point of magnesium. Also, a 74.2 Na-25.8 Mg mixture produces mixed

salts melting at 650°C. The eutectic salt melting point of 450°C is obtained with a 58.8 Na-41.2 Mg mixture. Thus any metal mixture containing 24.0 to 74.2 per cent Na brings the melting point of the resulting salts down below that of magnesium (650°C).

Another advantage of using such mixtures arises from the fact that the heat conductivity of NaCl is about twice that of $MgCl_2$. Consequently, hot spots are not liable to occur as readily within the reaction crucible.

The easy fusibility of the salt mixture presents an advantage in salt removal by tapping and in the vacuum-distillation step. With $MgCl_2$ as reaction product, accretions form in the vacuum retort in the area of the water jacket. These accumulations of salt become hot enough to resublime to the upper part of the retort, and the pressure build-up of the gaseous chloride interferes with the removal of the chloride entrapped in the sponge. However, a eutectic mixture of $NaCl/MgCl_2$ runs further down into the collector can from which it does not evaporate because of the lower temperature.

Lowering the melting point of the salt mixture below 650°C also permits an early start of the reaction because solid-salt crusts do not form above the melting point of magnesium. Sodium itself starts reacting below the melting point of the eutectic and solid crusts of NaCl supposedly form at this low temperature. However, sodium communicates the heat of its reaction with $ZrCl_4$ to the solid magnesium, thus contributing heat to the fusion of this reagent and speeding up the reaction process as a whole.

Another advantage in the use of a sodium addition is the fact that the resulting salts are much less hydroscopic than pure magnesium chloride, which makes handling them in air easier.

The heats of formation of solid Na, Mg, and $ZrCl_4$ are 98.4, 153.2, and 269.0 kg-cal, respectively. When $ZrCl_4$ is reduced with Na or Mg, there are 124.6 and 37.4 kg-cal liberated. Therefore, the reaction of Na and $ZrCl_4$ is much more exothermic than the one with Mg. This also appears from the fact that Na can be used as a reducing agent for $MgCl_2$ with evolution of 43.6 kg-cal. Experimentally, this reaction is not reversible despite the fact that Na is more volatile than Mg. As long as $MgCl_2$ is present, no free Na can appear in the reaction mixture even in a good vacuum. The Na reacts first when a mixture of both metals is used.

The excess heat of reaction with Na as a reducing agent and the volatility of this metal limit its use even in mixture with Mg in the reduction of $ZrCl_4$ and accentuate the heat-dissipation problems. Sodium at its boiling point, 880°C, disperses in the reaction room and condenses on cool walls. Gaseous $ZrCl_4$ reacts outside the crucible wherever vaporized sodium has condensed. Sodium is more expensive than Mg per equivalent, and the costs for the reducing agent would be increased by a factor of 1.7 when using Na instead of Mg. Also, the mixed salts obtained when reducing with a Na-Mg mixture have a lower value than pure $MgCl_2$, if these salts were to be used as a feed in a fusion electrolysis cell in view of reclaiming chlorine and Mg.

The lower specific gravity of the NaCl reduces the capacity of the equipment seriously. It may also cause larger amounts of fused magnesium to remain entrapped in the sponge within the salt, the uplift in the low-density salt bath being lower. The lower vapor pressure of the NaCl, which at 925°C is about half that of $MgCl_2$, might cause trouble in the salt separation when evaporating in a vacuum. If the available vapor-pressure data (10) are correct, one might expect that NaCl would tend to remain entrapped in the sponge to a larger degree than $MgCl_2$.

It is reasonable to conclude that replacing about 12 per cent by weight of Mg with the equivalent of Na would fulfill the required purpose. Higher additions, up to the formation of the $NaCl/MgCl_2$ eutectic (mp 450°C), would ease salt tapping; but with more sodium it is quite certain that, on an industrial scale, difficulties will arise from the low boiling point of the metal, aggravated by the fact that much more heat is developed when $ZrCl_4$ is reduced with this reagent than when Mg is used.

The possibility of reacting gaseous Na with $ZrCl_4$ gas was not considered because in such a process the operation margin is too narrow, since Na boils at 880°C, and Fe alloys with Zr at 940°C leaving only 60°C as safety limit. Cast iron or graphite as materials of construction for the reactor would give more leeway as to the upper temperature of reduction, but no advantages are apparent over reduction below the boiling point of sodium. Similar considerations apply to the use of gaseous magnesium as reactant.

Some advantages could be derived from the addition of fluxing agents such as NaCl or KCl in the reduction of zirconium chloride with magnesium, providing these salts are free of oxide. The disadvantages of this procedure have been stressed above.

Experimental

Purification of Raw Chloride, Transfer of Purified Gaseous Chloride to Reaction Vessel, Tapping of Salts, and Refilling of Reaction Crucible with Magnesium

The apparatus used is shown in Fig. 1. It consists essentially of a $ZrCl_4$ gas producer (2, 3) reactor, heated pipe (7), and heated stopcock (8). During the run all parts are heated above 331°C, the condensation temperature of $ZrCl_4$.

The reactor contains the reaction crucible (16) with the magnesium. The top cover is provided with a water-cooled rubber gasket (12). A small lead-seal safety valve is arranged in the center of the cover (14). It is heated separately with an electric furnace. Pressure built up in the gas producer can be released through this safety valve indicating that the passage through the heated pipe and stopcock is free. Gas producer and reactor are connected by way of a pipe, cockstop, and two flanges (9) bolted tightly to a metal asbestos joint. Helium can be admitted to the reactor with a needle valve whenever needed,

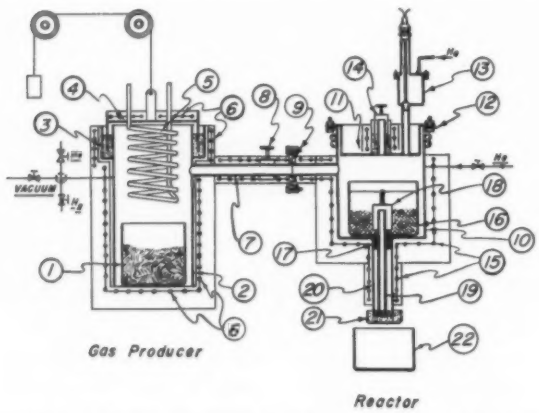

FIG. 1. Reaction apparatus—1. nickel can with raw zirconium chloride powder, 2. iron shell of the gas producer, 3. trough with lead-alloy seal, 4. floating top, 5. water-cooled coils, 6. heating elements, 7. heated transfer pipe for gaseous chloride, 8. heated stopcock, 9. heated flange, 10. heat-resisting steel shell of the reactor, 11. inserted top, 12. water-cooled rubber gasket and bolts, 13. magnesium ladle held under helium, 14. heated lead-alloy safety valve, 15. heating elements of the reactor, 16. reaction crucible with siphon, 17. threaded joint, 18. siphon, 19. siphon outlet, 20. drain pipe, 21. lead joint, 22. mold for the salts.

especially in the moment when magnesium is charged through the lead-seal valve.

The tapping device is built in the reaction crucible. It is essentially a siphon (18) constituted of a sleeve, welded tight on one end, and inserted over the tapping pipe. The crucible with the tapping siphon is screwed into the center of the reaction vessel. The outlet of the siphon is inserted in a larger drain pipe (20) or discharge tube that is welded in the center of the reactor. It can be heated externally (15). A small pot with lead is used to plug the lower end of the discharge (21). After the opening of the discharge tube is freed by removing the lead seal, pressure is applied to the reaction vessel by bleeding helium into it, while the stopcock between this vessel and the gas producer is sealed. The fused $MgCl_2$ is now forced into the siphon, through which it empties into a mold that is held in readiness below the drain pipe.

The following procedure was used. A double charge, 4800 grams, of crude, anhydrous $ZrCl_4$ was placed in the purification vessel and a regular 600-gram charge of magnesium in the reaction crucible. After the lead-alloy seal was frozen, the entire system of the two connected vessels was evacuated and the stopcock valve in the heated transfer pipe closed. The reactor vessel was back-filled with helium, the purification vessel with hydrogen.

The temperature of the purification vessel was raised to 250°C and maintained for a minimum of 2 hours. At 30-minute intervals the hydrogen and any hydrogen chloride formed were evacuated and replaced with fresh hydrogen. After the final evacuation, the purification vessel was back-filled with helium and the lead seal around the lid melted.

In the meantime, the reaction vessel temperature had been slowly increased to a temperature just below the melting point of $MgCl_2$ in preparation for the beginning of the reaction. The temperature of the purification vessel, which was now the supplier for $ZrCl_4$ gas, was increased to slightly above 330°C and the stopcock valve in the heated transfer pipe was opened. The purified gaseous $ZrCl_4$ was passed through the pipe and reacted with the magnesium in the regular manner at a temperature of approximately 800°C. After 4 hours, a static condition in the $ZrCl_4$ gas pressure indicated that most of the available magnesium had reacted.

The drain or salt-tapping pipe was heated electrically to 800°C and the stopcock in the transfer pipe closed. A slight positive pressure of helium was maintained in both systems at all times. When the various thermocouples, located at important points on the apparatus, indicated the proper temperatures, the lead seal on the drain pipe was removed, and the helium pressure in the reaction vessel was boosted sufficiently to force the salt through the siphon arrangement in the reaction crucible and out into an open pot. Immediately after the salt ceased draining, the lead seal was replaced and allowed to freeze and reseal the drain pipe opening.

At this point in the experiment, the reaction crucible contained approximately the same amount of zirconium sponge normally produced in a single batch zirconium operation of this size, but with only about 15 per cent of the salt normally present and, of course, a small amount of unreacted magnesium. Since the temperature was maintained at 800°C, it was a simple matter to introduce a second charge of 600 grams of molten magnesium from a special helium-sealed ladle with bottom pour, open the stopcock in the transfer pipe, and continue the reaction with the remaining charge of purified gaseous zir-

conium chloride. In about 4 hours, the reaction was again considered complete, and again the salt formed was drained in the same manner as described above. The apparatus was allowed to cool to room temperature under helium and the crucible containing the double batch of zirconium sponge, some undrained salt, and excess magnesium was removed from the reaction vessel, placed in the vacuum retort, and given the regular vacuum-distillation treatment.

In this experiment, 1800 grams of zirconium metal were produced as compared to 900 grams in a similar single-stage operation not involving salt tapping and addition of magnesium. The zirconium sponge produced analyzed less than 0.09 per cent iron, indicating that satisfactory iron removal is possible if the raw chloride is given the proper hydrogen treatment and sublimed directly through the transfer pipe into the reaction vessel and reacted with the magnesium.

The first salt tapping gave 1350 grams of $MgCl_2$ and the second or final tap gave 1600 grams. The remaining $MgCl_2$ and excess magnesium were removed in the vacuum retort.

As can be seen from this experiment, it was possible to eliminate the iron of the raw chloride by reducing the $FeCl_2$ with hydrogen at about 250°C without subliming the chloride to water-cooled coils. It was easy to tap the salts repeatedly and to refill the crucible with magnesium. In a number of experiments the output of the crucible was doubled in this way.

Cast Iron Crucibles

As indicated previously, cast iron was found suitable as crucible material, resisting the action of hot zirconium very well. Comparative runs, made with a plain iron crucible and one of cast iron in which the temperature inside the salt separation retort was held at 950°C, resulted in the formation of large quantities of "tears" in the first case, while the cast-iron crucible yielded a sponge that had less than 0.1 per cent iron. The graphitic and combined carbon contained in the cast iron form a barrier of zirconium carbide, and only the free iron present at the surface can react with the zirconium. The highest temperature at which cast-iron crucibles can be used depends on the creep strength of cast iron. Creeping was observed with large cast-iron pots held at 950°C for 10 hours in pilot-plant operation. Alloying may reduce this creeping. Cast-iron crucibles have to be heavier than those made of mild steel. The experiments have shown conclusively that the temperature in the reduction as well as in the salt separation can safely be increased by about 50°C above that used when operating with a mild steel crucible. A runaway in the reduction does not result in piercing the crucible by reaction of the sponge with the iron, because the unfusible carbide layer that is formed blocks the penetration of zirconium into the iron wall.

Use of a Mixture of Magnesium and Sodium as a Reducing Agent

A series of fused mixtures of sodium and magnesium was reacted in the experimental apparatus described above. The following mixtures of sodium and magnesium were used (in per cent):

5 Na-95 Mg 50 Na-50 Mg
15 Na-85 Mg 80 Na-20 Mg
30 Na-70 Mg

To this a 20 per cent excess of reducing agent as magnesium was added.

It was observed that the reaction with Na started at temperatures as low as 500°C. Even with the highest Na addition, the heat evolution was not excessive, but it is questionable whether heat-dissipation problems might not arise when operating on a commercial scale. The batches with Na contents high enough (more than 15%) to produce large quantities of salt eutectic showed evidence of the fact that salt eutectic melted out in the salt separation retort long before the distillation or sublimation of residual salt and magnesium started. The fusible salt collected in the can arranged below the inverted reaction crucible and secondary evaporation from this salt was not observed.

The reaction between sodium and magnesium chloride is not reversible under the conditions prevailing in the salt-distillation procedure. Even with the highest sodium additions used, no sodium was ever found in the distillate from the salt separation. One would have expected that sodium could be reduced from its chloride by the excess magnesium in a vacuum, since sodium is much more volatile than magnesium. These facts show that if there is any vapor pressure of sodium over the reaction mixture of $Na + MgCl_2$, it must be below the order of 1μ at 925°C, at which pressure and temperature most distillations were carried out.

The experiments indicate that sodium can be used to replace magnesium in the reduction of anhydrous zirconium chloride. Pilot-plant operation will have to show whether the disadvantages in using this reducing agent do not outweigh the advantages that may be derived from its use.

Conclusions

This investigation shows that raw zirconium chloride powder can be freed of its iron trichloride content by reduction with hydrogen at about 200°C. Sublimation of the chloride and its condensation on water-cooled coils can be omitted. The gaseous chloride can be transferred directly through a heated pipe

and stopcock to a shorter separate reaction vessel. This makes the reaction crucible readily accessible for stirring of the batch as well as for filling in fused magnesium after tapping the salts. The tapping of the magnesium chloride does not offer any difficulties. This permits using the crucible capacity for two or three consecutive reductions.

Cast iron is a better material of construction for the reaction crucible than mild steel because of a zirconium carbide barrier produced on the surface which obstructs the diffusion of iron into the zirconium and vice versa.

Sodium can be used to replace magnesium in the magnesium reduction of zirconium chloride. Mixtures of sodium and magnesium containing up to 80 per cent sodium were tested successfully. No sodium appears in the condensate of the salt-distillation furnace, showing that the reaction between sodium and magnesium chloride, which yields magnesium metal, is not reversible, even in a vacuum at 925°C.

The gaseous transfer of chloride from a gas producer to a reaction vessel, the use of sodium magnesium mixtures as a reducing agent and that of a cast-iron crucible apply quite as well to the production of titanium.

Acknowledgment

This investigation was sponsored by the Atomic Energy Commission, to which the authors extend their appreciation for permission to publish the results of this work.

Any discussion of this paper will appear in a Discussion Section, to be published in the June 1951 issue of the Journal.

REFERENCES

1. W. J. Kroll, A. W. Schlechten, and L. A. Yerkes, *Trans. Electrochem. Soc.*, **89,** 263, (1946).
2. W. J. Kroll, A. W. Schlechten, W. R. Carmody, L. A. Yerkes, H. P. Holmes, and H. L. Gilbert, *Trans. Electrochem. Soc.*, **92,** 99, (1947).
3. W. J. Kroll, C. T. Anderson, H. P. Holmes, L. A. Yerkes, and H. L. Gilbert, *J.* (*and Trans.*) *Electrochem. Soc.*, **94,** 1, (1948).
4. W. J. Kroll and W. W. Stephens, "Pilot Plant for the Production of Malleable Zirconium," A.I.M.E. meeting, New York (February, 1950).
5. W. J. Kroll, *Trans. Electrochem. Soc.*, **78,** 35, (1940).
6. H. Freudenberg and Deutsche Gold und Silberscheideanstalt, "Titanium," U. S. Pat. 2,148,345, Feb. 21, 1939. Also, J. S. Smatko, "Titanium Metal Produced by Degussa," FIAT Final Report No. 798 (May 15, 1946).
7. "Gmelin, Handbuch der anorganischen Chemie," 8th Edition, System No. 6, Chlorine, p. 221, Verlag Chemie, Berlin (1927).
8. *Ibid.*, page 99.
9. W. Klemm and P. Weiss, *Z. anorg. Chem.*, **245,** 281, (1940).
10. C. G. Maier, Bureau of Mines Tech. Paper 360 (1925).

Preparation of Ductile Vanadium by Calcium Reduction[1]

R. K. McKechnie and A. U. Seybolt

Knolls Atomic Power Laboratory, General Electric Company, Schenectady, New York

ABSTRACT

A method is described for preparing ductile vanadium of about 99.5 per cent purity by calcium reduction of vanadium pentoxide. On the scale investigated, metal so reduced collects in a solid regulus weighing about 100 grams and can be cold worked directly from the button to thin foils without annealing. Oxygen is the principal cause of embrittlement in vadium produced by this technique.

Introduction

Of the metals in the fifth group of the periodic table of the elements, vanadium has been least studied metallurgically, and very few properties of the pure metal have been reported. Because of this lack of information an investigation was initiated to produce vanadium and to study its properties. As a preliminary step, some research on the reduction of the metal was necessary because vanadium was not available commercially in a form sufficiently pure to be ductile. The following is a report of the metal-preparation phase of this work.

While there appears to be very little known regarding the properties of the pure metal, there is moderately extensive literature dealing with the reduction of the metal from its compounds, particularly halides and oxides. It is not necessary to review this literature in detail as this was done by Van Arkel (1) in 1933 and more recently by Pearson (2). Pearson's review serves to point up the fact that little has been published since the review of Van Arkel, the state of vanadium reduction being essentially as described by him. All of the various methods used appear to have yielded a powdered or granular product, usually heavily contaminated with oxide and sometimes other impurities. Because of the position of vanadium in the periodic table of the elements, it would be anticipated that its preparation would be attended by the same difficulties encountered with columbium which lies just below vanadium in Group V-A. That is, the danger of contamination and consequent embrittlement by oxygen, hydrogen, and nitrogen would be great, especially in the case of methods which produce a finely divided product. Van Arkel's (1) review of the various methods used to obtain metal and the results thereof amply confirm this expectation.

It seemed obvious at the start that an effort should be made to find a method of producing metal in massive form, thus tending to reduce the likelihood of gas contamination by decreasing the metal surface to volume ratio. Of the various methods outlined by Van Arkel (1), that of Marden and Rich (3) appeared to hold the most promise as it seemed to be capable of yielding a high purity product, and it is a rather simple procedure requiring materials which are readily available. In addition, it appeared that the method of Marden and Rich (3) might yield, with some modification, massive metal instead of beads or powder. This method is the calcium reduction of V_2O_5 carried out in a strong steel vessel or "bomb". These investigators considered the reaction

$$V_2O_5 + 5Ca + 5CaCl_2 = 2V + 5CaO \cdot CaCl_2.$$

It is clear that the calcium chloride plays no actual part in the reduction, but may function as it does in thorium reduction (4), i.e., as flux, fluid medium, and seal. They found the metal in the form of beads, 6 to 9 mm in diameter. These beads were very ductile, and could be hammered or rolled inside of a steel tube until they became sufficiently elongated to be worked without a steel jacket. The vanadium assay found by chemical analysis was high—between 99.4 and 100 per cent. The only impurities reported were iron and silicon which were respectively about 0.20 and 0.05 per cent by weight.

Experimental Procedure and Results

The reaction studied was

$$5Ca + V_2O_5 \rightarrow 5CaO + 2V.$$

From the data of Thompson (5), $\Delta F°$ for this reaction is about -340 kcal in the range of 450° to 600°C, while ΔH is about -350 kcal. The large amount of heat generated is sufficient to melt the vanadium (melting point about 1750°C) and allow some agglomerating into a massive form (depending upon the heat losses in the system).

It is necessary for obvious reasons to carry out this reaction in a closed container of considerable

[1] Manuscript received April 18, 1950. This paper prepared for delivery before the Cleveland Meeting, April 19 to 22, 1950.

strength, high melting point, and nonreactivity with the charge.

Materials and Equipment

The V_2O_5 used was finely divided powder of C.P. grade in the calcined or "air-dried" condition, available from several suppliers. Distilled calcium metal of high purity was obtained through the procurement services of the Atomic Energy Commission. This material was used as powder of nominal 30-mesh size, but subsequent work showed that particle size over a wide range made no appreciable difference in results.

The bombs used were made from standard 4-inch (10 cm) steel tubing of $\frac{3}{8}$-inch (0.96 cm) wall thickness, and were 11 inches (28 cm) high, welded shut

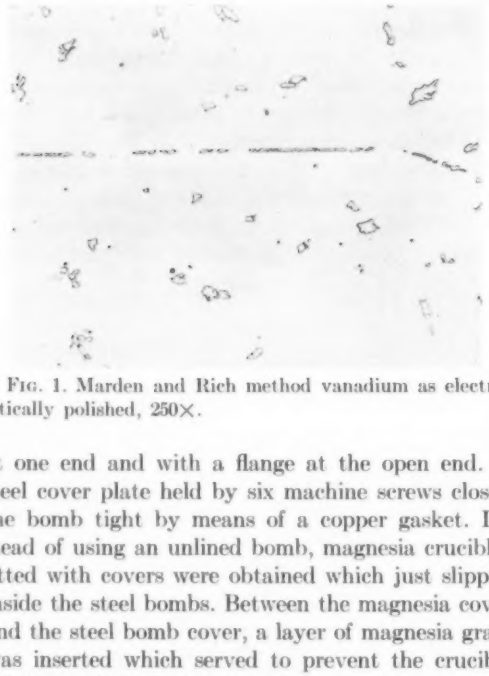

FIG. 1. Marden and Rich method vanadium as electrolytically polished, 250×.

at one end and with a flange at the open end. A steel cover plate held by six machine screws closed the bomb tight by means of a copper gasket. Instead of using an unlined bomb, magnesia crucibles fitted with covers were obtained which just slipped inside the steel bombs. Between the magnesia cover and the steel bomb cover, a layer of magnesia grain was inserted which served to prevent the crucible lid from lifting during the bomb reaction.

A 50-kw vacuum tube oscillator of about 220-kilocycles frequency was used as a power source for bomb heating. The time required for "firing" the bomb (usually about 12 minutes) could be determined by plotting the outside temperature of the bomb as a function of time. At the time of firing, the rate of heat production increased suddenly, sometimes accompanied by a cracking noise or even by a jumping of the bomb a large fraction of an inch off the fire brick upon which it rested.

Preliminary Bomb Reduction Experiments

The first attempt to produce vanadium metal in this investigation consisted of a more or less faithful reproduction of the conditions used by Marden and Rich (3).

Duplicating their charge, 175 grams of V_2O_5, and 300 grams each of ground calcium metal, and C.P. calcium chloride were mixed and placed in the magnesia crucible and the bomb assembled. Instead of placing a small quantity of sodium or potassium for gettering purposes in the bomb cavity as they did, the air was evacuated and replaced by argon. The bomb was heated to approximately 700°C at which point it "fired" as evidenced by a sudden rise in temperature of the steel wall. After cooling to room temperature, the contents of the bomb were examined and found to be substantially as described by Marden and Rich (3). The vanadium metal was in the form of beads ranging from the size of a pea down to very fine powder with the bulk of the metal in the range around $\frac{1}{8}$ of an inch (0.3 cm) in diameter. The metal recovered weighed 43 grams out of a possible yield of 98 grams, or 44 per cent theoretical yield. The pellets were very ductile and could be hammered flat without fracture.

A second charge was prepared, this time using 115 grams of iodine with an additional 30 grams of calcium to combine with the iodine. The use of iodine and other boosters for added heat in bomb reductions has been described previously (6, 7). Calcium and iodine combine directly to form calcium iodide, a reaction which is thermally initiated near 425°C, and releases about 100 kcal per mole (8). Hence, the formation of calcium iodide acts as a starting or triggering reaction, generating enough heat to start the main reaction. In addition, the calcium iodide by combining with the nonmetallic reaction products tends to lower the melting point of the slag, thus aiding in separating the dross from the metal. A noticeable improvement in yield was obtained since the amount of recoverable metal increased by 10 grams to 53 grams, or 54 per cent theoretical yield; however, the vanadium still appeared as beads and powder.

The benefits ascribed to the use of calcium chloride by Marden and Rich (3) could not be observed in this investigation. After a few more experiments varying the amount of calcium chloride in the bomb, the use of this salt was eliminated in all subsequent work since it seemed to be detrimental to the production of high yields and good consolidation of the product. However, the quality of the beads was high; a chemical assay showed a vanadium content of 99.1–99.6 per cent vanadium with a carbon content of 0.06 to 0.20 per cent. No other chemical analyses were performed.

Fig. 1 shows the typical microstructure of a bead. While there is still some uncertainty, the inclusions have been tentatively identified as vanadium car-

bide, VC. However, since VC and VN are isomorphous, there is a possibility that the so-called carbide inclusions are solid solutions of VC-VN.

Attempts to Lower the Melting Point of the Oxide Slag

In an effort to lower the melting point of the slag (mainly CaO with some CaI_2) and thus secure better settling of the reduced metal to the bottom of the bomb, aluminum metal, aluminum oxide, and mixtures of both were added, maintaining the weight of the V_2O_5 at 250 grams for most runs, and the iodine at 36 grams. The calcium oxide-aluminum oxide phase diagram (9) shows a range of composition close to 50 per cent by weight Al_2O_3 where the melting point is about 1450°C. Hence, it appeared that, if a 50–50 mixture of CaO-Al_2O_3 were present in the bomb, the melting point of the slag should be about 1450°C. These expectations were borne out, and excellent collections of the vanadium were obtained. Yields were between 82 and 97.5 per cent, giving a more or less smooth button weighing close to 130 grams. It made no difference whether the aluminum was added as metal or as oxide or both; the results were about the same. The difficulty was that the metal produced was uniformly brittle, apparently owing to aluminum contamination. The work on the addition of aluminum to the bomb charge was, therefore, discontinued and further experimentation was limited to the use of V_2O_5, calcium, and iodine in the charge.

Production of Ductile Reguli

A series of eight reductions was made using 280 grams of V_2O_5, 622 grams of calcium, and 78 grams of iodine. This amount of calcium was approximately 100 per cent in excess of that required to reduce V_2O_5 taking into account the amount needed to combine to form CaI_2, and was used in an attempt to drive the reaction as far as possible to completion. The yield in vanadium metal under these conditions occurred as a massive button or regulus which was always close to 65 per cent theoretical and weighed about 100 grams. In every case the metal was very ductile, and could be rolled directly from the as-reduced state to thin foil with no evidence of cracking. Naturally, the quality of the sheet or foil was not very good because of cold shuts and other defects attributable to lack of regular geometry in the starting material. The Vickers hardness number was about 140.

At this stage in the investigation, the original lot of V_2O_5 was exhausted and reductions were commenced on a second lot which unexpectedly yielded only brittle metal. Since no other variable in the method had been changed, it appeared obvious that some impurity not controlled in the C.P. oxide was the cause of embrittlement. The gas content of the metal was suspected at once because of the known behavior of columbium. Since a large amount of oxygen was already present in the V_2O_5, it appeared that the nitrogen or hydrogen content would be a likely source of trouble. Also, since V_2O_5 is prepared by the thermal decomposition of ammonium metavanadate (NH_4VO_3), nitrogen and hydrogen would be suspected from this source if the vanadate were incompletely converted to V_2O_5. If the ammonium vanadate were prepared in an atmosphere of insufficient oxygen content, there is danger of some of the nitrogen from the NH_3 combining with the V_2O_5 to form other nitrogen compounds (10). A moisture analysis showed that the V_2O_5 contained no detectable amount of water at 200°C. Unfortunately, none of the original lot of V_2O_5 was available for nitrogen analysis by the time it was suspected that this element in the second lot of oxide was causing embrittlement of the metal.

Nitrogen was determined by the Kjeldahl method, modified to allow the determination of nitrogen present originally as ammonia, imides, amides, and nitrates. Subsequent investigations using vanadium nitride showed that this type of nitrogen is not included in the above determination. There was little or no NH_3 nitrogen but there was about 0.15 per cent total in the other forms. This amount of nitrogen is relatively large, and efforts were made to (*a*) prepare V_2O_5 of very low nitrogen content, and (*b*) eliminate the nitrogen content from the commercial V_2O_5. After considerable experimentation, a simple treatment was devised to treat the commercial V_2O_5 in order to lower the nitrogen content to a tolerable value. This consisted of heating the oxide to 400°C in a stream of wet oxygen for a period of about 18 hours; after this treatment, the nitrogen determined by the Kjeldahl analysis fell to about 0.012 per cent, or about one-tenth of its former value.

Using the "denitrided" V_2O_5, ductile metal was produced using bomb charges similar to those described above. The brittle metal previously made from this batch had a Vickers hardness ranging from 180–250, but now the Vickers hardness was in the neighborhood of 115.

As yet, the optimum amount of excess calcium had not been established. After several bomb reductions had been made in which only the amount of calcium was altered, it became clear that about 60 per cent excess calcium was required in order to secure a good yield of ductile metal. Lesser calcium contents tended to produce smaller amounts of a definitely more brittle metal. The brittleness associated with lower amounts of excess calcium appears to be caused by the oxygen content.

Table I lists the gas content of the metal made

under various conditions. While the data are not comprehensive enough to draw quantitative conclusions, they strongly suggest that a lower excess calcium content results in a high oxygen content. No definite statement can be made at this time with regard to the amount of hydrogen, nitrogen, or oxygen necessary to cause brittleness, but it is intended to report on the specific effects of these gases in a separate paper. It appears highly probable that any of the three gases shown in Table I can make vanadium brittle if present in sufficient amount.

TABLE I. *Gas analyses and hardness of vanadium reduced from V_2O_5**

Run No.	V_2O_5 treatment	% Excess Ca	O_2 per cent	H_2 per cent	N_2 per cent	Remarks	Vickers hardness
D-1	none (first lot)	100	0.070	0.004	0.028	ductile	153
D-2	" "	100	0.052	0.002	0.017	ductile	145
D-3	" "	100	0.046	0.007	0.022	ductile	
D-4	" "	100	0.042	0.003	0.002	ductile	
X-1	none (second lot), 0.15% N_2	10	0.510	0.010	0.030	brittle	336
X-2	" "	25	0.350	0.005	0.018	brittle	281
X-4	" "	100	0.091	0.004	0.065	brittle	141
V-45	18 hr wet O_2 treatment, 0.012% N_2	25	0.240	0.010	0.011	brittle	245
V-49	" "	40	0.120	0.007	0.006	brittle	183
V-44	" "	50	0.017	0.002	0.013	ductile	110
V-48	" "	60	0.029	0.003	0.006	ductile	114
V-43	" "	100	0.031	0.005	0.016	ductile	116

* Gas analyses, courtesy of Manley W. Mallett, Battelle Memorial Institute, and A. F. Torrisi, Pittsfield Works, General Electric Company.

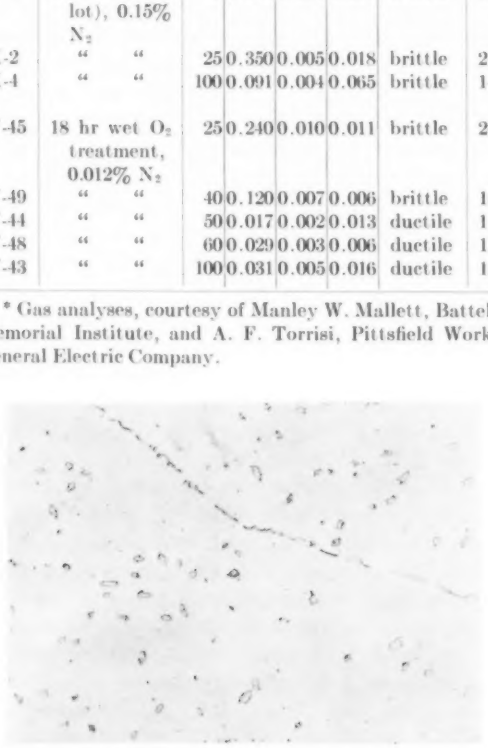

FIG. 2. Typical structure of massive ductile vanadium as electrolytically polished, 250×.

TABLE II. *Purity of ductile vanadium reguli*

Sample No.	V assay	C	Fe	Si	Ca	O_2	H_2	N_2
V-42	99.1	0.23	<0.01	0.01	0.011	0.025	0.002	0.016
V-43	99.0	0.21	<0.01	0.04	0.023	0.031	0.005	0.016
V-44	99.0	0.20	<0.01	0.001	0.014	0.017	0.002	0.013
V-46	99.6	0.29			0.015			
V-48	99.5	0.21			0.016	0.029	0.003	0.006

Optimum Bomb Charge

A typical optimum charge using a bomb with an effective volume of 1.5 liters is the following: 300 grams V_2O_5, 552 grams Ca, 150 grams I_2. This corresponds to a 60 per cent excess of calcium and 0.2 mole iodine for each mole of vanadium. The yield is generally about 125 grams of vanadium or 74 per cent of the theoretical yield.

When iodine was first added to the charge, it was used in the ratio of 0.1 mole iodine to every mole of vanadium produced. This had a beneficial effect in the case of the Marden and Rich type of charge described above, and this improvement in the vanadium yield persisted throughout. Later, the amount of iodine charged per mole of vanadium was doubled; this caused a reproducible 5 per cent increase in the yield of metal without any deleterious effect on qual-

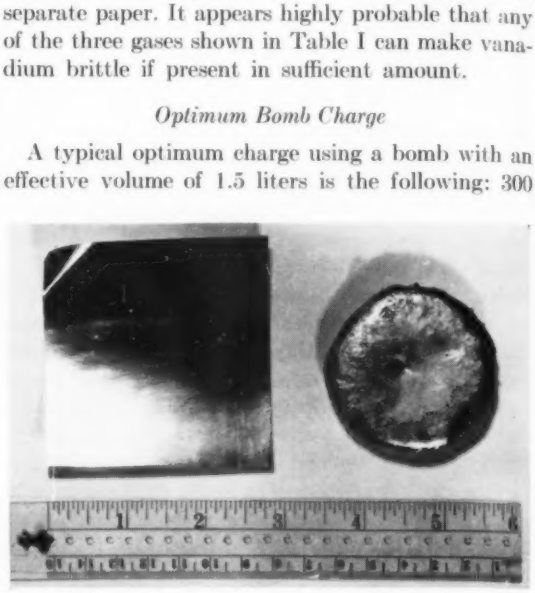

FIG. 3. As-reduced button and rolled sheet

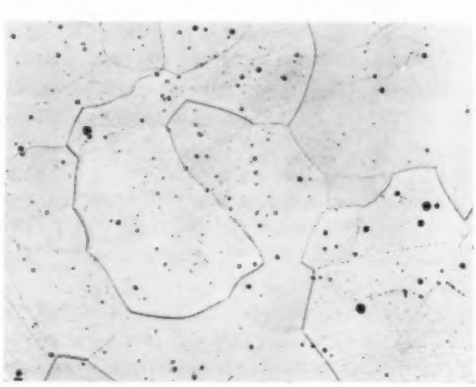

FIG. 4. Hot-worked structure, electrolytic HCl etch, 100×.

ity. This subject was not investigated further, as it appeared that since quality was not affected, an increase of a few per cent more in theoretical yield was not worth the additional cost in iodine.

Fig. 2 shows a photomicrograph of a typical ductile vanadium button reduced from V_2O_5.

The level of purity in recent V_2O_5 reductions is shown in Table II.

Carbon is introduced into the metal by the reagents calcium and vanadium pentoxide. Analysis for carbon in calcium has not been performed; however, 0.05 per cent carbon has been found in the C.P. pentoxide which is calcined from ammonium metovanadate at 400°–450°C.

Fig. 3 shows a typical oxide reduction and some 0.003 inch (0.008 cm) thick foil rolled directly from an as-reduced button without annealing.

Fig. 4 shows the structure of a sample which has been hot worked at 900°–1000°C. Note that the carbides have apparently been partially dissolved and redistributed in a random manner.

Conclusions

1. A method has been developed for the production of small amounts of massive ductile vanadium of approximately 99.5 per cent purity.
2. There appears to be no reason why the same technique could not be scaled-up to produce metal of equal purity in several-pound lots.
3. The major source of brittleness in vanadium made by this technique is oxygen, which should not exceed approximately 0.05 per cent.
4. The wet oxygen treatment of the V_2O_5 lowers the nitrogen content of the oxide and aids in obtaining ductile metal by lowering the oxygen content by some unknown mechanism.

Acknowledgments

The authors wish to make due acknowledgment to Dr. Leo Epstein for valuable discussions on the thermodynamical aspects of this work and to Dr. Richard Gale for his interest in some of the chemical problems involved. The bomb reduction experiments were largely carried out by Mr. John Hartwell and Mr. Robert Gray.

Any discussion of this paper will appear in a Discussion Section, to be published in the June 1951 issue of the Journal.

References

1. A. E. Van Arkel, "Reine Metalle," J. Springer, Berlin (1933).
2. W. B. Pearson, *J. Iron Steel Inst. (London)*, **164,** 149 (1950).
3. J. W. Marden and M. N. Rich, *Ind. Eng. Chem.*, **19,** 786, (1927).
4. J. W. Marden and H. O. Rentschler, *Ind. Eng. Chem.*, **19,** 97 (1927).
5. M. DeK. Thompson, "The Total and Free Energies of Formation of Oxides of Thirty-Two Metals," The Electrochemical Society, New York (1942).
6. F. H. Spedding, H. A. Wilhelm, W. H. Keller, and D Peterson, Manhattan District Report CT-816, (July 1943).
7. F. H. Spedding, H. A. Wilhelm, and W. H. Keller Manhattan District Report CT-2712 (June, 1945).
8. L. L. Quill, "Chemistry and Metallurgy of Miscellaneous Materials: Thermodynamics," National Nuclear Energy Series IV, Vol. **19B**, Paper 6, McGraw-Hill Book Co., Inc., New York (1950).
9. G. A. Rankin and F. E. Wright., *Am. J. Sci.* [4], **39,** 11, (1915).
10. Fritz Ephraim, "Inorganic Chemistry," Interscience Publishers, New York (1943).

Heat Resistance of Zirconium in Several Mediums[1, 2]

E. T. Hayes, A. H. Roberson, and R. H. Robertson

Bureau of Mines, U. S. Department of the Interior, Albany, Oregon

ABSTRACT

Zirconium sheet was heated in carbon monoxide, carbon dioxide, hydrogen, sulfur dioxide, propane, and steam at atmospheric pressure. Weight changes and tensile properties were determined, metallographic structures discussed, and safe heating temperatures for the metal exposed to the various gases deduced.

Introduction

The production of zirconium in constantly increasing quantities by the Bureau of Mines, U. S. Department of the Interior, has been the result of continued interest and expanding demand for this new and potentially important metal.

Since considerable interest has developed in the corrosion resistance of zirconium, this paper is concerned with the behavior of the metal in atmospheres of CO, CO_2, SO_2, H_2, propane, and steam. A previous paper by two of the authors (1) outlined the behavior of the metal in air, oxygen, and nitrogen as an approach to the problems encountered when the metal is forged and rolled in air.

Although a number of papers have been published on the chemical reactions of zirconium with gases, they have been confined largely to the behavior of oxygen, hydrogen, and nitrogen at very low pressures. Gulbransen and Andrew (2) have listed the reaction products of O_2, H_2O, CO_2, CO, and N_2 with zirconium as evaluated from thermodynamic data as follows:

1. $Zr(s) + O_2(g) = ZrO_2\ (s)$
2. $2Zr(s) + CO_2(g) = ZrO_2(s) + ZrC(s)$
3. $3Zr(s) + 2CO(g) = ZrO_2(s) + 2ZrC(s)$
4. $Zr(s) + 1/2\ N_2(g) = ZrN(s)$
5. $Zr(s) + 2CO_2(g) = ZrO_2 + 2CO(g)$
6. $Zr(s) + 2H_2O(g) = ZrO_2(s) + 2H_2(g)$

In the case of SO_2 the reaction probably is $Zr(s) + SO_2(g) = ZrO_2(s) + S(g)$. The letters (s) and (g) refer to the solid and gaseous states, respectively.

Guldner and Wooten (3) have made detailed studies on the sorption of O_2, N_2, CO, and water vapor at low pressure and showed that the metal forms stable solid solutions or compounds with all of the gases except hydrogen. Nitrogen produces stable nitrides, and the CO and CO_2 dissociate to form ZrO_2 and ZrC.

[1] Manuscript received April 3, 1950. This paper prepared for delivery before the Buffalo Meeting, October 11 to 13, 1950.

[2] Published by permission of the Director, Bureau of Mines, U. S. Department of the Interior. Not subject to copyright.

At temperatures up to 800°C and at atmospheric pressure, hydrogen forms ZrH_2, which remains stable until it is heated to between 800° and 900°C. In this temperature range the hydride decomposes with the evolution of large amounts of hydrogen. Apparently the breakdown is associated with the allotropic alpha-beta transformation, since the hydride is decomposed by heating to 900°C and reforms on cooling back to 800°C when the experiment is carried out in a closed system and at atmospheric pressure. The decomposition occurs at much lower temperatures when the pressure is lowered.

Materials and Methods

The metal sheet used in this work was a representative example of industrial metal sheet and contained the following impurities: 0.2 per cent carbon, 0.06 per cent iron, 0.07 to 0.08 per cent oxygen, 0.01 per cent nitrogen, 0.02 to 0.05 per cent aluminum, and 1.8 per cent hafnium. It had been forged and rolled in air at 650°C, sandblasted, and the remaining oxide removed by pickling. The cleaned sheet was cold rolled about 25 per cent before being cut into specimens. All specimens were thoroughly degreased before weighing. Any oxide on the samples was the result of room-temperature oxidation, the surface of the metal being more or less passivated in this way. If the sheets had been heated in a good vacuum for an hour at 1000°C, the surface oxide would have been dissolved and a clean and activated surface presented for the metal-gas reactions, which undoubtedly would then have been more rapid. The vacuum annealing was not undertaken, however, since it was desired to simulate conditions that would be encountered in the normal use of zirconium metal.

The specimens were heated to their critical temperatures, usually 700° to 900°C, in quartz tubes under atmospheric pressures of the dry gases for 1-hour and 24-hour periods. Weight gains were determined on $\frac{3}{4}$ in. x 1 in. x $\frac{1}{16}$ in. (1.8 cm x 2.5 cm x 0.16 cm) specimens cut from cold-rolled, high-hafnium (0.8%) sheets. Standard 8-inch (20 cm) flat

tensile specimens were heated at the same time to determine the effects of the various gases on the tensile properties of zirconium.

Individual specimens were held upright by alundum supports placed in alundum combustion boats, and the entire assembly was placed in a quartz combustion tube.

Positive pressures of the gas on the inside of the tubes were maintained by connecting to the tubes 12-inch (30 cm) surgical balloons filled with gas, thus assuring constant pressure at all times. The quartz tubes were inserted in tube furnaces, evacuated, and back-filled several times with the dry gas, and then heated at the desired temperatures. After the heating period the tubes were withdrawn from the furnace, cooled in air, and the specimens removed.

TABLE I. *Weight gain of zirconium heated in carbon monoxide*

Temp °C	Weight gain, mg/dm²	
	1 hr	24 hr
600	30	200
700	115	275
800	150	600
900	90	500
1000	60	120

Carbon Monoxide

Zirconium specimens were heated in dry commercial-grade carbon monoxide at temperatures ranging from 600° to 1000°C for 1 and 24 hours. Tensile specimens were heated at the same time for mechanical testing. Results of these tests are shown in Table I and Fig. 2.

Some of the values tabulated are the average of five runs, since the results frequently varied as much as 15 per cent. These variations arose from the breakdown of CO and the deposition of a carbon film which hindered diffusion. Weight gains showed a progressive increase up to 800°C, where a maximum was reached, and then a marked decrease as the temperature approached 1000°C.

The pronounced maximum at 800°C in this series is not readily explained. The controlling reactions are:

$$2CO \rightleftharpoons C + CO_2 \qquad (I)$$

$$Zr + 2CO_2 \rightleftharpoons ZrO_2 + 2CO \qquad (II)$$

It is believed that since less oxygen is available in the CO atmosphere the weight gains are less than those found for CO_2. It seems probable that the decreasing weight gains above 800°C arise from the fact that CO is more stable than CO_2; thus the equilibrium shifts to the left in equation (I), in the temperature range 800° to 1000°C. On the other hand, the decrease in reaction rate may be related to the fact that ZrO_2 may catalyze the decomposition of CO at various temperatures, while at higher temperatures the oxide may dissolve in the metal and not be available.

Tensile properties of the treated specimens are shown in Table II. In order to provide a basis for comparison, a standard specimen that was not exposed to the gas also is included in the tabulation.

These data bear out the weight-gain findings that there is a pronounced maximum at 800°C. This is not an unusual phenomenon, since carbon monoxide behaves similarly toward other metals at elevated temperature. It is essentially a cracking phenomenon, the maximum being a function of the metal to which the gas is exposed.

TABLE II. *Tensile properties of zirconium heated in carbon monoxide*

Temp °C	Yield strength 0.2% offset × 1000 psi		Ultimate strength × 1000 psi		Elongation % in 2 inches (5 cm)	
	1 hr	24 hr	1 hr	24 hr	1 hr	24 hr
Standard	38.8		69.7		21.0	
700	36.3	38.9	69.6	60.1	17.0	—
800	41.7	58.0	69.1	80.3	14.2	7.2
900	—	56.6	62.6	62.5	9.5	—

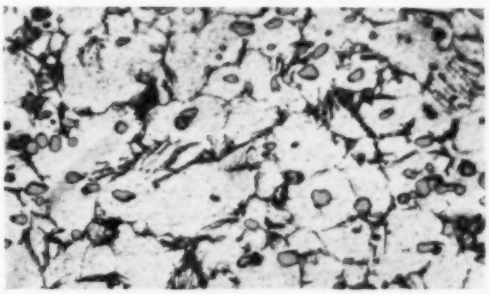

Fig. 1. Zirconium heated in CO, 900°C, 24 hr. Etchant: Vilella's reagent, 250×.

Metallographic study showed the presence of a second phase at 700°C which was attributed to oxide absorption. At temperatures below 1000°C, the oxide occurs as a dark grain-boundary constituent, sharply outlining individual grains. In this series the second phase appeared first as fine spheroids in the grain boundaries. With increasing temperatures they become continuous lines and finally a broadening grain-boundary constituent as shown in Fig. 1, which illustrates the appearance of the specimen exposed for 24 hours at 900°C. The rounded inclusions scattered at random through the metal are zirconium carbide, which was formed when the metallic sponge was consolidated by melting in a graphite crucible. They

should not be confused with the carbides formed when zirconium is heated in the various carbon-containing atmospheres. The oxide forms a solid solution with zirconium at temperatures above 1000° C and cannot be distinguished as a discrete phase.

In spite of the increasing amounts of oxygen at the grain boundaries, the tensile strength was not impaired at 900°C for the 1-hour specimen.

Tensile bars heated at 900°C for 24 hours showed a marked decline in ultimate strength and increase in brittleness. The brittleness exhibited in these specimens was attributed to the rapid oxygen pene-

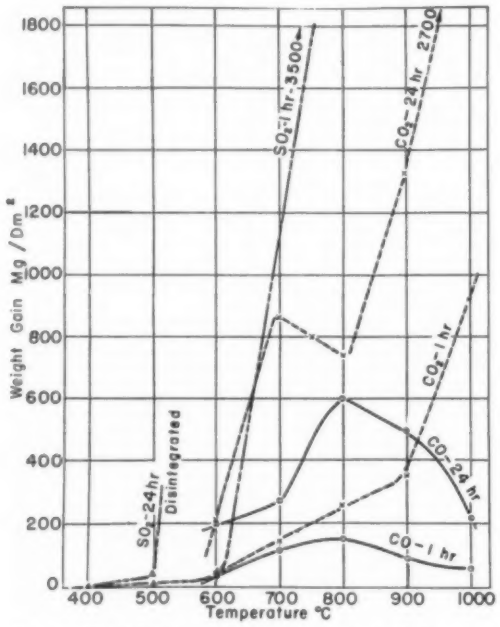

FIG. 2. Weight gain of zirconium sheet heated in carbon monoxide, carbon dioxide, and sulfur dioxide.

tration always noted when the metal is heated through the transformation temperature in the presence of oxygen.

From the standpoint of 0.1 ipy[3] corrosion (600 mdd[4]), zirconium has an upper limit of 1 hour at 900°C or 24 hours at 700°C in carbon monoxide. On the basis of tensile properties, however, maximum yield and ultimate strengths were obtained from specimens heated for 24 hours at 800°C.

Carbon Dioxide

Studies using commercial-grade (dried) carbon dioxide were conducted along the pattern outlined for other sections of this investigation.

Weight gains for the various temperatures are listed in Table III and shown graphically in Fig. 2.

[3] Inches per year.

[4] Milligrams per square decimeter per day.

In the 1-hour specimens, weight gains increase steadily and regularly to 900°C and then take a sudden upswing. The rapid increase in weight at 1000°C was attributed to activation of the metal surface due to the diffusion of oxides and carbides, allowing clean surfaces for the gaseous attack. Acceleration of the reaction $Zr + 2CO_2 \rightleftharpoons ZrO_2 + 2CO$ at temperatures above 900°C likewise may account for the increased rate.

The 24-hour specimens showed a marked departure from the behavior of the 1-hour group. Weight gain increased rapidly to 700°C, then declined at 750° and 800°C, and finally rose sharply at 900° and

TABLE III. *Weight gains of zirconium sheet heated in carbon dioxide*

Temp °C	Weight gain, mg/dm²	
	1 hr	24 hr
600	37	220
700	150	864
750	—	790
800	265	740
900	365	1325
1000	900	2700

TABLE IV. *Tensile properties of zirconium heated in carbon dioxide*

Temp °C	Yield strength 1000 psi		Ultimate strength 1000 psi		Elongation % in 2 inches (5 cm)	
	1 hr	24 hr	1 hr	24 hr	1 hr	24 hr
Standard	38.8		69.7		21.0	
800	39.8	45.9	61.1	66.2	17.0	12.5
900	42.0	—	72.9	63.8	13.5	3.0

1000°C. Reference to the curves for CO_2, shown in Fig. 2, indicates that the upper heating limits should not exceed 900°C for the 1-hour samples or 650°C for 24 hours if a corrosion rate of 0.1 ipy (600 mdd) is not to be exceeded.

Tensile data are shown in Table IV.

Tensile data for the 1-hour specimens showed only small variations in the yield strength at 800° and 900°C. Ultimate strength increased about 15 per cent, while elongation decreased about 30 per cent.

Both ultimate strength and elongation declined in the 24-hour specimens heated at 900°C, indicating oxide penetration at this temperature. The rapid decrease in elongation with the 24-hour specimens indicates that the metal should not be used at temperatures exceeding 800°C in applications where brittleness is a disadvantage.

Carbon deposits were found on the zirconium heated from 600° to 1000°C in both CO and CO_2 atmospheres, and there was no evidence of carbide

formation in the body of the specimen. Guldner and Wooten (3) in their work with CO and CO_2 observed that at 800°C oxygen diffused through the specimens while the carbide remained on the surface. The weight gains shown in this work, then, can be assigned primarily to oxygen absorption. Undoubtedly, at higher temperatures, appreciable carbide formation would take place to form a definite zirconium carbide case.

The anomaly occurring between 700° and 800°C when zirconium is heated 24 hours in CO_2 is believed to arise from this carbon deposit and slow diffusion of the oxygen. Above 800°C the oxygen becomes sufficiently mobile to keep moving into the metal and the weight gains again increase.

TABLE V. *Weight gain of zirconium heated in sulfur dioxide*

Temp °C	Weight gain, mg/dm²	
	1 hr	24 hr
400	—	1.1
500	20	40
600	4000	Decomposed
700	5500	do.

TABLE VI. *Weight gain of zirconium heated in hydrogen*

Temp °C	Weight gain, mg/dm²	
	1 hr	24 hr
300	95	93
400	95	95
500	95	95
600	93	2540
700	95	—

Sulfur Dioxide

The sulfur dioxide series followed the familiar pattern of increasing weight gains with increasing temperature. There was a marked difference from the other zirconium-gas systems investigated, in that there was a well-defined critical temperature. The data for this series are given in Table V and Fig. 2.

These data show conclusively that, although there is little effect at 500°C, the SO_2 oxidizes zirconium rapidly between 500° and 600°C. The samples heated to above 600°C were almost completely decomposed to a voluminous oxide. X-ray analysis of these oxidation products showed that they were mixtures of tetragonal and monoclinic oxides of zirconium. Free sulfur was deposited in the cool ends of the tube.

Tensile data confirmed the above values, in that the mechanical properties were unaffected by exposure of zirconium to SO_2 for 24 hours at 500°C. It was not possible to obtain valid strength values on specimens heated to higher temperatures.

Zirconium metal is quite sensitive to the presence of dry sulfur dioxide, and it would be expected that the presence of water would accelerate the corrosion. It appears that the precautions used in exposing stainless steel to SO_2-bearing gases will have to be followed for zirconium. Any application involving the exposure of zirconium to combustion products will have to be carefully investigated under specific test conditions.

Hydrogen

Experiments with hydrogen atmospheres over a temperature range of 300° to 700°C showed trends similar to those of the SO_2 series. Weight gains are listed in Table VI. In this series the usual standard for weight gains cannot be applied, since any variation in weight is due to hydride formation rather than oxidation.

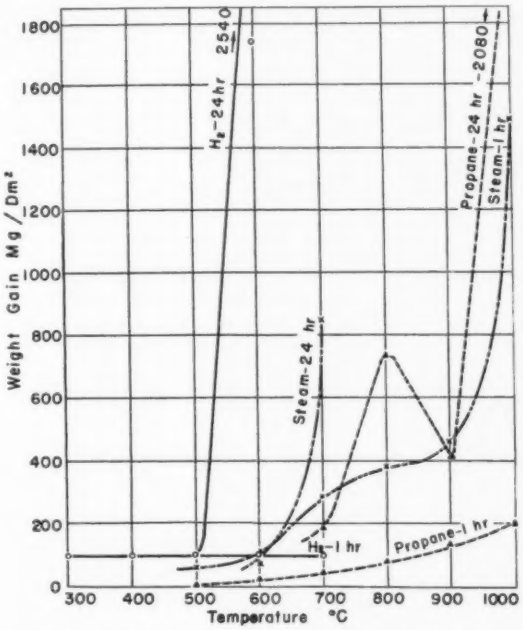

FIG. 3. Weight gain of zirconium sheet heated in hydrogen steam, and propane.

Weight gains remained virtually constant in the 1-hour tests, indicating that no difficulty would be encountered in short-term exposures at 700°C. Results of the 24-hour runs showed that the maximum temperature should not exceed 500°C for longer heating times. The critical temperature appeared to be only slightly above 500°C, since there was such a large increase in weight between 500° and 600°C. These results are shown graphically in Fig. 3.

Tensile data are shown in Table VII.

In the 1-hour specimens, yield and ultimate strengths remained constant to 600°C, with the ultimate showing a sharp drop in the 700°C specimen.

Elongation declined slowly to 500°C, fell about 25 per cent at 600°C, and then dropped sharply at 700°C. The safe temperature for heating in hydrogen for 1 hour appears to be 600°C. The 24-hour group appeared to follow a similar pattern, with little change in ultimate strength, although there was a sharp decline in elongation at 500°C. Zirconium should not be heated above 400°C in a hydrogen atmosphere for extended periods.

The addition of hydrogen to zirconium actually reduces the hardness of the metal. A specimen which had been heated in hydrogen for 24 hours at 800°C—the optimum temperature for hydride formation—had a Knoop hardness of 185, while the value for the unexposed sheet was 243. Retreatment of the hydrided specimen at 700°C in vacuum to expel the hydrogen raised the hardness to 226.

TABLE VII. *Tensile properties of zirconium heated in hydrogen*

Temp °C	Yield strength × 1000 psi		Ultimate strength		Elongation % in 2 inches (5 cm)	
	1 hr	24 hr	1 hr	24 hr	1 hr	24 hr
Standard Zr	38.8		69.7		21.0	
300	38.7	39.0	62.5	71.6	27.0	19.0
400	39.0	39.3	70.2	69.7	20.0	21.0
500	41.9	—	72.9	69.1	22.0	—
600	41.9	—	72.5	67.7	16.5	2
700	—	—	56.3	64.8	3.0	1

The presence of hydrogen likewise reduces the ductility of the metal, completely hydrided material being readily pulverized in a mortar. Ductility is restored by heating the hydrided metal in a vacuum at 700°C.

The limited amount of exposed area and the passivated surface of the specimens definitely control hydride formation. This is especially evident in the 1-hour specimens, where it was possible to heat them well above the critical temperature without any pronounced weight change, and probably accounts for the rapid increase in absorption about 500°C. Increased temperature results in a more rapid solution of the surface oxide, thereby presenting an activated surface for hydride formation. Gulbransen and Andrew (2) and Guldner and Wooten (3) indicate that hydride formation on properly activated surfaces begins near 300°C and is quite rapid at 500°C.

In this work metallographic examination showed little structural difference in specimens heated at 400°, 500°, and 600°C, although there was a very marked weight gain in the 600°C specimen. Specimens heated at 300°C for 24 hours showed very fine intergranular areas of hydride and indicated that some hydride was formed below 300°C, even in a specimen without an activated surface. Hydrogen penetrated the metal completely, forming intergranular second-phase areas that widened with increasing hydrogen. Rapid absorption did not occur below 500°C at atmospheric pressure. Although weight-gain data were not recorded for temperatures above 600°C, metallographic sections showed a marked increase in the amount of hydride in the 700°C samples. The structure shown in Fig. 4 indicates that nearly all of the field was composed of hydride at 800°C.

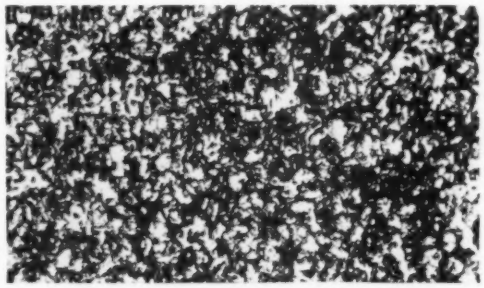

FIG. 4. Zirconium heated in hydrogen, 800°C, 24 hr. Etchant: Vilella's reagent, 250×.

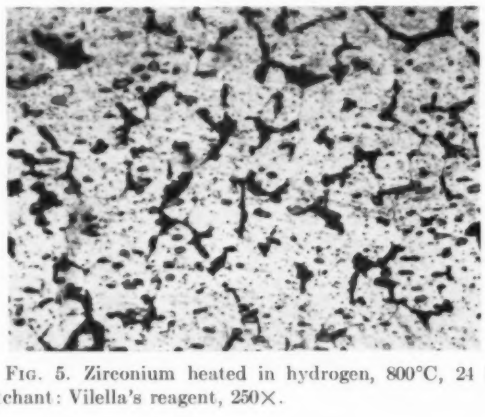

FIG. 5. Zirconium heated in hydrogen, 800°C, 24 hr. Etchant: Vilella's reagent, 250×.

Fig. 5 shows the appearance of a sample from the specimen which was heated in hydrogen at 800°C for 1 hour and then held in a vacuum at 700°C until hydrogen desorption was complete. Comparison of Fig. 4 and 5 shows that most of the second phase was destroyed by this treatment and definitely establishes the second phase as zirconium hydride.

The constant weight-gain value for the 1-hour specimens over the entire heating range may be attributed to an insulating effect of the oxidized surface or to the gettering of a small amount of impurity in the commercial hydrogen. Increased time at temperature accounted for the diffusion of the oxide into the metal, leaving a clean surface which was more susceptible to hydride formation.

Propane

The propane series followed the same procedures set up for other atmospheres and produced a customary pattern of increasing weight gains with increasing temperatures.

Table VIII and Fig. 3 show the weight gains for the specimens used in this test.

The 24-hour runs showed a sharp break above 800° C, the 900°C weight gain being 150 mg/dm² less. The upward trend was resumed in the 1000°C specimen.

Weight gains of 0.1 ipy as standard of suitability cannot be used in this series, since hydrides and carbides rather than oxides are the products of the reaction. Theoretically, the reaction should be:

$$7Zr(s) + C_3H_8(g) = 3ZrC(s) + 4ZrH_2(s)$$

TABLE VIII. *Weight gains of zirconium sheet heated in propane*

Temp °C	Weight gain, mg/dm²	
	1 hr	24 hr
500	15	—
600	39	—
700	50	193
800	85	760
900	143	420
1000	205	2080

However, propane does not decompose completely, the final products being methane, hydrogen, and carbon. After long-term runs above 600°C the quartz tubes contained light tars, dark liquids, and crystals assumed to be napthalene, which resulted from polymerization of some of the intermediate carbon and hydrocarbon dissociation products.

Hagg (4) has shown that hydrogen is more soluble in beta than in alpha zirconium. It is also known that at atmospheric pressure zirconium hydride decomposes between 800° and 900°C, giving off large volumes of hydrogen. The 24-hour curve for propane shown in Fig. 3 indicates that hydrogen is absorbed up to 800°C and then liberated during the alpha-beta transformation at 862°C. Above 900°C the metal is entirely beta, which combines rapidly with hydrogen to produce the immediate, large increase in weight. Carbide formation also occurs at higher temperatures,, and it is believed that weight gains above 900°C are due to the formation of both hydrides and carbides.

Metallographic studies verify the weight-gain curves. The 700°C specimen heated for 24 hours showed fine acicular needles along the grain boundaries, which were very similar to the hydrides. At 800°C the specimen contained a much larger amount of the second phase, which was still in the grain boundaries and had a lamellar appearance. The fact that the 900°C specimen contained less second phase is due to the absence of the hydride, which partly decomposes between 800° and 900°C. The specimen heated to 1000°C contained greatly increased amounts of the second phase.

Salient features of the effect of C_3H_8 in the tensile properties are shown in Table IX.

Yield-strength data indicate that propane has little effect below 900°C, and it appears that heating at 900°C for both 1 and 24 hours is permissible. However, at 1000°C yield and ultimate strengths increase rapidly and elongation is sharply reduced.

TABLE IX. *Tensile data for zirconium heated in propane*

Temp °C	Yield strength		Ultimate strength		Elongation	
	1 hr	24 hr	1 hr	24 hr	1 hr	24 hr
Standard	38.8		69.7		21.0	
700	43.5	40.1	65.1	59.8	17.5	20
800	43.4	42.0	62.0	60.0	12.0	7.0
900	43.1	50.5	63.0	67.5	12.5	4.0
1000	55.6	56.0	75.4	80.0	4.5	1.0

TABLE X. *Weight gain of zirconium heated in steam*

Temp °C	Weight gain, mg/dm²	
	1 hr	24 hr
500	—	72
600	73	107
700	284	860
800	385	—
900	464	—
1000	1496	—

Steam

The effect of steam on zirconium at temperatures from 500° to 1000°C was determined by passing steam from a boiler through a quartz tube containing the specimens, the tube being heated in an electric tube furnace. A trap at the discharge end of the tube prevented the entrance of air.

Weight-gain data are shown in Table X and Fig. 3.

Weight gains in the 1-hour suite showed a gradual increase through 900°C, followed by a sharp gain at 1000°C, which can be explained on the basis of the allotropic transformation from alpha to beta zirconium. The transition temperature (862°C for pure zirconium) is shifted upward by the addition of oxygen. At this temperature diffusion of the oxide into the metal is rapid, and shifting of the transition point not at all unlikely. It has been shown previously that oxidation is greatly accelerated by the volume change and reorientation that accompany

the phase change. The sharp weight gain noted here is attributed to this cause.

The 24-hour group showed a rapid increase between 600° and 700°-C. Specimens heated at 800°C and above were completely oxidized, with only a loose mound of white powder remaining at the end of the heating period.

Tensile properties were not determined above 600° C, since tests indicated that properties were sharply altered in specimens exposed for 24 hours at 600°C. The data are shown in Table XI.

Although the yield and ultimate strengths at 600° C are comparable to those of the untreated standard sheet, the marked decrease in elongation was taken as an indication that 600°C was the probable upper limit at which zirconium could be heated in air and still retain most of its useful properties.

TABLE XI. *Tensile properties of zirconium heated in steam for 24 hours*

Temp °C	Yield strength 0.2% offset × 1000 psi	Ultimate strength 1000 psi	Elongation % in 2 inches (5 cm)
Standard	38.8	69.7	21.0
500	46.0	72.5	20.0
600	42.8	66.3	3.0

Steam produces a comparatively high corrosion rate, being second only to SO_2 among the atmospheres used in this series of tests. Zirconium can be heated in steam at 900°C for 1 hour, or 600°C for 24 hours without exceeding the tentative 600 mdd standard that has been suggested for zirconium. However, the decline in mechanical properties limits the temperature to 600°C for extended periods.

Summary

Zirconium sheet was heated in CO, CO_2, SO_2, C_2H_2, steam, and hydrogen atmospheres at elevated temperatures. Heat resistance was determined on the basis of weight gains, metallographic structures, and tensile properties. A summary of the individual systems follows:

Carbon Monoxide.—Weight gains and tensile strengths of zirconium heated in carbon monoxide at temperatures from 600° to 1000°C show that a maximum is reached in the specimens heated at 800°C. From the standpoint of a corrosion rate of 0.1 ipy of zirconium as an upper tolerance limit, the metal should not be heated above 900°C for 1 hour or 700°C for 24 hours. Tensile data indicate that maximum properties were developed in the specimens heated at 800°C for 24 hours.

Carbon Dioxide.—Weight gains for this system present an irregularity at 800°C which is caused by a carbon coat on the metal surface and the slow diffusion rate of the oxide. Above 800°C the oxygen becomes mobile enough to keep moving into the metal, and the weight gains increase in a normal fashion. The metal should not be heated above 650° C for extended periods if excessive corrosion is to be avoided. Tensile properties are impaired above 800°C.

Sulfur Dioxide.—The sulfur dioxide series followed the familiar pattern of increasing weight gains with increasing temperature. A well-defined critical temperature was established between 500° and 600°C. Samples heated to 600°C decomposed rapidly to oxide powder. Weight gains were negligible, and tensile properties were unimpaired at 500°C.

Hydrogen.—Excessive weight gains and a marked deterioration in tensile properties were caused by heating zirconium specimens in hydrogen above 500° C for 24 hours. Hydride formation embrittled the metal and reduced its ductility. Heating the hydrided specimens at 700°C in a vacuum restored the ductility.

Propane.—Zirconium was heated in propane at temperatures from 500° to 1000°C. The weight gain curve showed a sharp dip at 900°C and then a continued rise to 1000°C. Weight gains up to 800°C were due to hydrogen absorption, with the drop between 800° and 900°C caused by decomposition of the hydride. Above 900°C the increase in weight is a result of hydride and carbide formation. Heating to 900°C did not impair yield and ultimate strengths although elongation was reduced at 800°C and above.

Steam.—Steam produced a very high corrosion rate, being second only to sulfur dioxide among the atmospheres studied. The decline in both corrosion resistance and tensile properties indicated that the metal should not be heated above 600°C in steam.

The extreme sensitivity to sulfur dioxide and water vapor singly indicates that a combination of the two might be especially corrosive. Any application involving the exposure of zirconium to combustion products should be carefully investigated for specific conditions.

Discussion

The choice of 0.1 ipy as the maximum allowable rate was purely arbitrary, and is admittedly high. It was selected as a possible guide for the designer who might be interested in zirconium as a construction metal.

It should be recognized that corrosion rates reported in these studies do not imply a total time of exposure, but rather a rate over the indicated periods, and may or may not indicate a rapid initial rate and a less rapid final rate. Therefore, little re-

liance can be placed on the extrapolation of 24-hour data to one-year periods. This is particularly true where intergranular attack may result in changes of strength of material. The tensile properties given in this paper indicate the decrease in strength resulting from exposure of zirconium to the various atmospheres, and should provide a valuable addition to the corrosion rate data in applications where tensile strength is a design factor.

Any discussion of this paper will appear in a Discussion Section, to be published in the June 1951 issue of the JOURNAL.

REFERENCES

1. E. T. HAYES AND A. H. ROBERSON, *J.* (*and Trans.*) *Electrochem. Soc.*, **93,** 142 (1949).
2. E. A. GULBRANSEN AND K. F. ANDREW, *J. Metals* (*Trans. Am. Inst. Mining Met. Engrs.*) **185,** 515 (1949).
3. W. G. GULDNER AND L. A. WOOTEN, *J.* (*and Trans.*) *Electrochem. Soc.*, **93,** 223 (1948).
4. G. HÄGG, *Z. physik. Chem.*, **B 11,** 433 (1931).

Studies on Alternating Current Electrolysis

I. The Nature of Polarization Capacity and Polarization Resistance[1]

MANUEL SHAW AND A. EDWARD REMICK

Department of Chemistry, Wayne University, Detroit, Michigan

ABSTRACT

The work here reported involves impedance bridge measurements on electrolytic cells subjected to alternating currents. A study of the cleaning and conditioning of platinum electrodes was followed by a study of reversible and irreversible oxidation-reduction systems. Relationships were sought among the following variables: polarization capacity, polarization resistance, reversibility, frequency, current density, concentration, and redox ratio. It was found that the polarization capacitance is compounded of three different kinds of capacitance: C_o, C_h and C_p, and that C_p is a function of the reversibility and the redox ratio. It was also found that the number of coulombs passing per half cycle at the capacitive elevation point is independent of the frequency and of the electrolyte (water was always present).

INTRODUCTION

No adequate review of the field of alternating current electrolysis has been published, but a reasonably good picture of the field up to the year 1939 can be obtained by reading the papers of Reichenstein (1), Shipley (2), and Shipley and Rogers (3). Only the literature most closely related to our research is reviewed here.

It has been established that when an alternating current passes through an electrolytic cell, the cell shows both dissipative and reactive characteristics. These were considered by Kohlrausch (4) to consist of the resistance of the electrolyte, R_T, in series with a capacitance, C_S. Wien (5) showed the presence of an additional resistance, R_Δ, called the polarization resistance. Hence, if the measured effective series resistance of the cell is designated as R_S, it follows that

$$R_S = R_T + R_\Delta. \qquad (I)$$

A number of investigators, usually employing platinum electrodes in aqueous sulfuric acid or neutral salt solutions, found that the cell capacity is independent of the current density only at very low values of the latter. At higher current densities, the capacity rises. The limiting value of the capacity as the current approaches zero was called the initial capacity (C_i) by Blandlot (6). The point at which the capacity first starts to rise with increasing current density we shall call the "capacitive elevation point" (C.E.P.). Neumann (7) predicted, on the basis of Warburg's (8) mathematical theory, that the C.E.P. should be frequency dependent. The dependency of polarization capacitance on the frequency has been much studied, and curiously divergent results have been obtained. A number of investigators (4, 9) have reported that these two variables are independent; others (1, 7, 10) have reported that the relationship

$$C_S = k\omega^{-1} \qquad (II)$$

(in which ω is the frequency in radians per second) is accurately or approximately obeyed. Still others (11) preferred the relationship

$$C_S = k_1 + k_2\,\omega^{-1} \qquad (III)$$

and a few investigators (12) have found it desirable to give the negative exponent in equation (II) values ranging from 0.1 to 1.0.

Similar attempts have been made by many of these same investigators to establish a relationship between R_Δ and ω. Their findings for the most part can be expressed by the equation

$$R_\Delta = k\omega^{-n} \qquad (IV)$$

in which n varies from 0.5 to 1.0.

It is by no means impossible that both C_S and R_Δ may be caused, at least in part, by the presence of an adsorbed layer of air, electrolytic gases, other electrolytic products, or impurities in the solution which form a poorly conducting surface layer on the electrode (12*a*, 13). Good evidence that such films are formed electrolytically at higher current densities has been presented by Scott (14) and Shipley (2), and Wien (5*c*) showed that air adsorbed on palladium electrodes alters the value of C_S. Neverthe-

[1] Manuscript received July 5, 1949. This paper prepared for delivery before the Chicago Meeting, October 12 to 15, 1949. The subject matter of this paper was abstracted from a dissertation presented to the Graduate School of Wayne University by Manuel Shaw in partial fulfillment of the requirements for the Ph.D. degree.

less, it appears from experiments of Wolff (15), which were checked by Jones and Christian (10*e*), that in the range of the initial capacitance, at any rate, these thin gas films do not contribute appreciably to the production of the cell capacitance. The same conclusion was reached by Taylor and Acree (16) using a different method.

Despite the fact that the initial capacitance behaves in many ways like a geometrical capacitance, it has been found that its value is too high (10 μf cm^{-2} and greater) to be accounted for as a geometrical capacitance involving a uniform dielectric between the electrodes (17). Eventually much evidence accumulated to show that this high capacitance is due to the formation of Stern electrical double layers at the electrode interfaces (18).

The question as to whether each electrode behaves as an ideal electrostatic condenser [ideal polarized electrode (19)] or as a leaky condenser in the range of the initial capacity has been definitely answered. Grahame (19) has found that the ideal polarized electrode corresponds to a limiting condition which can be approached but never completely achieved. The closest approach to this ideal was realized with scrupulously clean mercury at low voltages. In this case, the capacitance and resistance were found to be independent of the frequency.

The rapid rise of C_s above the C.E.P. has not, as far as we are aware, been definitely explained, but it is presumably closely similar to, if not identical with, a rise in capacitance observed by Grahame (20) in investigating the reduction of cadmium chloride. He used a dropping mercury cathode, which was polarized by direct current, and superimposed a small alternating current by means of which the cell capacitance could be measured on an impedance bridge. He found that very rapid rise in capacitance occurred at the polarographic decomposition potential. This excess capacity which arises from the reversible electroreduction of ions he termed "pseudocapacity." It is interesting to note that he found no "noticeable" pseudocapacity when irreversible processes such as the reduction of oxygen or of nitrate or hydrogen ions were studied. This work proves that reversible electrochemical action gives rise to a very high capacitance.

Most investigators agree that C_s increases with the concentration. A purely physical theory of this effect, which would presumably apply in the range of the initial capacity, has been given by Erdey-Gruz and Kromrey (21).

The theory of the polarization resistance R_Δ which accompanies C_s has also been the subject of much speculation. Its discoverer, Wien (5*a*), pointed out that its existence proves nothing except that there occurs an energy loss of some kind in addition to that associated with the true conductivity of the solution itself. He suggested, but did not prove, that it might be due to a poorly conducting surface layer on the electrode, in which case the lost energy would be degraded, or it might be due to "spontaneous depolarization," i.e., to some process which would prevent the reversal of the electrochemical change on current reversal. In this case, the lost energy would not necessarily all be degraded. A further possibility is that even in cases in which the primary process is completely reversed, there will be an entropy increase attending this cyclic process if a potential barrier exists at the electrode surface (22). Wien's (5*c*) observations that preliminary degassing of electrodes in vacuo reduced R_Δ indicates clearly that the adsorbed air is partially responsible for the existence of R_Δ.

Warburg (8) was the first to attempt the development of a mathematical theory of the dispersion of C_s. His mathematical analysis was extended by Rosebrug and Miller (23) and by Miller and Gordon (24). Warburg's theory was developed for unpolarizable electrodes. C_s was considered to be chemical in nature and the slow process responsible for the dispersion was considered to be diffusion. This theory predicts that C_s should be inversely proportional to the square root of the frequency. Another dispersion theory has been presented by Thon (25) who pointed out that if the equivalent circuit of an electrolytic cell is represented by the resistance of the electrolyte in series with a parallel combination of a capacitance and another resistance, then the application of ordinary alternating current theory predicts dispersion effects for C_s and R_Δ, both of which would be inversely proportional to the square of the frequency under certain conditions.

The only case on record in which Thon's predicted relationship between resistance and frequency has been observed is that furnished by Grahame's experiments with dropping mercury cathodes on which octyl alcohol had been adsorbed, and, even in this case, the relationship was not even approximately obeyed except near the electrocapillary maximum (19*b*). Thon's predicted relation of capacity to frequency has never been observed.

Grahame's experiments, especially those dealing with dispersion, throw additional light on the nature of R_Δ. His observation that the resistance of an ideal polarized electrode does not vary with the frequency is interpreted by him to mean that R_Δ is zero since R_Δ has been reliably shown to be a function of the frequency. This fact combined with the definition of an ideal polarized electrode forced him to conclude that R_Δ is brought into existence by electrochemical action.

A complete survey of the literature indicates even

more forcibly than the above review that there is much discord both in regard to experimental observations of C_s and R_Δ and to their theoretical explanation. We feel that this discord has resulted in no small measure from the diversity of equipment and conditions used by different investigators, rendering comparisons impossible. We therefore undertook an experimental reinvestigation of C_s and R_Δ so that all the variables whose relationships are of

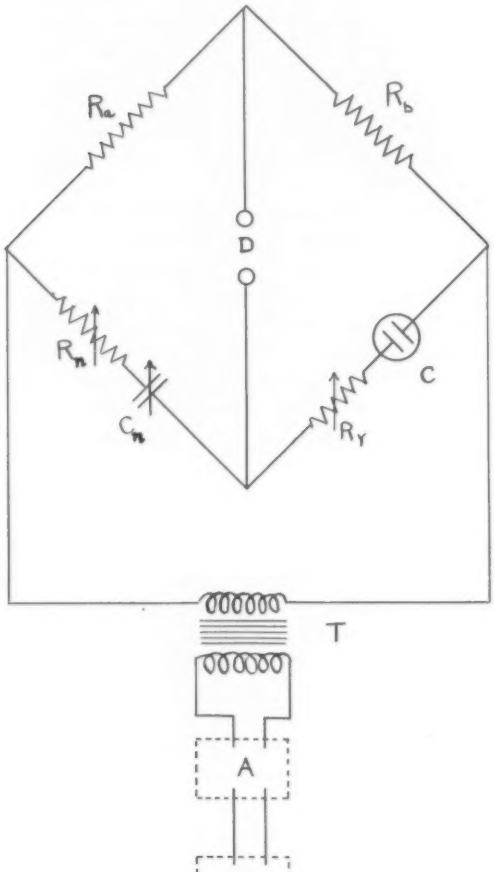

FIG. 1. Schematic diagram of impedance bridge

interest could be determined under comparable conditions. Other objectives were: (*a*) to study more carefully than has been done the effect of immersion time of the electrodes on the values obtained for C_s, (*b*) to study the effect of pertinent variables on the C.E.P., (*c*) to study oxidation-reduction systems of the ferrous-ferric type which are characterized by the simultaneous presence of both oxidant and reductant in the solution (no such study had ever been published), and (*d*) to glean such theoretical knowledge as may prove possible from these experimental results. Our entire study aspires to no higher aim than a preliminary survey of a rather large field.

APPARATUS

The electrolytic cell, C, was introduced into one branch of an impedance bridge, Fig. 1, which was constructed in the laboratory. R_a and R_b are non-inductive IRC wire-wound precision resistors ($\frac{1}{4}$% tolerance), R_n and R_y are General Radio type 602-J decade resistance boxes, and C_n is a General Radio type 219-M decade capacitor. In view of the large capacitances encountered in this work it was frequently necessary to connect two calibrated Cornell Dubilier decade capacitors, model CDC-5, in parallel with C_n. Vacuum tube voltmeters, connected with the bridge through a suitable switchboard, were used for reading voltages across any part of the circuit desired. The current through the cell was calculated from the voltage across R_y. The output of the oscillator, B (a Ferret, model 610), was amplified by a push-pull amplifier, A, and coupled with the bridge through a General Radio type 578-A shielded transformer. Either phones or a Dumont cathode ray oscillograph, type 208-B, could be connected through the switchboard to the detector terminals, D. When the phones were used, the signal was amplified by means of a Ballentine electronic voltmeter, model 300, which may be made to serve this purpose. The switchboard also allowed the oscillograph to be connected across R_y or C to check wave-forms. No distortion of the voltage waves across either of these circuit elements could be detected visually in any of the observations reported in this paper. All leads were made with shielded cables whose shields were grounded. The small capacitances thus introduced were negligible in comparison with the high cell capacitance. The shielding was necessary to minimize the electrical disturbances originating outside the laboratory. The oscillograph, oscillator, and amplifier were all suitably grounded.

The electrodes used in the cell, C, consisted of smooth platinum disks (area 0.30 cm^2) sealed in L-shaped glass tubes as close to the end as possible and in such a way that the sealing process did not reduce the area. Sealed in this manner, no sharp edges were exposed and only one face of the electrode was in contact with the solution. The electrodes were mounted in a rubber stopper so that they were parallel, their positions relative to one another being maintained constant by a suitable clamp. The stopper also carried a third electrode, which served as anode for the electrolytic cleaning of the working electrodes, and inlet and outlet tubes for nitrogen. The nitrogen was purified by passing over reduced

copper in a tube furnace. The nitrogen stream was used in all experiments involving ferrous salts.

All experiments were made at 30° ± 0.1°C in a constant temperature bath. All chemicals used were of the best commercial grades available.

Experimental Results

Experiments on the cleaning of electrodes, made in order to get reproducibility, yielded only one satisfactory method. The two working electrodes were tied together so that they served jointly as cathode during an electrolysis in an alkaline cyanide solution having the composition: NaOH, 50 g/l; KCN, 10 g/l; Na_2CO_3, 50 g/l. The third electrode mentioned above served as anode, the cell being subjected for 10 to 20 minutes to as high a current density as possible (about 35 ma cm^{-2}) so that a vigorous evolution of gas resulted. The electrodes were then suitably washed.

Effect of Immersion Time on the Polarization Capacity

These experiments were carried out for the purpose of gaining some understanding of the immersion time dependency of C_s. All measurements were made in the range of the initial capacity (0.5 ma cm^{-2}) and at a frequency of 1000 c/sec.

The following systems were studied: (1) 0.5*M* H_2SO_4, (2) 0.5*M* Na_2SO_4, (3) glycerol saturated with KI, and (4) absolute ethanol saturated with KI. Readings of C_s were taken every few minutes for an hour or more, the current being left on only as long as required to balance the bridge. In system (1), the C_s readings dropped to a fairly constant value of 13.1 μf cm^{-2} in about 45 minutes; in system (2) they rose to a peak value of 23.3 μf cm^{-2} in 76 minutes and then dropped again; in systems (3) and (4) the values of C_s became remarkably constant at 8.5 and 5.2 μf cm^{-2} respectively in 2 or 3 minutes and stayed constant within 0.2 μf cm^{-2}.

In another experiment on system (1) the electrodes were immersed for one hour before taking a reading. The result checked well with that obtained above, in which the current was flowing a fair portion of the time, thus showing that the changes taking place, whatever their nature, were essentially independent of any application of current.

A very significant experiment was performed in which the electrodes were removed from the sulfuric acid at the end of an hour, washed with distilled water, and replaced in the acid, with the result that C_s did not change. The experiment was repeated using water at 50°C and again at 70°C with the same result. Finally, the electrodes were put in distilled water and heated for at least 10 minutes at 96°–98°C. After cooling to 30°C they were returned to the cell and C_s was immediately determined. It was found to have increased considerably but in 3 minutes it had returned to its "one hour value." Only on re-cleaning the electrodes by electrolysis in the alkaline cyanide solution was the effect of the conditioning process completely obliterated.

An investigation of the effect of temperature on the rate of decrease of the initial capacity was made on 10*M* H_2SO_4 over a temperature range of 30° to 80°C. The rate of decrease was greater, and the final value of C_s lower, at higher temperatures. Similar

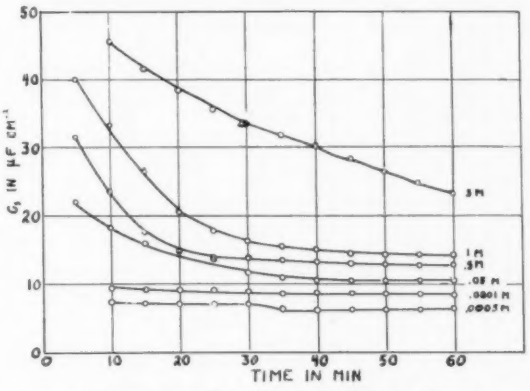

Fig. 2. Effect of concentration of sulfuric acid on the rate of decrease of initial capacity with time.

TABLE I. *Effect of frequency on the capacitive elevation point* (I_c)

System							
1		2		3		4	
f	I_c	*f*	I_c	*f*	I_c	*f*	I_c
1000	5.0	4000	2.0	200	1.0	1000	5.0
3000	12.7	6000	3.3	400	3.3	2000	11.0
5000	21.3	8000	3.3	600	5.0	4000	21.7
10000	42.7	10000	5.0	800	5.0	10000	50.0
				1000	6.7		

experiments were made at 30°C on sulfuric acid solutions of various concentrations. The results are shown in Fig. 2. Simultaneous measurements of the resistance showed that it did not change significantly during the first hour. However, after 3 hours it started to rise and after 24 hours standing it had, in one instance, risen from 41 ohms to 70 ohms.

Effect of Frequency on the Capacitive Elevation Point

It will be recalled that Neumann predicted an increase in the C.E.P. (I_c) with the frequency. As far as we are aware, this prediction has never been verified experimentally; therefore, we collected the data in Table I to check it. The following systems were used: (1) 0.1*M* $FeSO_4$ + 0.1*M* $Fe_2(SO_4)_3$ in 0.5*M* H_2SO_4 (aqueous), (2) glycerol saturated with KI, (3) 0.5*M* H_2SO_4 saturated with capryl alcohol,

and (4) 3.8M H_2SO_4 (aqueous). The frequency is given in cycles per second and I_c in rms ma cm^{-2}. It is evident that I_c increases with frequency as predicted. Furthermore, when the data are plotted graphically, it is found that all four systems can be represented by straight lines going through the origin. This linear relationship is obeyed quite accurately by the two aqueous solutions, systems (1) and (4).

The value of I_c was not obtained from curves (e.g., Fig. 3) but by increasing the current very

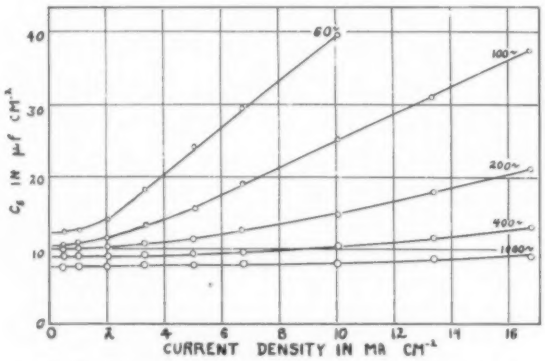

FIG. 3. Effect of current density on polarization capacity at various frequencies for a saturated solution of potassium iodide in glycerol.

TABLE II. *Calculated values of* q_c

System	q_c (microcoulombs/cm^2)
1	2.0
2	2.1
3	3.0
4	2.3

slowly up to the point where the bridge balance was first noticeably disturbed.

The following equation, in which I is the effective current and q_1 is the number of coulombs passing per half cycle, can easily be derived from alternating current theory.

$$I = \frac{q_1 f}{2} \qquad (V)$$

If I is replaced by I_c, the current density at the C.E.P., then q_1 also becomes a function of the C.E.P. and may be symbolized as q_c. Equation (V) shows that the observed linear relationship between I_c and f means that q_c is a constant for a given system independent of the frequency. Furthermore, Table II indicates that q_c is not much different for three of the systems used. The higher value observed when capryl alcohol was used may be related to the adsorption of the alcohol on the electrode. Although the near constancy of q_c for the other three systems may not look impressive at first sight, it must be remembered that the C.E.P. cannot be determined with great precision.

Effect of Frequency on the Polarization Capacity

The ferrous sulfate in aqueous sulfuric acid solution was stored in an atmosphere of nitrogen and at no time was exposed to the air. Both the ferrous and ferric sulfate solutions were standardized potentiometrically by Jacob Silverman. Bridge measurements of C_s were recorded only after the electrodes had been immersed in the electrolyte for a time sufficient to insure essential constancy of the capacitance (about one hour, usually). The experimental results are given in the following figures. Fig. 3 gives a good example of the extension of the range of the initial capacitance accompanying increasing frequencies.

Fig. 4 shows that the dispersion of C_s is much greater above the C.E.P than below it. In order to study this effect in greater detail, it was deemed desirable to construct a series of dispersion curves at different current densities. This would demand that the capacity must remain independent of the rather long time required for the completion of such a series of measurements. The system best meeting these requirements is glycerol saturated with potassium iodide. The results obtained with this system are shown in Fig. 5.

The trends observed in all the dispersion experiments are obvious from the graphs. Attention should be drawn to the fact, however, that the studies involving the ferrous-ferric and the ferrocyanide-ferricyanide systems involve as an additional variable the "redox ratio." This term will be used by us to represent the ratio $[Ox]/[Red]$ where $[Ox]$ and $[Red]$ represent, respectively, the molar concentrations of the oxidized and reduced forms of a reversible oxidation-reduction system.

The dispersion curves shown in the figures are all examples of I-dispersion, i.e., dispersion observed at constant current density. It is also possible to measure dispersion at constant half-wave area (q_1); this we will call Q-dispersion. Comparison of the examples given in Table III (all of which are above the C.E.P.) with those in Fig. 5 shows that Q-dispersion is much less pronounced than I-dispersion.

Effect of Frequency on the Polarization Resistance

For all measurements of the polarization capacity made in this study, simultaneous readings were taken for the total cell resistance, R_s. The data for low frequencies (below 600 c/sec) were of greatest interest in both cases, but unfortunately the values of R_s are subject to great error in this range owing to poor sensitivity of the impedance bridge for re-

sistance measurements in the presence of the high capacitive reactance existing at low frequencies. The experimental results are shown in Fig. 10 and 11.

Discussion and Conclusions

The experiments made on the conditioning of electrodes indicate that while the electrodes are immersed in the aqueous solutions some process is occurring at the electrode surface which is independent of the small currents used, increases with the concentration of the sulfuric acid, is absent in the experiments in which sulfuric acid was absent, and is not appreciably undone by heating the electrode in water. Adsorption of sulfuric acid or possibly impurities in the acid is thus a likely explanation. At higher temperatures, diffusion to the electrode is faster and the final adsorption equilibrium is more quickly attained, giving a lower equilibrium value of C_s because thermal agitation decreases the concentration of ions in the compact double layer and increases the thickness of the diffuse double layer (26).

Our dispersion experiments gave data for which we were able to derive, in all cases, satisfactory empirical equations of the general form:

$$C_s = C_o + kf^{-m} \qquad \text{(VI)}$$

or

$$R_s = R_o + kf^{-n} \qquad \text{(VII)}$$

where C_o and R_o are constants independent of the frequency, f, and represent the values of the capacitance or resistance, respectively, at infinite frequency.

It is of passing interest to note that none of the previous investigators who worked with solutions ever suggested the use of equation (VI) for capacitive dispersion, but von Schweidler (27) showed that the capacitance of practical condensers, unlike ideal condensers, varies with the frequency according to such an equation. Jones and Christian (10*e*), working with silver electrodes in silver nitrate solution, obtained data which they tried to fit to Warburg's equation: $C_s = k\omega^{-\frac{1}{2}}$. Actually, their data are in much better accord with equation (VI). It is the frequency dependent term of (VI) which should be used to test the Warburg theory. Application of this equation to the data of Jones and Christian gives $m = 0.5$ as required by the Warburg theory. The values of m obtained from our experiments vary between 0.23 and 1.34. We do not consider that our results should be used to test the Warburg theory since that theory is restricted to "electrodes of the first kind."

Since C_o is independent of the frequency, it must be caused by a different agency than the frequency-dependent part of C_s. Frequency-independence of C_s is a characteristic of an ideal polarized electrode, whose capacitance has been convincingly shown to be the electrostatic capacitance of an electrical double

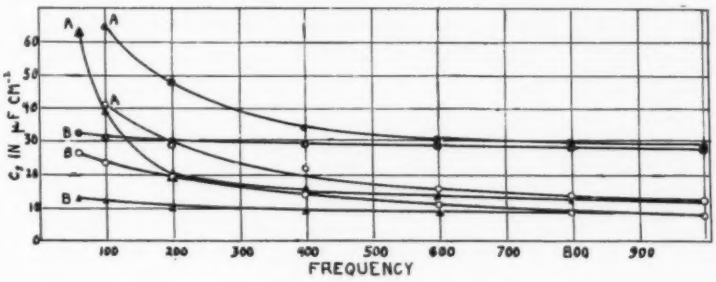

Fig. 4. Capacitive *I*—dispersion. ○—0.0005*M* sulfuric acid, ●—5*M* sulfuric acid, ▲—ethanol saturated with picric acid, A—above the C.E.P. (16.7 ma cm^{-2}), B—below the C.E.P. (0.5 ma cm^{-2}).

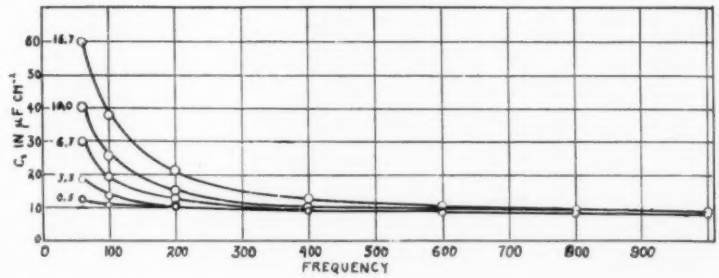

Fig. 5. Effect of current density (ma cm^{-2}) on the capacitive *I*-dispersion of glycerol saturated with potassium iodide.

TABLE III. *Q-dispersion for glycerol saturated with potassium iodide*

Frequency	Current density	C_s
60 c/sec	2.0 ma cm^{-2}	14.7 μf cm^{-2}
100 c/sec	3.3	13.7
200	6.7	13.1
400	13.3	12.0

layer (18). Another characteristic of an ideal polarized electrode is that the frequency dependent R_Δ is zero. This is also the characteristic of an electrolytic cell at very high frequencies, as shown by equation (VII). Thus in two important respects a cell in which $C_s = C_o$ behaves like an ideal polarized electrode. It is not unreasonable, therefore, to identify C_o with the capacitance of the electrical double layer. An additional argument in favor of this theory is that the observed values of C_o are of the same order of magnitude as the often-measured double layer capacity.

The corresponding term in equation (VII), viz., R_o, is commonly accepted as being identical with R_T of equation (I). It then follows from equations (I) and (VII) that

$$R_\Delta = kf^{-n}.$$

This relationship is generally accepted as correct (10*c*).

The interesting observation that q_c, the half-wave area at the C.E.P., has nearly the same value in three different redox systems suggests that q_c may be a property of some common component of those systems. The only common components were platinum and water (the glycerol was not anhydrous) and the only likely common reaction is the electrolysis of water. Evidence that the C.E.P. is associated with the onset of the electrolytic decomposition of water may be obtained as follows.

For each electrolyte, C_i is independent of the current density and directly proportional to the electrode area (5, 28). In the region of the initial capacity, therefore, the electrode simultates a practical condenser and justifies the use of common alternating current theory in connection with the C.E.P. which terminates this region. Representing peak values of current and voltage at the C.E.P by the symbols I_c and E_c, equation (V) is readily transformed into the equation:

$$E_c = q_c/2C_i \qquad \text{(VIII)}$$

in which E_c is the amplitude of the potential drop across the double layer. The observed constancy of q_c would demand a constant E_c if an ideal condenser were involved. However, C_i, like the capacity of a practical condenser, is slightly frequency-dependent, as shown by all of our dispersion curves. Strictly speaking, this means that equation (VIII) is no longer applicable, but it seems certain that it may still be applied semiquantitatively at the C.E.P. It would demand that E_c increase with increasing frequency since C_i decreases. Values of E_c were calculated by the use of equation (VIII) together with the experimental data on our least time-variable system, glycerol saturated with potassium iodide. Values of I_c were obtained from the linear plot of I_c against f (data from Table I). A plot of log I_c against E_c (Fig. 12) proved to be linear. Its equation is

$$E_c = 0.10 + 0.03 \log I_c \qquad \text{(IX)}$$

which is reminiscent of the Tafel equation for overvoltage. E_c is presumably compounded of a polarization voltage and a thermodynamic voltage, but this should not affect the value of the slope (0.03) which is remarkably close to the value 0.029 found for hydrogen overvoltage at low overvoltage cathodes (29). Of course, since alternating current was used, oxygen overvoltage is probably also involved, but the value of the slope is not much different in this case (30). These relationships strongly suggest, but do not prove, that the process which is starting to occur at the C.E.P. is the decomposition of water.

The frequency-dependence of C_i shows that C_i cannot be strictly the same as C_o of equation (VI). However, both of them have values of the same order of magnitude as the double-layer capacity, which suggests that below the C.E.P. the electrode together with its double layer is acting like a slightly leaky condenser. The demonstrated applicability of equation (VI) below the C.E.P. justifies the description of the double layer capacity by the equation

$$C_i = C_o + C_k$$

where C_k is a frequency dependent term.

It is well known that a decrease in the concentration of electrolyte around an electrode increases the thickness of the diffuse double layer and thereby decreases C_i. This is observed for sulfuric acid in Fig. 2 and 4.

The frequency dependence of C_k is adequately explained in terms of the highly developed theory of capacitive dispersion occurring in liquid dielectrics (31). In the range of frequencies used in our experiments, dispersion in liquid dielectrics is caused by the motion of ions and it is found that large loss angles occur in the frequency range in which capacitance decreases with increasing frequency. Furthermore, the loss angle becomes a maximum at the point at which dispersion reaches a maximum. Expressed in the language of the chemist, R_Δ increases with the capacitive dispersion in leaky dielectrics.

The capacitive I-dispersion for picric acid in ethanol and for aqueous sulfuric acid below the C.E.P., shown in Fig. 4 and 10, is of the same order of magnitude as that found in practical condensers. This perhaps means that the dispersion of C_k is caused by the same influence, viz., the slow movement of ions. But comparison of the curves below the C.E.P. with those above it shows that the

large increase in capacitive dispersion as the C.E.P. is exceeded is not accompanied by much increase in R_Δ (it should be recalled that $R_\Delta = R_s - R_o$).

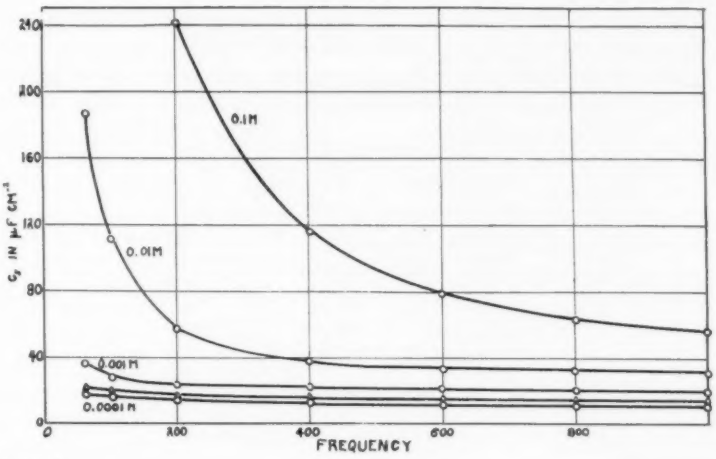

FIG. 6. Effect of concentration on the capacitive *I*-dispersion of the ferric-ferrous system in 0.5*M* sulfuric acid (given concentration = concentration of ferric sulfate = concentration of ferrous sulfate). ○—ferric-ferrous system in 0.5*M* sulfuric acid, △—0.5*M* sulfuric acid.

This would not be the case with practical condensers. The conclusion is that above the C.E.P. a new kind of capacitance is introduced. Our previous arguments suggest that it is a pseudocapacitance (C_p) and the experimental data just cited indicate that its dispersion is associated with a much lower R_Δ than is that of C_h.

The very high values of C_s associated with the reversible ferrous-ferric and ferrocyanide-ferricyanide systems (Fig. 6, 7, 8, and 11) must, because of their magnitude, be largely due to pseudocapacitance. The small double layer capacitance must also be present, however, so that $C_s = C_o + C_h + C_P$.

It is important to recognize that although pseudocapacitance is observed both in the reversible systems and in aqueous sulfuric acid, there are two important differences between these groups: (1) reversibility and (2) concentration of the molecular or ionic species undergoing oxidation and reduction. We shall distinguish these two cases by the symbols $C_{P(r)}$ for the reversible systems and $C_{P(w)}$ for solutions in which water is electrolyzed.

It was shown above that the large dispersion of $C_{P(w)}$ is not associated with a large R_Δ. That this is true also for $C_{P(r)}$ is shown by a comparison of Fig. 10 and 11. It is seen that the capacitive dispersion for the ferrous-ferric system in sulfuric acid is vastly larger than that for the acid alone whereas R_Δ is about the same in each.

In certain regards the *I*-dispersions of $C_{P(r)}$ and $C_{P(w)}$ seem to differ. The dispersions observed with the reversible systems (Fig. 6 and 7) can reasonably be explained qualitatively on the basis of Warburg's idea that diffusion is the slow process involved. Frequency dependency would follow. In the case of $C_{P(w)}$, however, a glance at Fig. 3 (sulfuric acid gives curves entirely similar to Fig. 3) shows that another factor is also involved in the dispersion. A dispersion curve can be constructed from Fig. 3

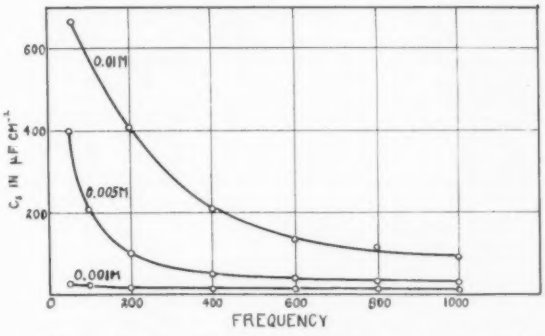

FIG. 7. Capacitive *I*-dispersion for the ferrocyanide-ferricyanide system (redox ratio unity and current density 0.05 ma cm^{-2} in each case).

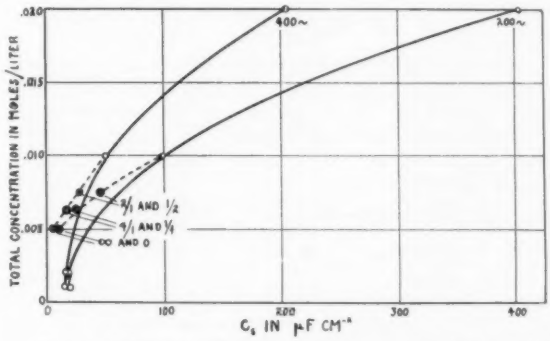

FIG. 8. Effect of redox ratio and concentration on the capacitive *I*-dispersion of the ferrocyanide-ferricyanide system in aqueous solution.——Redox ratio unity, - - - - variable redox ratio given by Figures. Current density 0.5 ma cm^{-2}.

by drawing a vertical line at any chosen value of current density and plotting its intersections with the given curves against C_s. The dispersion shown by the

resulting plot will depend upon how far beyond the C.E.P. the vertical line cuts each of the given curves. It will also depend on the slopes of the given curves. These slopes are quite possibly dependent on diffusion rates but the former factor cannot be. It is dependent on the factor which causes the C.E.P. to increase with the frequency. This must in turn be largely determined by the relationships of alternating

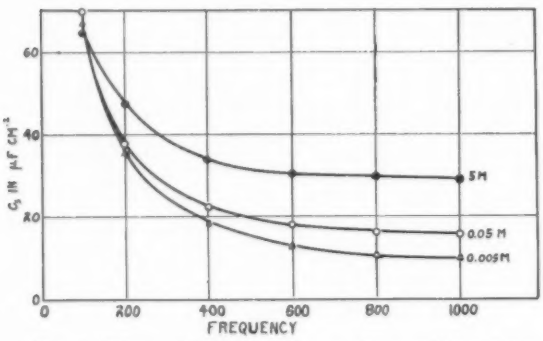

FIG. 9. Effect of concentration on the capacitive I-dispersion of sulfuric acid above the C. E. P. (current density 16.7 ma cm^{-2}). ●—$5M$, ○—$0.05M$, △—$0.005M$.

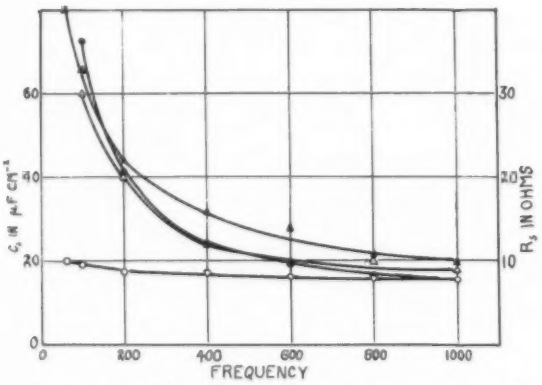

FIG. 10. Resistive and capacitive I-dispersions for $0.5M$ sulfuric acid. ○—C_S below the C.E.P. (0.5 ma cm^{-2}), ●—C_S above the C.E.P. (16.7 ma cm^{-2}), △—R_S below the C.E.P. (0.5 ma cm^{-2}), ▲—R_S above the C.E.P. (16.7 ma cm^{-2}).

current theory expressed in the equation

$$I_c = \frac{E_c}{X_c} = E_c C_i \omega. \qquad (X)$$

If, as a first approximation, we say that E_c and C_i are constants independent of the frequency and the current density, then I_c will increase with ω. Actually, however, both C_i and E_c (cf. Fig. 12) are slightly dependent on frequency so that equation (X) is not strictly valid. It is hard to believe, however, that it does not present an essentially correct picture of why the C.E.P. increases with the frequency.

$C_{P(r)}$ and $C_{P(w)}$ also differ in that the former is independent of current density and the latter increases with current density. If, as we believe, the C.E.P. is related to the activation energy hump associated with the electrolysis of water, then an increase in current density and the attendant increase in E would increase the reaction rate and hence increase $C_{P(w)}$. This influence would be absent when reversible systems are used. C.E.P.'s were,

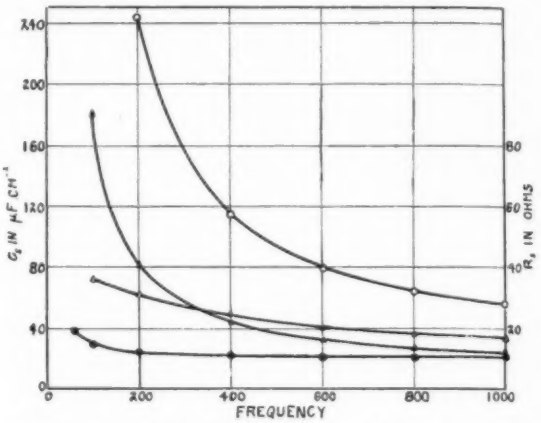

FIG. 11. Resistive and capacitive I-dispersions for the ferric-ferrous system in $0.5M$ sulfuric acid. ○—C_S for $0.1M$ ferrous sulfate, $0.1M$ ferric sulfate; ●—C_S for $0.001M$ ferrous sulfate, $0.001M$ ferric sulfate; △—R_S for $0.1M$ ferrous sulfate, $0.1M$ ferric sulfate; ▲—R_S for $0.001M$ ferrous sulfate, $0.001M$ ferric sulfate.

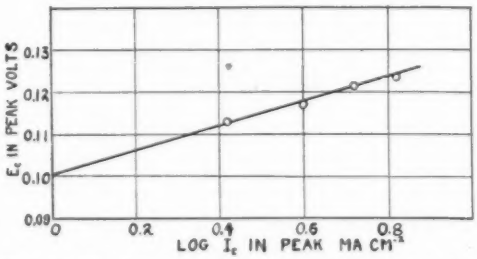

FIG. 12. The linear relation of E_c and log I_c for glycerol saturated with potassium iodide.

nevertheless, observed with our reversible systems (cf. Table I). Since the current densities used with these systems were far above the corresponding polarographic diffusion currents, it is likely that the range of initial capacitance exists because all of the active ions in the compact double layer react during the first small fraction of a cycle of alternating current (probably too small a time interval to give any evidence of distortion in the oscillographic wave). Beyond this point the electrolytic current is replaced largely by charging current, and an essentially constant capacitance results until the C.E.P. corresponding to the electrolysis of water is reached.

The effect of concentration on $C_{P(r)}$ is shown in

Fig. 6 and 7. It is adequately explained by recognizing that, at a given frequency, decreasing concentration results in fewer ions reaching the electrode per cycle. In the case of $C_{P(w)}$, the very high concentration of water at the electrode surface in all sulfuric acid solutions means that concentration of acid should have little effect on $C_{P(w)}$. Fig. 9, however, shows a divergence of the curves at higher frequencies where $C_{P(w)}$ is probably replaced largely by C_i, which is sensitive to changes in ionic concentration. The contrasting convergence of the curves at high frequencies shown in Fig. 6 means that, as

TABLE IV. *Effect of the redox ratio on the dispersion of the polarization capacitance in aqueous ferrocyanide-ferricyanide solution for M/200 oxidant. Current density: 0.5 ma cm⁻²*

Frequency	Redox ratio			
	1/1	2/1	4/1	∞
50	400 μf cm⁻²	200	70.0	14.3
100	204	100	40.4	13.0
200	100	46.5	25.2	12.0
400	50.3	29.0	16.6	11.0
600	40.0	22.7	16.2	10.5
800	34.0	19.8	15.1	10.3
1000	32.4	18.4	14.4	10.0

TABLE V. *Effect of the redox ratio on the dispersion of the polarization capacity in aqueous ferrocyanide-ferricyanide solutions for M/200 reductant. Current density: 0.5 ma cm⁻²*

Frequency	Redox ratio			
	1/1	1/2	1/4	0
50	400 μf cm⁻²	200	46.5	17.3
100	204	100	30.4	16.1
200	100	46.5	22.0	14.8
400	50.3	28.7	17.0	13.8
600	40.0	21.7	15.7	13.3
800	34.0	19.7	14.7	12.9
1000	32.4	18.0	14.0	12.5

$C_{P(r)}$ drops out, C_s approaches the almost constant value of C_i which is largely determined by the concentration of the acid serving as solvent.

The effect of the redox ratio is shown in Fig. 8 and in Tables IV and V. The dotted lines in Fig. 8 were constructed from the data in those tables. The curves make clear that the observed effect is only partially the effect of total concentration. It can also be shown by similar plots that the redox ratio exerts an influence that cannot be interpreted solely in terms of the concentration of the least concentrated component of an oxidation-reduction system. The data presented seem to justify the conclusion that the polarization capacitance of a reversible oxidation-reduction system decreases as the redox ratio departs from unity when the total concentration is constant. It is particularly significant that a reversal of the redox ratio from 2/1 to 1/2 makes no appreciable difference. The reversal from 4/1 to 1/4 points to the same conclusion, although here the agreement is not as good. There are several alternative theoretical explanations of these results between which we cannot choose at the present time. We hope to solve the problem by further experimental work. We can say, however, that the observed influence of the redox ratio is probably related to its significance in the Nernst equation and it thus constitutes some small measure of additional evidence in favor of the theory that the high capacitances observed with our reversible redox systems have a chemical origin.

Acknowledgment

We wish to express our deep appreciation to Dr. W. H. Bixby of Wayne University's Department of Electrical Engineering for his generous help in designing the amplifier used in our work and for much helpful advice. We are also indebted to Dr. D. C. Grahame of Amherst College for his critical reading of our original manuscript.

Any discussion of this paper will appear in a Discussion Section, to be published in the June 1951 issue of the JOURNAL.

REFERENCES

1. D. REICHENSTEIN, *Z. Elektrochem.*, **15,** 913, (1909).
2. J. W. SHIPLEY, *Can. J. Research*, **1,** 305 (1929).
3. J. W. SHIPLEY AND M. J. ROGERS, *Can. J. Research*, **17B,** 147 (1939).
4. (*a*) F. KOHLRAUSCH AND W. A. NIPPOLDT, *Ann. Physik u. Chem.* [1], **138,** 280 (1869).
   (*b*) F. KOHLRAUSCH, *Ann. Physik u. Chem.* [1], **148,** 143 (1873); "JUBELBAND," *Ann. Physik u. Chem.* [1], 290 (1869).
5. (*a*) M. WIEN, *Ann. Physik u. Chem.* [3], **58,** 37 (1896).
   (*b*) *Ibid.*, **59,** 267 (1896).
   (*c*) *Ibid.* [4], **8,** 372 (1902).
6. R. BLANDLOT, *J. Phys.*, **10,** 277 (1881); **18,** 275 (1924).
7. E. NEUMANN, *Ann. Physik u. Chem.* [3], **67,** 500 (1899).
8. E. WARBURG, *Ann. Physik u. Chem.* [3], **67,** 493 (1899).
9. (*a*) A. OBERBECK, *Ann. Physik u. Chem.* [3], **19,** 213, 265 (1883); **21,** 139 (1884).
   (*b*) C. M. GORDON, *Ann. Physik u. Chem.* [3], **61,** 1 (1897).
   (*c*) P. SCHONHERR, *Ann. Physik u. Chem.* [4], **6,** 116 (1901).
   (*d*) N. THON, *Compt. rend.*, **200,** 54 (1935).
10. (*a*) F. KRUGER, *Z. physik. Chem.* **45,** 1 (1903).
    (*b*) E. MERRITT, *Phys. Rev.*, **17,** 524 (1921).
    (*c*) C. B. JOLIFFE, *Phys. Rev.*, **22,** 298 (1923).
    (*d*) K. F. SUN, *Phys. Rev.*, **23,** 617 (1924).
    (*e*) G. JONES AND S. M. CHRISTIAN, *J. Am. Chem. Soc.*, **57,** 272 (1935).
11. (*a*) W. A. TAYLOR AND H. L. CURTIS, *Phys. Rev.*, **6,** 61 (1915).
    (*b*) R. T. LATTEY, *Phil. Mag.*, **50,** 444 (1925).

12. (*a*) H. F. Haworth, *Trans. Faraday Soc.*, **16,** 365 (1920).
(*b*) C. C. Murdock and E. E. Zimmerman, *Physics*, **7,** 211 (1936).
13. D. Gunther-Schulze, *Z. Physik*, **6,** 237 (1921).
14. A. M. Scott, *Ann. Physik u. Chem.* [3], **67,** 388 (1899).
15. I. Wolff, *Phys. Rev.* [2], **27,** 755 (1926).
16. W. A. Taylor and S. F. Acree, *J. Am. Chem. Soc.*, **38,** 2415 (1916).
17. W. G. Smiley and A. K. Smith, *J. Am. Chem. Soc.*, **64,** 624 (1942).
18. D. C. Grahame, *Chem. Rev.*, **41,** 441 (1947).
19. (*a*) D. C. Grahame and R. B. Whitney, *J. Am. Chem. Soc.*, **64,** 1548 (1942).
(*b*) D. C. Grahame, *J. Am. Chem. Soc.*, **68,** 301 (1946).
20. D. C. Grahame, *J. Am. Chem. Soc.*, **63,** 1207 (1941).
21. T. Erdey-Gruz and G. G. Kromrey, *Z. physik. Chem.* **157A,** 213 (1931).
22. B. Breyer and F. Gutmann, *Disc. Faraday Soc.*, **1,** 19 (1947).
23. T. R. Rosebrugh and W. L. Miller, *J. Phys. Chem.*, **14,** 816 (1910).
24. W. L. Miller and A. R. Gordon, *J. Phys. Chem.*, **35,** 2785, (1931).
25. N. Thon, *Compt. rend.*, **198,** 1681 (1934).
26. O. Stern, *Z. Elektrochem.*, **30,** 508 (1924).
27. E. von Schweidler, *Ann. Physik u. Chem.*, **24,** 711 (1907).
28. E. Bouty, *Compt. rend.*, **116,** 628 (1893).
29. S. Glasstone, "Introduction to Electrochemistry," D. van Nostrand Co., New York (1942).
30. J. O. M. Bockris, *Disc. Faraday Soc.*, **1,** 232 (1947).
31. (*a*) A. Gemant, "Liquid Dielectrics," pp. 78–96 John Wiley & Sons, New York (1933).
(*b*) J. B. Whitehead, "Lectures on Dielectric Theory and Insulation," McGraw-Hill Book Co., Inc., New York (1927).

Studies on Alternating Current Electrolysis

II. Oscillographic Studies[1]

JACOB SILVERMAN[2] AND A. EDWARD REMICK

Department of Chemistry, Wayne University, Detroit, Michigan

ABSTRACT

Reichenstein's oscillographic study of the alternating current electrolysis of aqueous sulfuric acid was repeated. His contention that the instantaneous value of the cell voltage at zero instantaneous current, corrected for iR drop, approaches a limiting maximum value as the rms value of the current increases was found to be true; but his statement that this maximum voltage is the thermodynamic decomposition potential of water was not verified. Actually, it turns out that this voltage includes the associated overvoltage. Oscillographic studies were also made on two reversible redox systems. Variations produced by changes in current density, concentration, frequency, and redox ratio were explained in terms of a qualitative theory.

INTRODUCTION

The field of alternating current electrolysis seems to offer rich possibilities of obtaining important fundamental knowledge related to reaction mechanisms, especially in view of the possibility of using modern electronic equipment. The cathode ray oscillograph, in particular, seems to hold great promise, and it is, therefore, surprising to find almost no published evidence of its use in this field, although it has been rather extensively used in polarography.

The first attempt to use the oscillograph in studying alternating current electrolysis was made in 1909 by Reichenstein (1) who used a very crude instrument. He obtained oscillograms (Lissajou's figures) which showed the instantaneous values of current and voltage across an electrolytic cell. In order to compensate for the iR drop of the solution so that the oscillogram would show only the voltage associated with the capacitive reactance of the cell, he determined the solution resistance, R_T, independently. Subtracting the instantaneous values of iR_T from the instantaneous values of the cell voltage and plotting the difference, e_b, against the instantaneous values of the current, i, gave figures which he referred to as "pure characteristics." In a study of aqueous sulfuric acid, using platinized platinum electrodes, he made two important observations: (1) the maximum value of e_b always occurs at the point where $i = 0$ and (2) as the voltage is increased the values of e_b at $i = 0$ approach a maximum of 1.2 volts, which is very close to the thermodynamic decomposition potential of water. Reichenstein considered that his method could be used for the determination of this potential.

A few years prior to Reichenstein's work, Hopkinson, Wilson, and Lydall (2) devised a mechanical method by means of which they could pick off instantaneous values of current and voltage across an electrolytic cell and plot an e-i cyclogram. Furthermore, they attempted to use a probing electrode between the electrolyzing electrodes to follow the variations in potential at a single electrode. Their results shed little light on the nature of electrode phenomena. Furth (3) also used a similar device, but, beyond a description of the device, no experimental data were given.

Interesting oscillographic studies were made by Acree, Bennett, Gray and Goldberg (4), who devised a method of studying the rate of cell discharge when the alternating current was interrupted at any desired point during a cycle. These studies revealed that the rate of discharge was fastest at peak current and slowest at zero current, thus showing that the back emf of the cell is capacitive in nature and lags the current by 90°.

Recently two papers of related interest have appeared (5). Sevcik (5*a*) utilized an alternating current whose wave-form was triangular. Randles (5*b*) devised an oscillographic method by means of which he was able to determine the rate constant for the electrode reaction occurring when a dropping amalgam electrode was subjected to an alternating potential relative to the solution.

Very little work has been done on the interpretation of distorted wave-forms observed during al-

[1] Manuscript received July 20, 1949. This paper prepared for delivery before the Chicago Meeting, October 12 to 15, 1949. It is an abstract of the thesis presented by Jacob Silverman to the graduate faculty of Wayne University in partial fulfillment of the requirements for the Ph.D. degree.

[2] Ethyl Corporation Fellow. Present address: Department of Chemistry, University of Southern California, Los Angeles, California.

ternating current electrolysis at sufficiently high current densities. The theoretical papers of Cooper (6) and Shipley (7) leave much to be done.

Purpose of Investigation

Reichenstein's claim that the limiting value of e_b at $i = 0$ corresponds to the thermodynamically reversible cell potential in the case of aqueous sulfuric acid is so important in its implications that his experiments deserve verification by the use of modern equipment. This verification was the first objective of our study. Our second and major objective was to study the wave distortion accompanying alternating current electrolysis of sluggishly reversible systems, like aqueous acids, and of actively reversible ones, like the ferric-ferrous system, when the current densities employed fall in the range between the capacitive elevation point (8) and the critical current density (9), i.e., in the range in which cyclical electrochemical reaction occurs without the net production of electrolytic products. Since oscillographic studies of the periodic variations of cell voltage show only the additive instantaneous effects of each of the electrode processes plus the iR drop across the cell, we faced the additional problem of devising a technique whereby the variations of potential occurring at a single electrode could be studied.

Experimental

Apparatus.—The cell and the electrodes were constructed in the manner described in the first paper of this series (8) except that the rubber stopper carried also a thermometer in the experiments of Part 1 of this paper, while in the experiments of Part 2 it carried, in addition to the two "working electrodes," a third electrode (hereafter referred to as the "dummy electrode") consisting of a long platinum wire which was bent into a planar curve resembling a sine wave. The dummy electrode was placed halfway between the working electrodes with its plane parallel to them. The electrodes used in Part 1 were parallel, one centimeter apart and each one had a surface area of 0.14 cm². In Part 2, the electrodes were approximately one centimeter apart and parallel; each one had an area of 0.45 cm². The electrodes were cleaned by electrolysis in an alkaline cyanide solution as previously described (8).

In both series of experiments the source of the alternating current passing through the electrolytic cell was a Jackson Audio-Frequency oscillator, Model 652, whose output was amplified by a push-pull amplifier. The oscillograph was a Dumont instrument, type 208B, which was powered by the Detroit Edison Company's supply through a Sola constant voltage transformer, Model 30806, as was also the oscillator. All voltage readings in Part 1 were taken with a Radio City Products electronic voltmeter, Model 664, and in Part 2 by a Ballentine electronic voltmeter, Model 643, whose range was 0.001–100 rms volts. A "Queen" potentiometer, Model E-3040, was used when it was necessary to measure d-c voltages. This instrument is capable of reading voltages down to 10^{-6} v.

Experiments—Part 1

These experiments were made for the purpose of checking Reichenstein's work. The circuit which was used is pictured in Fig. 1. A is the alternating current source, C is the electrolytic cell, R a Leeds & Northrup decade resistance #4776, and S is the oscillograph. With connections made as shown, the oscillograms registered the current on the vertical axis and the cell voltage on the horizontal axis. The electrolytic solution consisted of 20 per cent aqueous sulfuric acid and was prepared from Baker's C.P. acid by approximate dilution. Quantitative knowledge of the acid concentration was unnecessary.

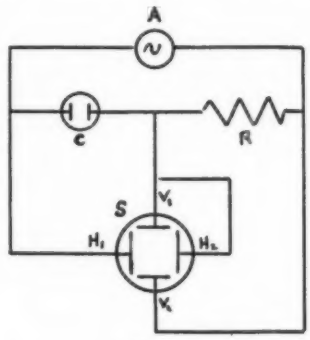

Fig. 1

The horizontal axis of the oscillograph was calibrated in instantaneous volts in an obvious manner by substituting a pure resistance for the cell in Fig. 1. There was no need to calibrate the vertical axis since the only readings of interest were the instantaneous values of the voltage when $i = 0$ (hereafter referred to as v_o). The values of v_o are not, of course, associated with any iR drop.

Reichenstein never performed any experiments other than those with platinized electrodes and at current densities at and below 1.0 amp cm^{-2}. In our studies, the values of v_o were measured over a wide range of current densities and electrode conditions at a frequency of 60 cycles per second.

The data listed in Tables I and II are typical of the results obtained. It was realized, of course, that the listed current densities, especially when platinized electrodes were used, are apparent values

only. Currents (I) are given in rms amperes, and current densities in rms amp cm^{-2}.

In the experiments using bright platinum electrodes, the electrode surfaces appeared at the end of each run to be covered with a thin, uniform layer of platinum black. This behavior of platinum electrodes in alternating current studies has been noted by many previous investigators.

The temperature rises observed are in no case a serious source of error since even a 5 degree rise would decrease v_o by only 0.01 v.

TABLE I. *Variation of v_o with current density (I_d) using bright platinum electrodes*

Temperature (°C)	Cell voltage ($i = 0$)(v_o)	Current density (I_d)
27.5	0.90	0.15
27.5	1.18	0.29
27.5	1.44	0.50
27.5	1.55	0.72
27.5	1.64	0.93
28.0	1.66	1.14
28.1	1.64	1.28
28.5	1.66	1.43

TABLE II. *Variation of v_o with current density using heavily platinized electrodes (area 0.07 cm²)*

Temperature (°C)	v_o (volts)	I_d (amp/cm²)
27.0	0.37	0.71
27.0	0.51	1.43
27.5	0.79–1.10	2.14
27.9	1.18	2.86
27.9	1.24	3.57
28.1	1.22	4.28
28.5	1.32	5.00
28.9	1.38	5.72
29.0	1.47	6.43
29.7	1.58	7.14
29.9	1.63	7.85
30.0	1.66	8.58
30.1	1.66	9.29
30.2	1.66	10.00
30.7	1.66	10.70

Table I shows that the limiting value of v_o with initially bright platinum electrodes is 1.66 v. When lightly platinized electrodes were used, this limiting value rose to 1.72 v. In another experiment, in which the electrodes were very lightly platinized by a-c electrolysis in aqueous sulfuric acid, 1.64 v was the limiting value of v_o.

When heavily platinized electrodes were used, it was found impossible to attain a limiting value of v_o at the highest currents our amplifier could deliver, so smaller electrodes had to be used. The results are shown in Table II. It is of interest to note that at $I_d = 2.14$ amp cm^{-2}, there is a sudden rise in v_o. The attendant instability is again replaced by stability at 3.57 – 4.28 amp cm^{-2}, where v_o seems to have little tendency to change. It is perhaps significant that here the value of v_o is close to Reichenstein's limiting value of 1.2 v. But further increase of the current density results in a further increase of v_o values until the final limiting value of 1.66 v is again attained. At the end of the experiment the electrodes appeared gray instead of black, as they were initially, indicating a loss of platinum.

Experiments—Part 2

These experiments were concerned chiefly with making photographic records of oscillograms, some of which are reproduced in this paper. All measuring instruments and circuit elements were connected through a switchboard which enabled the operator to alter circuit arrangements and make various oscillograph and voltmeter measurements across any or

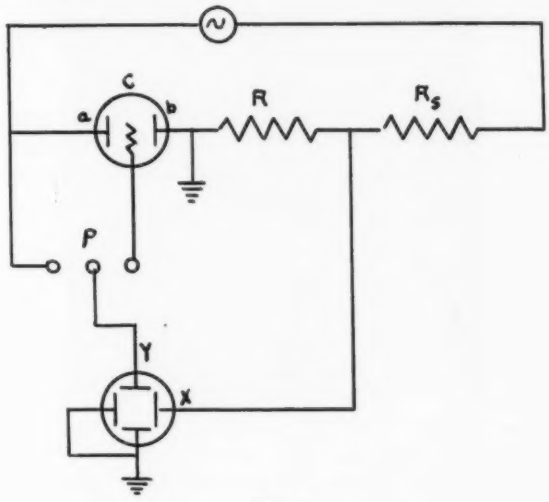

FIG. 2

all of the circuit elements in rapid succession. All wiring was done with shielded cable. The circuit diagram is shown in Fig. 2. The cell, C, contains two working electrodes, a, and b, as well as the dummy electrode. A requirement for a sinusoidal current through the cell is that $R_s + R >> Z_{cell}$. For this purpose, $R_s + R$ should be about 2000 ohms. With the circuit shown, the oscillograph will register cell voltages on the vertical plates and current variations (i.e., iR) on the horizontal plates. The switch P makes possible two different choices of electrode pairs: either a and b or b and the dummy.

Oscillograms involving the voltage drop between the two working electrodes are of very little use in studying the mechanism of electrode processes, since each electrode is undergoing variation and the recorded voltage at any instant is merely the sum of these two variable voltages, plus the iR drop. How-

ever, since no current is passing through the dummy electrode, its potential is constant and hence the variations in potential between the dummy and one of the working electrodes shows in reality the potential variations at a single electrode, plus about half of the iR drop through the solution between the two working electrodes. Fig. 3 shows two cyclograms obtained by double exposure of the photographic film. The larger one shows the variations in full-cell potential while the smaller one shows the corresponding variation in the half-cell potential. A glance at the smaller cyclogram will show that the changes taking place at the anode are by no means equal and opposite to those taking place at the cathode—a point of the utmost importance which is obscured entirely in the full-cell cyclogram.

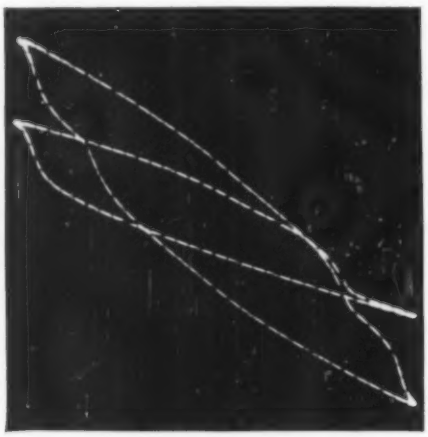

FIG. 3. 0.1M $FeSO_4$ in N H_2SO_4 at 100 c/sec

All of the experiments recorded in this section were made with smooth platinum electrodes. All chemicals used were of the best analytical grades obtainable commercially. The stock solution of ferrous sulfate was stored under purified nitrogen. The ferrous salt was standardized potentiometrically by titration with standard dichromate in a nitrogen atmosphere at constant temperature. The ferric sulfate was standardized with the standard ferrous sulfate solution by the potentiometric method of mixtures. The standard solutions of potassium ferrocyanide and ferricyanide were prepared by weighing out suitable amounts of the dry salts on an analytical balance. Greater accuracy by standardization was deemed unnecessary in view of the relatively large errors involved in reading the oscillograph. All experiments were conducted at 30°C in a constant temperature oil bath.

Each of the photographs which show three cyclograms involve the following constant sets of conditions unless otherwise specified: (1) frequency, 100 c/sec; (2) calibration of vertical axis, 100 mv per scale division; (3) the three cyclograms correspond to current densities of 22.2, 55.5, and 88.8 rms ma cm^{-2}, respectively. The highest of these current density values is low enough to avoid platinization of the electrodes. (4) Cathodic potentials relative to the dummy electrode are above the horizontal axis.

Further discussion of the photographs will be given in the final section of this report.

Discussion

Part 1.—Our experiments with sulfuric acid lead immediately to two conclusions: (1) the values of v_o reach a maximum as the current density is increased, as Reichenstein claimed, and (2) the maximum value does not correspond to the reversible potential of the hydrogen-oxygen cell (1.23 v) as Reichenstein claimed it does, but rather to a higher value (1.64 to 1.72 v) which apparently depends somewhat on the extent of platinization of the electrodes. The closely similar value of the experimental decomposition potential of water (1.67 v for H_2SO_4) suggests very strongly that the maximum value of v_o includes the hydrogen and oxygen overvoltages. Presumably Reichenstein failed to discover this fact because his current densities were kept at or below 1.0 amp cm^{-2}. That the overvoltage should be involved does not seem at all strange in view of the modern theory of overvoltage [which considers that it is the primary step in both hydrogen and oxygen discharge which is the rate-controlling step (10)] especially in view of the fact that one-half wave of 60 cycle alternating current allows only 1/120 sec for reaction to take place. It would take a powerful catalyst indeed to bring a normally slow reaction to equilibrium in that length of time.

Part 2.—Before attempting to interpret the cyclograms in terms of fundamental theory, it is necessary that a few important points of a noncontroversial nature be explained.

The oscillograph is so constructed that the traces move in a clockwise direction. Furthermore, quadrants III and IV represent positive polarization of the working electrode relative to the dummy while quadrants I and II are those of negative polarization. An electron current flows to the electrode through quadrants III and II and away from it in quadrants I and IV.

The equivalent circuit representing an a-c electrolytic cell involves the following circuit elements: R_T, the "true" resistance of the electrolyte in the cell; R_Δ, the polarization resistance; C_d, the double-layer capacity; C_p, the pseudocapacity. The equivalent series resistance of the cell is designated as R_s; it is equal to the sum of R_T and R_Δ. The equivalent series capacitance of the cell is designated as C_s; it

is conveniently assumed to be equal to the sum of C_d and C_p. The characteristics of these quantities were discussed in the first paper of this series (8).

If the cell acted as a pure resistance, the cyclogram would consist of a straight line through the origin whose angle with the horizontal axis would be determined by the magnitude of R. If the cell combined the characteristics of a resistance and capacitance, the figure would be an ellipse and the angle between its major axis and the horizontal axis of the screen would again be determined by the magnitude of R. Any distortion in an ellipse may be ascribed to nonlinear circuit elements such as C_p and probably R_Δ.

When it is desired to study the polarization of an electrode, "pure characteristics" constructed in the manner of Reicheinstein are satisfactory only in the absence of an appreciable R_Δ. When half-cell cyclograms are involved, we may define a resistance, R_e, as: $R_e = R_T/2 + R_\Delta$ in which R_Δ is now understood to be the contribution made to the total polarization resistance by a single working electrode. If now a line representing iR_e be drawn through the the origin, a more satisfactory "pure characteristic" than Reichenstein's can be constructed graphically by subtracting instantaneous values of iR_e from the ordinates of the points on the ellipse. We do not yet know enough about R_Δ to state with certainty that this iR_e line would be linear. Nevertheless, it seems likely in view of evidence presented at the end of this paper that R_Δ is essentially constant. With this assumption, the iR_e line can be constructed graphically as shown in Fig. 6 by the X_1', X_2' axis which is drawn through the origin parallel to the straight line *dzf*. The justification for this procedure lies in the argument that throughout a linear portion of a cyclogram the potential of the working electrode is in phase with the current. There are two possible explanations: (1) if the potential be regarded as an impedance drop iZ, then the reactance must be zero; (2) if the potential be regarded as the sum of an iR_e drop and a back emf e_b, then e_b must be constant during the linear portion of the cyclogram. In either event, the linear portion would have the same slope as the iR_e line and hence the iR_e line will be parallel to it (or coincident with it) and will pass through the origin. It is to be noted that the second of the above explanations must apply to Fig. 6 since the linear portion does not pass through the origin.

For most purposes it is unnecessary actually to construct pure characteristics since they will look like the total characteristics except for a more condensed appearance and the fact that their axes will coincide with those of the oscillograph screen. Fig. 6 shows a simple method of constructing axes in terms of which the pure characteristics can be accurately visualized. In addition to the axis X_1 X_2, which has already been explained and which becomes the major axis of the pure characteristic, the lines Y' are drawn perpendicular to X_1X_2 and through the points where the total characteristic cuts the vertical axis of the screen. These points are the v_o points and are identical on both the total and pure characteristics. As X_1X_2 is rotated to a horizontal position in drawing a pure characteristic, the two Y' lines move toward the origin and pass through it in the pure characteristic. Thus, the points X_1, X_2, a and z represent the intersection of the pure characteristic with its own major and minor axes.

Another point of importance in interpreting cyclograms is the realization that convex portions (the point of observation is considered to be outside of the cyclogram) of the cyclograms may occur when de/dq (the rate of change of potential with the quantity of electricity which has passed during any portion of a half-wave) is increasing, is constant, or is decreasing slightly, but concave portions may occur only when de/dq is decreasing rapidly.

We are now ready to consider the points of basic physicochemical theory which are necessary for the interpretation of cyclograms. They are two in number. (1) When electrolysis of a mobile redox system is occurring, the ions which are close enough to the electrode enter into essentially instantaneous equilibrium with it; accordingly, the equilibrium in the electron transfer reaction involved may be described by means of the Nernst or the Peters equations (11). (2) In view of the statement just made, the fugacity (or escaping tendency) of the electrons on the electrode must at every instant of time equal the fugacity of the (bound) electrons in the layer of solution adjacent to the electrode. This means that the current will undergo a partition between electrode and solution in a manner regulated by the relative values of de/dq for the electrode charging process and for electrolysis. If at a given instant of time the redox system in the electrode layer is in its poised region, de/dq for electrolysis will be much smaller than de/dq for the charging of the electrode[3] and hence the former will be the rate-controlling process, i.e., de/dq will be regulated by the Nernst equation. Conversely, if the redox ratio is close to 0 or ∞, then de/dq for the charging of the electrode will be the rate-controlling process, i.e., de/dq will be regulated by the electrostatic capacitance of the electrical double layer. It is obvious, of course, that the instantaneous value of the redox ratio in the

[3] It is interesting to note that Grahame (12), in his study of the polarization capacitance of cadmium chloride, showed that the capacitance reached a maximum at about the half-wave potential. This is equivalent to the statement that de/dq is a minimum at the normal potential of the Cd-Cd^{++} system.

electrode layer is not generally the same as that in the bulk of the solution and is dependent on diffusion rates and on the magnitude and frequency of the alternating current.

With these few fundamental concepts in mind, we may now analyze the cyclograms obtained experimentally to see if the suggested theory is able to give an unambiguous interpretation of them.

(*A*) *Normal Sulfuric Acid*

The use of normal sulfuric acid as solvent for the ferric-ferrous studies made it mandatory that the effects of the solvent be distinguishable from those of the solute. Consequently, oscillographic studies were made on normal sulfuric acid in the range of

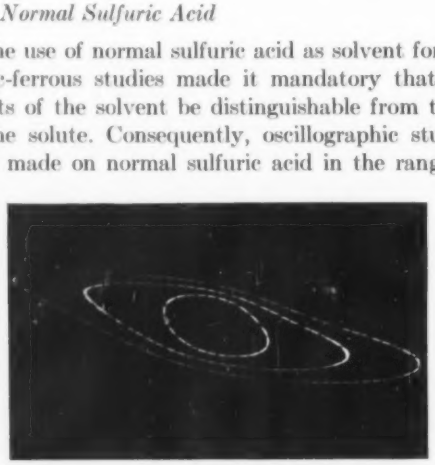

FIG. 4. *N* H_2SO_4

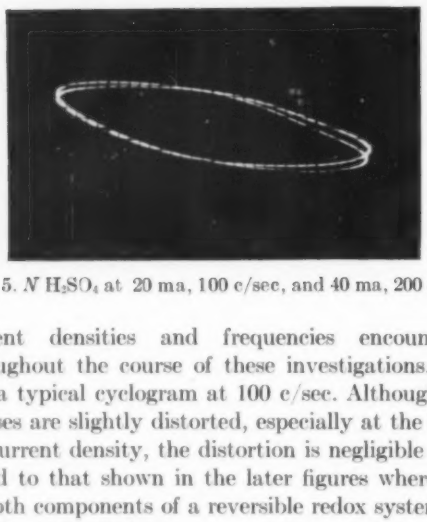

FIG. 5. *N* H_2SO_4 at 20 ma, 100 c/sec, and 40 ma, 200 c/sec

current densities and frequencies encountered throughout the course of these investigations. Fig. 4 is a typical cyclogram at 100 c/sec. Although the ellipses are slightly distorted, especially at the highest current density, the distortion is negligible compared to that shown in the later figures where one or both components of a reversible redox system are added as depolarizers.

(*B*) *The Reductant Solutions*

(*1*) *$FeSO_4$ in N H_2SO_4.*—Reference to Fig. 6 discloses striking similarities to the well-known d-c polarographic phenomena. The cyclograms are of 0.1*M* $FeSO_4$ and are interpreted strictly in terms of the pure characteristic based upon the new axis *X'*.

It is convenient to initiate discussion with point *b* at which time the electrode is an anode. The sharp anodic rise from *b* to *c* is quite analogous to the ordinary d-c electrode polarization preceding the discharge of an oxidizable ion. This is the region in which the rate-controlling process is primarily dielectric, i.e., de/dq is regulated by the electrostatic capacitance of the electrical double layer.

The concave region *c* represents the inauguration of oxidation of Fe^{++}. Similar to the d-c analogue, a region of 60–80 ma is traversed at *c* immediately prior to the entrance of the system into a region of almost constant potential *cdz* which represents the poised region of the thermodynamically reversible system Fe^{+++}/Fe^{++}.

At *z*, the electrode becomes a cathode and since the system Fe^{+++}/Fe^{++} is quite mobile, reduction of Fe^{+++} begins immediately at *Z* and proceeds at constant potential until the system reaches the extremities of the poised region at *f*. The region *zf* is,

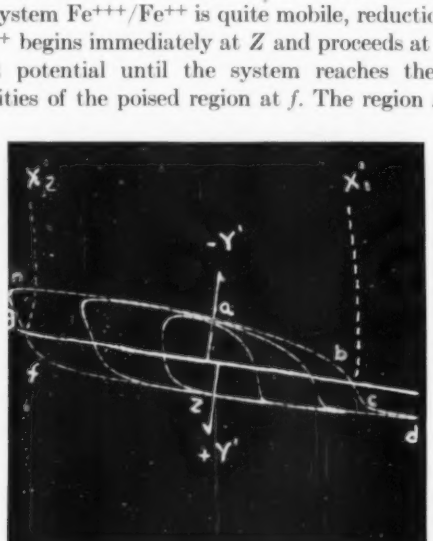

FIG. 6. 0.1*M* $FeSO_4$ in *N* H_2SO_4

consequently, one in which chemical polarization is rate-controlling and, as a matter of fact, $de/dq \approx 0$ in the poised region.

At *f*, as the system leaves the poised region, dielectric polarization reappears and subsequently predominates in the sharp cathodic rise *f* to *g*. The slight concavity at *g* suggests the inauguration of reduction although the unsharp character of the cathodic tail *gh* as compared to the sharp anodic tail *cd* indicates that the component reduced at *g* does not compare favorably in mobility to that oxidized at *c*. Realization that the only reducible component at *g* is H^+ lends strength to the above interpretation of *gh* since it is well known that H^+ is at best a sluggishly reducible ion at bright Pt. The segment *ha* shows a constancy in potential which compares favorably with the constancy of *cdz* and, in fact, is parallel to it. Thus, the segment *ha* is a region in which chemical action again is rate-controlling.

At *a*, the electrode becomes an anode again and,

as expected, the poor reversibility of the H^+/H system is manifest in the gradual anodic rise of *ab* immediately following reversal at *a*. The latter is in sharp contrast to the behavior of a thoroughly reversible system illustrated at current reversal point *z*.

An interesting development resulting from the study of such half-cell cyclograms is the following. Referring again to Fig. 6, it is noted that the anodic rise *bc* and cathodic rise *fg* do not take place at the same instant. Of course, it is obvious that these are segments of dielectric polarization. The interesting observation is that the cathode is reducing while the anodic rise *bc* takes place at the other working electrode and, conversely, the anode is oxidizing while the cathodic rise *fg* occurs. The conclusion which must be drawn is that *at any instant, there may be oxidation without reduction and vice versa.* Of course, over a complete cycle the amount of oxidation must equal the amount of reduction.

There is another point of importance already evident from Fig. 6. At *a* and *z*, the instantaneous values of current at both working electrodes are zero. Both points signify simultaneous current reversal. Since *a* and *z* represent the same instant of time at the two working electrodes, respectively, the difference in potential between *a* and *z* is the potential difference between two electrodes at $i = 0$, i.e., the cell potential v_o, exclusive of all iR drops. It is, furthermore, obvious that v_o approaches a maximum value in the region of 0.75 v. This maximum is independent of Fe^{++} concentration (above $0.03M$), frequency (100–300 c/sec), current density and distortion, and is reproducible within the experimental error involved in reading the oscilloscope, i.e., $\pm$ 0.015 v.

The existence of this maximum in the region of current densities employed is not unexpected. Since the point *z* is in the poised region of a completely reversible system, the potential at *z* will be determined by the Nernst ratio. For the Fe^{+++}/Fe^{++} system, this value is 0.78 v relative to the normal hydrogen electrode. The potential of the other electrode would be that of the sluggishly reversible hydrogen half-cell. This would be expected to be slightly more negative on the scale of reduction potentials than the value 0.00 v associated with the normal hydrogen electrode, so that the cell potential should be more than 0.78 v. We have just seen that the limiting value of v_o is about 0.75 v. Probably other factors are also involved.

An increase in frequency always results in a decrease in distortion. This would be expected if the chemical polarization is associated with a slow step, such as diffusion, for then a greater fraction of the coulombic charge is diverted to dielectric polarization. The same effect might also result from the fact that, working at constant current density, an increase in frequency would diminish the amount of electricity available during a half cycle so that less chemical polarization would ensue even if the partition of coulombic charge remained constant. Decreasing the concentration also lessens distortion, as would be predicted from the partition theory.

For any particular concentration, as evidenced in Fig. 6, increase in current density shifts the partition of electricity between chemical and dielectric polarization in favor of the former. This appears to be true at concentrations which are high enough so that the depolarizer available at the electrode surface is not exhausted by the highest current densities attained at that surface prior to current reversal. Exhaustion of depolarizer before current reversal results in loss of distinctive distortive character. Thus increase in current density at low concentration or decrease in concentration at constant current density leads to identical results, viz., loss of distinctive distortive character. In contrast, at reasonably high concentrations ($> 0.05M$ for Fe^{++}) increase in current density leads to sharper distortion.

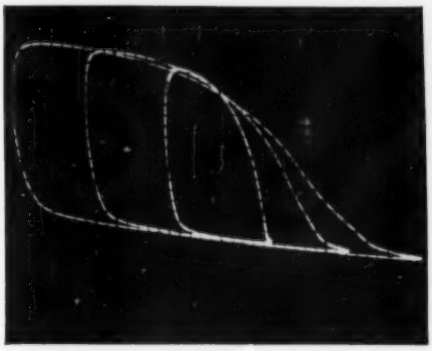

FIG. 7. $0.5M$ aqueous $K_4Fe(CN)_6$

(2) *$K_4Fe(CN)_6$ in water.*—Results with aqueous solutions of $K_4Fe(CN)_6$ are entirely similar to those obtained with $FeSO_4$. Fig. 7 is that of $0.5M$ $K_4Fe(CN)_6$. The absence of H_2SO_4 (necessary to prevent decomposition of depolarizer) necessitated the use of higher concentrations of reductant in order to make the conductance of the solution reasonably high. All the arguments previously mentioned apply equally well to the now familiar cyclogram distortion of the reductant solution. The cyclogram shows the existence of a maximum for v_o at 1.5 v. The magnitude of this maximum strongly suggests unusually high H_3O^+ discharge overvoltages. The same conclusion follows from a consideration of the character of the cathode to anode reversal point which indicates considerable dielectric character in the region of H_3O^+ discharge. Such a conclusion is further sup-

ported by the experimental fact that the value of v_o for $K_4Fe(CN)_6$ is susceptible to changes in frequency. As the frequency is increased and the half-cycle time available for H_3O^+ discharge is decreased, so that a larger percentage of the half-cycle coulombic charge is diverted to dielectric polarization, the maximum gradually fades, becoming nonexistent at 500 c/sec. No maximum would be expected, of course, for dielectric polarization.

(C) The Oxidant Solutions

Illustrative of the behavior of pure oxidant solutions is Fig. 8 showing characteristic cyclograms of $0.2M$ $Fe_2(SO_4)_3$ in N H_2SO_4. No reproducible results

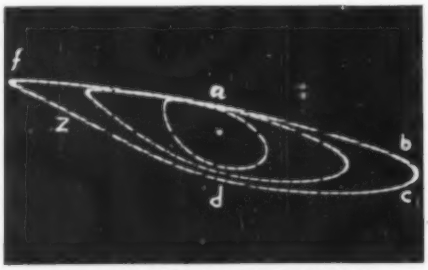

FIG. 8. $0.2M$ $Fe_2(SO_4)_3$ in N H_2SO_4

FIG. 9. $Fe^{+++}/Fe^{++} = 0.1M/0.1M$ in N H_2SO_4

were obtainable with aqueous solutions of $K_3Fe(CN)_6$ apparently because of reaction of the oxidant with the Pt, manifest by the formation of a blue-green crust at the electrode surface during electrolysis.

Reference to Fig. 8 discloses some points of major interest. The approximately straight line segment *fab* ($de/dq = 0$) again is interpreted as the reduction of Fe^{+++} and subsequent reoxidation of Fe^{++}. Interestingly enough, beyond *b*, the cyclograms show strong dielectric character suggesting little, if any, oxidation of any component subsequent to the oxidation of Fe^{++}. This occurrence is in full accord with expectations since the only oxidizable ions in solution are $(OH)^-$ and $(SO_4)^=$, both of which necessitate extraordinarily large discharge potentials not attained in these experiments. The view that the only reaction which takes place is

$$Fe^{+++} + e \rightarrow Fe^{++}$$

is supported by the apparent approach to a maximum at point *a* whose potential is completely determined by the Fe^{+++}/Fe^{++} ratio, and the complete lack of a minimum at point *d* which would be expected if dielectric polarization were principally operative.

The variation of the steady state of the oxidant solution with current density, frequency, and concentration of oxidant appears to follow the same pattern as that discussed for the reductant solution.

(D) The Oxidant-Reductant Systems

(1) The Ferric-Ferrous System (in N H_2SO_4).— The highly complex nature of the Fe^{+++}/Fe^{++} system

FIG. 10. $Fe^{+++/++} = 0.05M/0.025M$ in N H_2SO_4

FIG. 11. $Fe^{+++}/Fe^{++} = 0.05M/0.1M$ in N H_2SO_4

cyclograms makes them difficult subjects for discussion. The cyclograms show evidence of both Fe^{++} and Fe^{+++} oxidation and reduction, respectively. Typical are the cyclograms obtained for unit ratio ($0.1M/0.1M$) shown in Fig. 9. Both anodic and cathodic tails are in evidence. Furthermore, the behavior of the anodic and cathodic segments with change in frequency, current density, and concentration is quite consistent with expectations, and similar to those encountered with either pure oxidant or reductant.

An important feature of the experiments with various ratios of Fe^{+++}/Fe^{++} was the verifying association of the tails with the anodic and cathodic electrode reactions. Fig. 10–13 are illustrative.

In Fig. 12 and 13, changes in concentration of Fe^{+++} affect only the cathodic tail and have practically no effect on the anodic tail. Exactly the opposite

is true where only changes in concentration of Fe^{++} are involved. The trend in distortion is quite apparent. There is loss in specific distortive character with decrease in concentration of the component responsible.

(2) *Potassium Ferri- and Ferrocyanide in Water.*— In a thermodynamically reversible system, it is reasonable to expect that the dummy electrode would register a potential characteristic of the redox ratio. If the ratio were unity and the current density small enough, so that the oxidation and reduction would not displace the ratio from the poised region, then the difference in potential between the dummy and working electrodes should be no more than a few millivolts. Thus, within experimental error, de/dq should equal zero over the whole range of instantaneous current values and the resulting cyclogram should be a straight line. Exactly such results are illustrated in Fig. 14 which, like the others, involves three cyclograms.

FIG. 12. $Fe^{+++}/Fe^{++} = 0.025M/0.05M$ in N H_2SO_4

FIG. 13. $Fe^{+++}/Fe^{++} = 0.1M/0.05M$ in H_2SO_4

If the concentration of depolarizer is decreased (but maintaining unit ratio), then one should expect the development of definite differences in potential between dummy and working electrodes with increasing current density as the redox ratio at the working electrode is repeatedly carried away from the poised region. Fig. 15 again shows experimental evidence in accord with the hypothesis. The smallest cyclogram is a straight line but, with increasing current density, the expected potential differences develop.

For other than unit ratio, the effect of changes in current density is again predictable. At sufficiently low current densities, the cyclogram should be a straight line. At high current densities, as one component is exhausted at the working electrode, the cyclogram should be one in which the change from chemical to dielectric polarization is clearly apparent. Fig. 16 illustrates such behavior.

The effect of changing the concentration of only one component is observed by comparison of Fig. 16 and 17. The change in concentration of oxidant leads to changes in cyclogram distortion in the cathodic region exactly in the manner one would anticipate.

FIG. 14. $K_3Fe(CN)_6/K_4Fe(CN)_6 = 0.1M/0.1M$

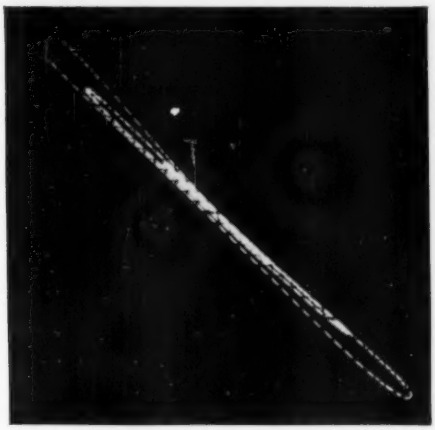

FIG. 15. $K_3Fe(CN)_6/K_4Fe(CN)_6 = 0.025M/0.025M$

The effect of frequency is interesting. At equivalent current densities, an increase in frequency causes a decrease in the current's half-wave area. Thus, at constant current density, an increase in frequency would tend to keep the redox ratio at the working electrode closer to that at the dummy. Potential differences between dummy and working electrodes would become smaller. Comparison of Fig. 16 and 18 bears out such expectations.

(*E*) *Special Experiments on* R_Δ.

In many respects, the polarization resistance R_Δ does not have the properties of a true resistance. It

varies with frequency and current density. Such behavior is analogous to that of the polarization capacitance.

If, therefore, R_Δ is dependent upon the polarization and shows properties usually associated with the polarization, then R_Δ should vary as the polarization varies. Specifically, it might be anticipated that the polarization resistance, R_Δ, would be zero when the polarization itself is zero. Acree, *et al.* (4) have shown that the reactance (X) is 90° out of phase with the current. Thus, at peak current (I), $IX = 0$ and, consequently, IR_Δ should be zero. The following experiment was devised and carried out in order to check the foregoing reasoning.

FIG. 16. $K_3Fe(CN)_6/K_4Fe(CN)_6 = 0.0125M/0.125M$

FIG. 17. $K_3Fe(CN)_6/K_4Fe(CN)_6 = 0.025M/0.125M$

The cell resistance of a $0.02M$ H_2SO_4 solution was measured on an impedance bridge at various frequencies. The cell resistance thus measured was extrapolated to infinite frequency in order to eliminate the effects of R_Δ. The extrapolated resistance was the true solution resistance, R_T, and was found to be 70 ohms.

A full-cell cyclogram was impressed on the scope such that the cell potential was measured on the vertical axis and current on the horizontal axis. The vertical axis calibration was 200 mv/division measured from the origin. Since the current was sinusoidal, there was no need to calibrate the horizontal axis.

Cyclograms were taken at 100, 300, 500, and 1000 c/sec. The trend is illustrated in Fig. 19 and 20. Current values are 5, 10, 15, 20 ma in each case.

If IR_Δ is zero at peak current, then the cell potential will be merely that calculated from IR_T. At 20 ma, this value is calculated as 1.97 volts. Since R_T is frequency independent, the cell potential IR_T should be frequency independent.

A glance at Fig. 19 and 20 shows that the cell potential at peak current (20 ma) is about 2.5 v and 2.1 v at 100 and 1000 c/sec, respectively. Obviously, IR_Δ is not zero at peak current. Since IR_T is frequency independent the decrease in cell potential at

FIG. 18. $K_3Fe(CN)_6/K_4Fe(CN)_6 = 0.0125M/0.125M$ at 300 c/sec.

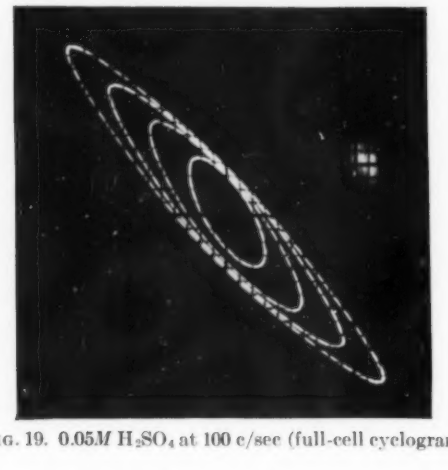

FIG. 19. $0.05M$ H_2SO_4 at 100 c/sec (full-cell cyclogram)

peak current with frequency increase can only be construed as being due to the decrease in the value of R_Δ.

The excellent elliptical character of the cyclograms indicates that R_Δ is constant over a complete cycle and that the iR_Δ drop is 90° out of phase with the IX drop. In this respect, R_Δ appears to be analogous to a true resistance in that it acts as a dissipative agency associated with electrode phenomena and, at constant frequency and rms current density, is independent of the variations in electrode polarization.

Fig. 5 shows two cyclograms, one at 100 c/sec and 20 ma and the other at 200 c/sec and 40 ma. Normal sulfuric acid was the electrolyte in each case.

The horizontal amplification of the oscillograph was readjusted for each current value so that the peaks of the current waves coincided. This arrangement makes possible the comparison of the instantaneous values of the voltage at different frequencies and current densities when the half-wave area (coulombs per half cycle) is held constant. The observed slight relative rotation of the cyclograms around the origin surely means that the polarization resistance has changed slightly. Otherwise, the two cyclograms are identical. Similar results were obtained over the four-

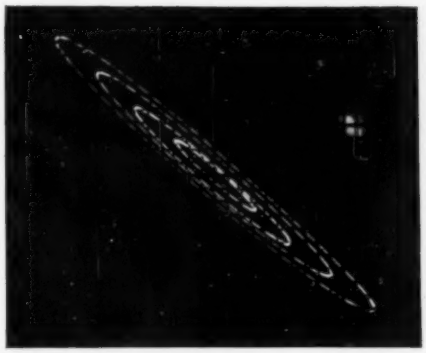

FIG. 20. 0.05*M* H_2SO_4 at 1000 c/sec (full-cell cyclogram)

fold frequency range from 100 to 400 c/sec. If we may consider that q and e are in phase with each other, then, when the two cyclograms are superimposed, their instantaneous values of q at any point must be equal. The conclusion follows that, within the limits of accuracy of our equipment and our method, q is the same function of e at different frequencies and current densities as long as the half-wave area is constant. Since the differential capacity is defined as $C = dq/de$, this means, in the terminology of Shaw and Remick (8), that there is no detectable capacitive Q-dispersion for normal sulfuric acid at current densities well above the capacitive elevation point. Nevertheless, there is a detectable resistive Q-dispersion in the same range. This property of the polarization resistance seems worthy of note, although its significance is not yet clear to us.

ACKNOWLEDGMENTS

The authors wish to express their gratitude to Dr. W. H. Bixby of the Electrical Engineering Department for many helpful discussions concerning some of the technical aspects of the equipment, and to Dr. D. C. Grahame of Amherst College for his critical study of our original manuscript. Thanks are also due to the Ethyl Corporation for the grant of a research fellowship to one of us (J. S.).

Any discussion of this paper will appear in a Discussion Section, to be published in the June 1951 issue of the JOURNAL.

REFERENCES

1. D. REICHENSTEIN, *Z. Elektrochem.*, **15,** 913 (1909).
2. J. HOPKINSON, E. WILSON, AND F. LYDALL, *Proc. Roy. Soc. London*, **54,** 407 (1893).
3. A. FURTH, *Z. Elektrochem.*, **32,** 467 (1926).
4. S. F. ACREE, E. BENNETT, G. H. GRAY, AND H. GOLDBERG, *J. Phys. Chem.*, **42,** 871 (1938).
5. (*a*) A. SEVCIK, *Collection Czechoslov. Chem. Communs.*, **13,** 349 (1948).
   (*b*) J. E. B. RANDLES, *Disc. Faraday Soc.*, **1,** 11 (1947).
6. W. R. COOPER, *Electrician*, **35,** 541 (1895).
7. J. W. SHIPLEY, *Can. J. Research*, **1,** 305 (1929).
8. M. SHAW AND A. E. REMICK, *J. Electrochem. Soc.*, **97,** 324 (1950).
9. (*a*) G. MENGARINI, *Electrician*, **27,** 304 (1891).
   (*b*) R. MALAGOLI, *Electrician*, **31,** 258 (1893).
   (*c*) J. W. SHIPLEY AND C. F. GOODEVE, *Eng. J.* (*Canada*) **10,** 1 (1927); *Trans. Roy. Soc. Can.* [3], **21,** 393 (1927); *ibid.*, **22,** 87 (1928).
10. S. GLASSTONE, "An Introduction to Electrochemistry," p. 473, D. Van Nostrand Co., New York (1942).
11. W. M. CLARK, "The Determination of Hydrogen Ions," Williams and Wilkins Co., Baltimore (1928).
12. D. C. GRAHAME, *J. Am. Chem. Soc.*, **63,** 1207 (1941).

The Voltage Balance in the Mercury Cell[1]

VITTORIO DE NORA

Impianti Elettrochimici, Milan, Italy

ABSTRACT

The distribution of voltage drop through a mercury cell has been calculated and directly measured at different current densities in an industrial de Nora cell which is described. The cell was operated at constant temperature and fed with 305 g/l sodium chloride solution at a rate proportional to current density. Voltage-current density curves corresponding to loads from 50 per cent to 150 per cent of rated capacity of the cell are reported and discussed.

INTRODUCTION

Very little has been known generally about mercury cells until recently when, following the investigations of German mercury cells by the Allied Intelligence Commissions, reports (1, 2) were published and interest was aroused in the United States. In the last few years a comparison of mercury and diaphragm cells was made by R. B. MacMullin (3) and a new model was described by W. C. Gardiner (4).

However, only general performance and operating data are available which include overall cell voltages at different loads.

The values of the several components of the cell voltage are of great interest, especially to determine if and how the total voltage of the cell may be lowered.

This study was originated by the attempt to improve operation of the mercury cell and it is based on a similar research carried out on diaphragm cells (5).

The distribution of the voltage drop through the cell was calculated so far as possible and measurements were taken on operating cells. Laboratory tests were made to check certain results which were doubtful because of difficulty encountered in carrying out measurements of some items of the voltage balance.

The data presented in this paper are a summary of a large number of measurements on de Nora type mercury cells and must be considered as average values. Adjustments have been made to apply some of the results to the type of cell which is described herein. Actually, experiments were carried out on different models which differed from one another only in some details of construction.

The voltage across a mercury cell for the electrolysis of sodium chloride consists of the following main factors:

(*a*) Anode potential.
(*b*) Cathode potential.
(*c*) Potential for overcoming the resistance of the electrolyte.
(*d*) Potential for overcoming the resistance of the first class conductors.
(*e*) Potential for overcoming the contact resistance.

Factors (*d*) and (*e*) are in turn the sum of different items.

The conclusions resulting from this study should be regarded as taking into account economical considerations which determine the capacity of the cell as well as the ideal size of the various elements of which the cell is composed.

THE MERCURY CELL

Mercury cell units for the production of chlorine, caustic, and hydrogen consist of two parts—the electrolysis cell, in which brine is electrolyzed to form chlorine gas and sodium amalgam, and the decomposer, in which the sodium amalgam reacts with water to form caustic and hydrogen.

The de Nora cell (6) presents some special features and will be described briefly with particular regard to the parts directly concerned with voltage drop. A perspective view of two cells, type 16 TD, is represented in Fig. 1. The electrolysis cell is a long, narrow, shallow trough of welded structural steel completely lined with corrosion-resistant plates. Electrical contact with the mercury flowing on the bottom of the cell is obtained by the upper flanges of steel structural tees welded to the trough at regular intervals. The upper level of these flanges is about $\frac{1}{8}$ in. (3.2 mm) lower than the top surface of the bottom lining so that even though no mercury were circulating there would be a layer of mercury over the steel plates, thus preventing exposure of

[1] Manuscript received February 16, 1950. This paper prepared for delivery before the Cleveland Meeting, April 19 to 22, 1950.

any steel part. The lining also restricts heat losses and permits satisfactory cell operation even under substantial changes in room or brine temperature.

The graphite anodes face the mercury cathode and are supported from the cell covers by means of graphite rods. Electrical connections are made by means of copper bars brazed to the underneath side of the cell and by means of copper collars clamped around the graphite rods. Each cell is provided with a disconnect switch for removing the cell from operation for anode replacement or maintenance.

Brine, saturated at the temperature at which it enters the cell, is fed at one end of the cell and is

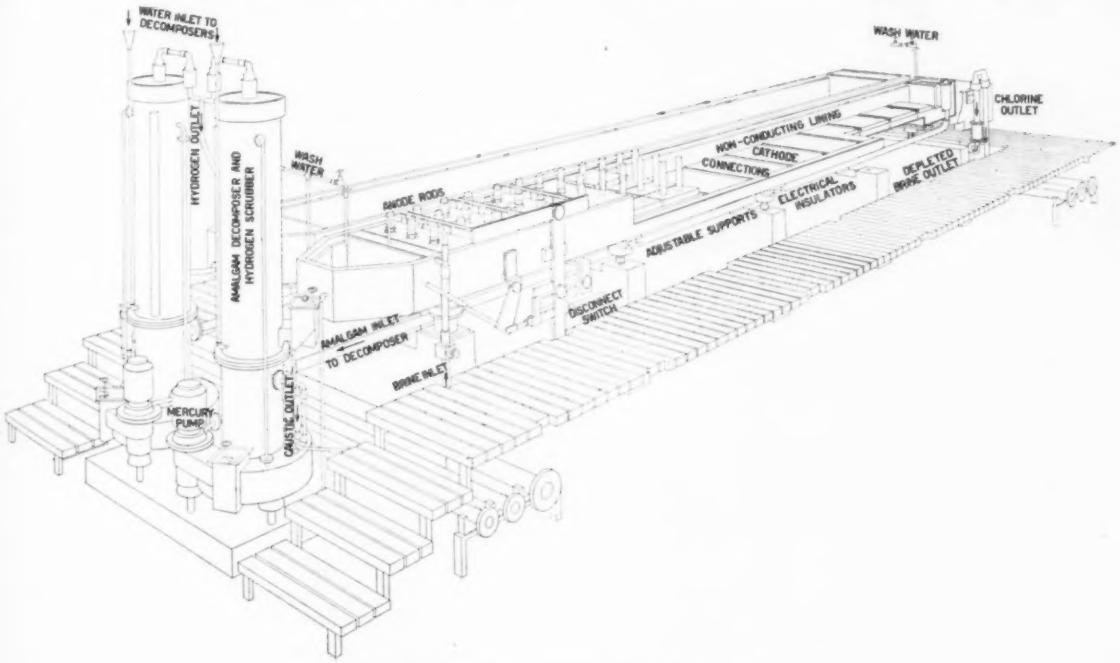

FIG. 1. Perspective view of two de Nora cells, Model 16 TD

electrolyzed between the graphite anodes and the mercury cathode. The depleted brine, leaving the cell at the opposite end, where the chlorine outlet is located, is resaturated and purified before returning to the cell.

The sodium amalgam flows by gravity from the cell to the decomposer in which, by electrochemical reaction with water, caustic soda and hydrogen are produced with simultaneous regeneration of mercury. The mercury is then pumped back to the cell.

The de Nora decomposer is of the tower type and has the particular feature of consisting of two stages: in the first stage the amalgam flowing from the cell is but partly decomposed and highly concentrated caustic can be produced; in the second stage, which is fed with water, the amalgam coming from the first stage is totally decomposed with production of dilute caustic which is fed to the first stage. Use of two stages gives great flexibility of operation under various amalgam concentrations and temperature conditions.

Another feature is that the rate of circulation of amalgam through the decomposer may be varied within wide limits while maintaining any desired constant flow of mercury through the electrolysis cell. The de Nora decomposer also has the function of serving as a scrubber for the evolved hydrogen gas. It is packed with pieces of graphite or carbon, flooded with caustic, and therefore requires only a small flow of mercury for efficient operation.

CELL DIMENSIONS

De Nora mercury cells are constructed in various sizes from 5000 to 30,000 amperes. The cross-section of a cell for a rated capacity up to 20,000 amperes is represented schematically in Fig. 2. The cell may be considered as formed by a number of similar sections, one of which is shown in Fig. 3 and comprises 4 anode sets of three plates each (terns, or triplets), the size of the plates being $7\frac{1}{2}$ in. x 21 in. x 2 in. (190 mm x 530 mm x 50 mm) thick. Thus each section has 12 anodes supported by 24—3 in. (76 mm) graphite rods. Each section also includes three cathode plates and is 7 ft 4 in. (2240 mm) long. The inside width of the cell where the mercury flows is 25 in. (640 mm). The mercury layer is about $\frac{3}{16}$ in.

(4.8 mm) deep at all points except over the steel cathode connections where the depth is increased to about $\frac{5}{16}$ in. (8 mm).

Current is fed to each section by an anode and a cathode busbar, each consisting of a double copper bar $\frac{1}{2}$ in. x 4 in. (12.7 mm x 101.6 mm). The anode busbar is connected to an anodic equalizing bar and the cathode busbar to the copper bar brazed to the cell.

The equalizing bar extends for the length of the cell thus equalizing the voltage at all sections. As the cells are arranged in pairs, the cathode bar has to be connected only to one cell of each pair.

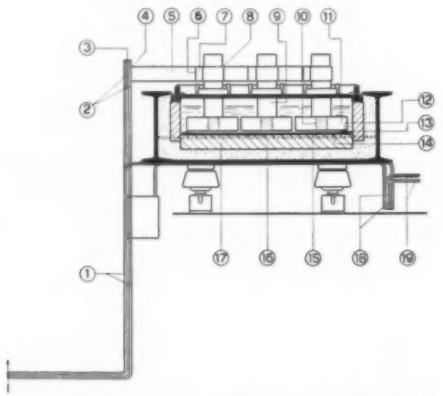

FIG. 2. Cross section of de Nora cell, Model T

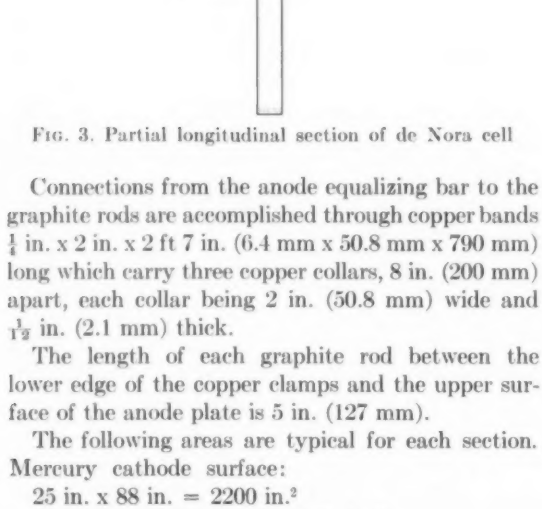

FIG. 3. Partial longitudinal section of de Nora cell

Connections from the anode equalizing bar to the graphite rods are accomplished through copper bands $\frac{1}{4}$ in. x 2 in. x 2 ft 7 in. (6.4 mm x 50.8 mm x 790 mm) long which carry three copper collars, 8 in. (200 mm) apart, each collar being 2 in. (50.8 mm) wide and $\frac{1}{12}$ in. (2.1 mm) thick.

The length of each graphite rod between the lower edge of the copper clamps and the upper surface of the anode plate is 5 in. (127 mm).

The following areas are typical for each section.

Mercury cathode surface:
25 in. x 88 in. = 2200 in.²
(640 mm x 2240 mm) = (143 dm²)

Anode surface facing mercury:
4 x 3 x $7\frac{1}{2}$ in. x 21 in. = 1890 in.²
(190 mm x 530 mm) = (122 dm²)

Electrolyte cross-sectional area conducting the current (assumed as being the mean value between anode and cathode surfaces):
= 2045 in.²
= (133 dm²)

Copper bars, cross-section:
2 x $\frac{1}{2}$ in. x 4 in. = 4 in.²
(13 mm x 100 mm) = (2600 mm²)

Graphite rods, cross-section:
24 x 7 in.² = 168 in.²
(45 cm²) = (1090 cm²)

Distance between cathode and anode surfaces:
= $\frac{3}{16}$ in.
(4.8 mm)

Operating Conditions

The experiments apply to approximately normal operating conditions.

The *brine* was fed at the rate of 0.3 gallons per minute (1.1 liters per minute) for each 1000 amperes and had the following average compositions:

NaCl	305 grams per liter
Na_2SO_4	2 to 4 grams per liter
$NaClO_3$	1 to 2 grams per liter
Ca	0.05/0.5 grams per liter

It was not possible to carry out all the experiments with a constant brine composition but the variations indicated above did not appreciably influence the results obtained.

It is to be noted especially that most of the earlier measurements were taken on cells operating with brine alkaline to NaOH (0.01 to 0.1 g/l) and Na_2CO_3 (0.01 to 0.2 g/l) but, later, cells were fed with acid brine (corresponding to about 0.01 g/l HCl). We suspect that cell voltage did diminish slightly but within the limits of experimental errors.

At the above feed rate, the depleted brine leaving the cell contained 275 grams per liter NaCl.

The average brine concentration throughout the brine, therefore, was 290 grams per liter.

The *temperature of the brine in the cell* was 70°C at the outlet and about 5° less at the inlet. The effect of temperature on conductivity of the brine was apparently compensated by the higher brine concentration where the temperature was lower.

The *rate of flow of mercury* was maintained at a value corresponding to an amalgam concentration of about 0.1 per cent Na at the exit, which corresponds to 0.264 U. S. gallons per minute (1 liter per minute) for each 1000 amperes.

All these conditions remaining the same, the ampere load through the cell was varied in order to take measurements at different values of the current den-

sity, which was the only independent variable taken into account.

The type T de Nora cell has a rated capacity of 3000 amperes per section which means a total current of 12,000 amperes for a 4-section cell (16 T type).

At this load the various current densities in the main parts of the circuit are the following:

(*a*) In the copper bars: 750 amp/in.^{2} (1.15 amp/mm^2)
(*b*) In the graphite rods: 17.8 amp/in.^{2} (2.75 amp/cm^2)
(*c*) At the anode plate surface: 1.59 amp/in.^{2} (24.5 amp/dm^2)
(*d*) At the mercury cathode surface: 1.36 amp/in.^{2} (21 amp/dm^2)
(*e*) Through the electrolyte: 1.47 amp/in.^{2} (22.6 amp/dm^2)
(*f*) At the contact copper to copper: about 100 amp/in.^{2} (0.15 amp/mm^2)
(*g*) At the contact copper to graphite: about 7 amp/in^2 (1.08 amp/cm^2)
(*h*) At the contact graphite to graphite: about 8 amp/in.^{2} (1.23 amp/cm^2)

These last three values are approximate and would correspond to the actual current densities only on the assumption that the contact between the two surfaces is perfect, which is not exactly the case, especially for the contact copper to graphite and graphite to graphite.

Distribution of Voltage Drop

The various terms making up voltage drop at the different parts of the cell are reported in Table I, where each part number corresponds to that indicated in Fig. 2.

Average values of all the measurements have been reported for current densities of 50%, 75%, 100%, 125% and 150% of rated current density.

In addition, the terms corresponding to partial voltage drops of the same nature have been added together in Table II, so that the total voltage is calculated from the sum of the anode potential (item 12), the cathode potential (item 14), the drop in the electrolyte (item 13), the total ohmic drop (items 1, 3, 5, 7, 9, 11, 15, 17, 19), and the total contact drop (items 2, 4, 6, 8, 10, 16, 18). The percentage of each drop referred to the total is also reported.

The graphs of Fig. 4 show the relative values of the various constituents of the total voltage, collected in the five significant categories mentioned above, and the way in which the total voltage and its constituents change with the current density when all other conditions remain the same.

Among the factors of the cell voltage, three of them, namely the anode and cathode potentials and the voltage drop in the electrolyte, deserve special consideration because of their strictly electrochemi-

TABLE I. *The voltage balance of the de Nora mercury cell*

	Current at 100% amperes	Voltage in millivolts at per cent of rated capacity				
		50	75	100	125	150
1 Interconnecting busbars copper bars ½ in. x 4 in. (13 mm x 100 mm), avg length 58 in. (1470 mm)	1500	17	25	34	42	51
2 Contact busbars/anode equalizing bar 32 in.^{2} (207 cm^2)	3000	2	3	4	5	6
3 Anode equalizing bar copper bars ½ in. x 4 in. (12.7 mm x 101.6 mm), avg length 7 ft 4 in. (2240 mm)	940	8	12	16	20	24
4 Copper equalizing bar/branch band 5 in.^{2} (32 cm^2)	375	2	3	3	4	5
5 Branch band copper band ¼ in. x 2 in. (6.4 mm x 50.8 mm), length 31 in. (787 mm)	280	7	10	14	17	21
6 Contact branch band/anode collars 4 in.^{2} (26 cm^2)	125	1	2	2	3	3
7 Anode collar copper band 1/16 in. x 2 in. (1.6 mm x 50.8 mm), avg length 10 in. (254 mm)	62	3	5	6	8	9
8 Contact anode collar/graphite rod 18 in.^{2} (116 cm^2)	125	20	30	40	50	60
9 Graphite rod diam 3 in. (76.2 mm), length 5 in. (127 mm)	125	14	21	28	35	42
10 Contact graphite rod/graphite plate 15 in.^{2} (97 cm^2)	125	9	14	18	22	27
11 Graphite plate 21 x 7.5 in.^{2} (1020 cm^2), thick. 2 in. (50.8 mm)	125	1	1	1	1	1
12 Anode potential		1500	1580	1660	1740	1830
13 Electrolyte path 3/16 in. (4.8 mm)	3000	110	180	240	300	370
14 Cathode potential		1740	1760	1780	1800	1820
15 Mercury cathode	3000	15	21	28	35	42
16 Contact mercury/steel plate 2½ in. x 25 in. (63.5 mm x 640 mm) voltage negligible	1000	—	—	—	—	—
17 From cathode steel plate to cathode bars	3000	25	36	45	53	60
18 Contact cathode bar/busbars 48 in.^{2} (310 cm^2)	3000	2	2	3	4	5
19 Busbars ½ in. x 4 in. (12.7 mm x 101.6 mm), avg length 27 in. (686 mm)	1500	8	12	16	20	24
Total		3484	3717	3938	4159	4400

cal nature and because they are outstandingly influenced by the operating conditions.

In the potentiometric determination of the potential drop in the electrolyte by means of two calomel electrodes, it was not possible to get very accurate data. This holds also for measurements of anode and cathode potentials at current densities such as those in an industrial mercury cell. In fact, if the position of the tip of the calomel electrode is moved by only $\frac{1}{32}$ in. (0.8 mm), there is a variation of 30–40 mv in the reading. Also control of the position of the tips during electrolysis required a special arrangement because of the difficulty of the experiments.

The only method available to judge the magnitude of the error was to compare the sum of the individual values of anode potential, cathode potential, and potential drop in the electrolyte with the value obtained by the voltmeter. An accuracy of ±10 mv is probably all that could be expected.

TABLE II. *Voltage distribution in the de Nora mercury cell*

	Voltage in millivolts at per cent of rated capacity					Per cent of total voltage at 100%
	50	75	100	125	150	
Anode potential (item 12)	1500	1580	1660	1740	1830	42.2
Cathode potential (item 14)	1740	1760	1780	1800	1820	45.1
Drop in the electrolyte (item 13)	110	180	240	300	370	6.1
Ohmic drops (items 1, 3, 5, 7, 9, 11, 15, 17, 19)	98	143	188	231	274	4.8
Contact drops (items 2, 4, 6, 8, 10, 16, 18)	36	64	70	88	106	1.8
	3484	3727	3938	4159	4400	100

Anode Potential

The value of the anode potential is the most important item in the voltage balance of the cell because its variation with current density is considerable and is greater than for the other partial drops. The factors governing the anode potential in a mercury cell are the same as in a diaphragm cell with the exception that brine concentration and current density are somewhat higher than those which are involved in diaphragm cells.

The chlorine discharge potential on graphite (British Acheson type X) as measured during electrolysis at 70°C with an auxiliary calomel electrode gave the values indicated in Table II. Measurements reported refer to graphite which had been used for about six weeks.

Assuming that the equilibrium anode potential is 1330 mv, a polarization results which is 170 mv at a current density of 0.79 amp/in.^{2} (12.2 amp/dm^2) and about 500 mv at 2.37 amp/in.^{2} (36.5 amp/dm^2).

The anode potential measured during the electrolysis was somewhat lower than that found in laboratory tests for the same value of current density. Apart from experimental errors, this can be explained by the fact that the actual current density at the surface of the anode of the cell is lower than that taken into account because the side surfaces of the anode plates are also active. Accurate measurements of anode potential at different points on the sides of the anode plates would give an indication of current distribution over the total surface.

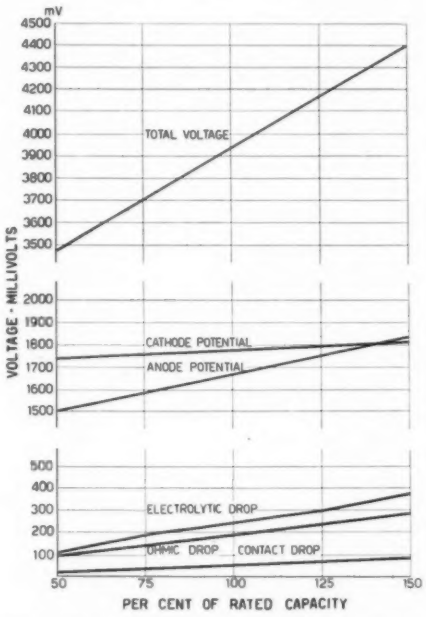

FIG. 4. Potentials changes with current density

Cathode Potential

The cathode potential is influenced but slightly by the current density. This is to be expected because polarization is notably influenced by current density only in case of gas evolution. Also changes in temperature and concentration of brine influence the cathode potential but slightly, whereas a larger effect is produced by a change in the amalgam concentration. Similar results have been obtained by Stender, Stroganov, and Zivotinsky (7).

The variation of the cathode potential is due mainly to concentration polarization resulting from impoverishment of sodium ions at the mercury surface, which is the more severe the higher the current density. More accurate experiments are being carried out concerning the potential of amalgams of different concentrations with respect either to brine or to caustic. These will be reported at some later date.

The variations shown in Table I have to be considered as an indication of the existence of a change in cathode potential rather than as the absolute values of this change.

Potential Drop in the Electrolyte

At rated current density the potential drop in the electrolyte is 230 mv. The value thus determined would correspond to a brine resistivity of 2.15 ohm-cm, if we assume that the current density is that calculated by taking the mean cross section between the electrodes and that the path from graphite to mercury is about $\frac{3}{16}$ in. (4.8 mm).

The value of the brine resistivity is affected by brine concentration and temperature, of course, the temperature being more important if the brine concentration decreases. Measurements taken at different points of the cell, where brine concentrations were not the same, gave no appreciable discrepancies; this can be explained by the limits of the experimental error and by the fact that current density would be a compensating factor.

Potential Drop in the First Class Conductors

This potential drop corresponds to the difference between the total voltage of the cell measured on the busbars, at points halfway between adjacent cells, and the voltage measured near the surface of the electrodes on the inside of the electrodes themselves. The measurements were taken by connecting the voltmeter to the anode through a lead sealed in the graphite plate. During all the measurements care was taken to keep the voltmeter (Weston with an internal resistance of 200 ohm/volt) far enough from the cells and the busbars to eliminate practically the influence of the electromagnetic field produced by the heavy currents involved.

The total potential drop measured corresponds within a few mv to that obtained by adding the different potential drops which were measured independently and which were also calculated whenever possible from the values of the cross sections, the length of the conductors, the resistivity of the material, and the current density.

It may be mentioned that the resistivity of the copper busbars, at the temperature of about 40°C, has to be considered practically as 2×10^{-6} ohm-cm and that the graphite used has a resistivity of about 800×10^{-3} ohm-cm at a temperature of 60°C.

The contact resistance copper to copper was in all cases fairly constant. On the other hand, the contacts copper to graphite and graphite to graphite varied appreciably according to the state of the surfaces and the pressure between the two materials. The data reported correspond to those of the great majority of the measurements, without taking into account those corresponding to poor contact or to particularly good ones.

It should be noted that by increasing the load of the cell the absolute value of the ohmic losses could be kept constant, if the dimensions of the conductors were increased correspondingly and if it were economically advisable.

Conclusions

Of the total voltage of the mercury cell about 42.2 per cent is the anode potential, 45.1 per cent the cathode potential, 6.1 per cent the potential necessary to overcome the resistance of the electrolyte, and 6.6 per cent the potential to overcome ohmic and contact drops.

In that anode potential increases with current density, this item is a very limiting factor of the capacity of one given cell.

The choice of current density is determined by economic considerations such as cost of power and capital investment.

The values of the ohmic drops in the electrolyte and in the conductors are affected appreciably by cell maintenance and operating conditions.

Improvements in total cell voltage can be expected only by the possibility of diminishing the anode potential by means of improvements in anode materials and shapes.

Acknowledgment

The author is indebted to Messrs. C. M. Dean and Patrizio Gallone for their valuable contributions and advice.

Any discussion of this paper will appear in a discussion section, to be published in the June 1951 issue of the Journal.

References

1. FIAT Final Report No. 816, "Horizontal Mercury Chlorine Cell," I. G. Farbenindustrie, A. G. (1946).
2. FIAT Final Report No. 797, "The Electrolytic Chlorine Plant in Hoechst on Main" (1946).
3. R. B. MacMullin, *Chem. Ind.*, **61**, 41 (1947).
4. W. C. Gardiner, *Chem. Eng.*, **54**, 108 (1947).
5. W. W. Stender, P. B. Zivotinsky, M. M. Stroganoff, *Trans. Electrochem. Soc.*, **65**, 189 (1934).
6. V. de Nora, "Progressi delle celle a mercurio per la produzione di cloro e di idrati alcalini," XXII Congrès de Chimie Industrielle, Barcelona (Oct. 1949).
7. W. W. Stender, M. M. Stroganov, and P. B. Zivotinsky, *Trans. Electrochem. Soc.*, **68**, 521 (1935).

THE ELECTROCHEMICAL SOCIETY, INC.

The Electrochemical Society is an international organization of individuals and companies concerned with or interested in Electrochemistry and allied subjects.

The Society is dedicated to the advancement of the theory and practice of Electrochemistry and related subjects, as shown in the following divisions:

Battery	Electro-Organic
Corrosion	Electrothermic
Electric Insulation	Industrial Electrolytic
Electrodeposition	Theoretical Electrochemistry
Electronics	

Among the means to this end are the holding of meetings for the reading and discussion of professional and scientific papers on these subjects, the publication of such papers, discussions, and communications as may seem appropriate, and cooperation with chemical, electrical, and other scientific and technical societies.

It is an incorporated society without capital stock. The affairs of the Society are managed by a Board of Directors under a Constitution and By-Laws. Officers are nominated by a nominating committee appointed by the Board of Directors and elected by the members.

Direct all general correspondence and inquiries regarding membership to Society headquarters at 235 West 102nd Street, New York 25, N. Y., c/o Mr. W. J. Holian, Assistant Secretary.

Officers of the Society

President ..... CHARLES L. FAUST
Past President ..... ALFRED L. FERGUSON
Vice-President ..... RALPH M. HUNTER
Vice-President ..... J. C. WARNER
Vice-President ..... ROBERT J. MCKAY
Treasurer ..... E. GIDEON WIDELL
Secretary ..... HENRY B. LINFORD